Final Report

Field Validation of Geologic Assessment of Features Sensitive to Pollution in Karst

Submitted to the Texas Commission on Environmental Quality

By
Susan D. Hovorka and Adrien Lindley
Bureau of Economic Geology
Scott W. Tinker, Director
John A. And Katherine G. Jackson School of Geosciences
The University of Texas at Austin

October 2007

Table of Contents

List of Tables

List of Figures

Summary

Karst on Cretaceous bedrock covered by thin soils are characteristic of the Edwards aquifer recharge zone in central and south Texas U.S.A. Upland areas containing karst features are undergoing rapid development in the aquifer recharge zone. This study undertakes an assessment of the hydrologic function of typical small-scale upland karst features. Features included in this study were located in both the Barton Springs and San Antonio segments and the Edwards aquifer contributing zone.

Texas state law (Edwards Rules (Title 30 Texas Administrative Code (TAC) Chapter 213) reduces risks of groundwater degradation by identifying geomorphic indicators of karst "sensitive features" as the most likely areas of direct connection between the surface and the aquifer where rapid recharge can occur. At these locations best management practices (BMPs) are required to mitigate the impacts associated with development. This project is designed to improve effectiveness these effort by measuring infiltration rates of typical abundant, small upland karst features to determine if they are sensitive under the Edwards Rules.

For the test program, selected typical small upland karst features were small soil-floored sinkholes, medium sinkholes with cobble-filled drains, a partially excavated solution cavity, and various background upland areas. Typical small upland karst features were with paired with non-karst control plots to determine if recharge was rapid at the karst features. Constant head infiltration measurements with a large diameter single ring infiltrometer was provide direct evidence of the net hydrologic function of the contained soil and bedrock system Microtopographical and soil thickness surveys, introduction of blue dye, followed by excavation were used to confirm that the karst features were of karst origin with central drains through which soil was lost by sapping. GPR over tested features failed to locate significant voids in the subsurface beneath the features tested.

Infiltration experiments show that even thin soil reduces hydraulic conductivity and recharge rate. Infiltration at small soil-filled sinkholes were only slightly higher than background, indicating that these features do not provide "rapid" recharge to the aquifer, and therefore do not qualify as "sensitive features" under the Edwards rules. The principle hydrologic function of small sinkholes is to pond water following major rainfall events, which will result in more sustained recharge beneath them. Soil sapping and limestone dissolution seems to be adequate to maintain a topographic depression. Excavation of the test features shows that although solution-enlarged karst features exist in the subsurface below small sinkholes, these fractures and conduits are plugged by the clay soil common in the uplands of the recharge zone. In contrast, those sites where visual inspection suggests higher infiltration through non-soil filled drains and cave access. High infiltration was measured, showing that the features should be classified as sensitive.

High infiltration was also measured at a location with no geomorphic evidence of karst, where the infiltrameter was set up around an ashe juniper on a hillside. At this site the water apparently moved along voids opened by roots and was discharged along bedding plains lower on the hillside.

This study generally validates that geomorphic method of identifying sensitive karst features by inspection for visible flow paths. It does not fully consider the inverse issue of how much recharge occurs at karst features with no geomorphic expression.

Background

Purpose and design of this study

Through the Edwards Rules (Title 30 Texas Administrative Code (TAC) Chapter 213), Texas has become a lead state in the implementation of a regional strategy for protection of recharge to a karst aquifer. Many areas, both internationally and in the US, recognize through regulation, research, and past contamination events that karst aquifers are both valuable water resources and uniquely vulnerable to contamination. The inventory of karst-management rules compiled (Hovorka, 2001a) shows that most regulation is done by local administrative regions (for example town or county building codes), and the procedures for assessing the need for karst protection, although in some locations rigorous, are generally not formally captured as public documents. In contrast, the Edwards Rules administered by Texas Commission for Environmental Quality (TCEQ) provide aquifer-wide water-quality protection measures and supply guidance on assessment of karst features and design of best management practices (BMP's).

The method of recharge protection described by the Edwards Rules uses geomorphologic characteristics to infer which areas of the landscape are most likely to contain subsurface karst conduits that focus flow. Because flow through karst conduits is preferential, pollution can be introduced into the aquifer rapidly and with little chance of either natural or human remediation. These geomorphically identified karst features (caves, sinkholes, fractures, etc.) that have potential for transmitting polluted surface water to the aquifer are called in the context of the Edwards Rules "sensitive features."

During revision of the TCEQ document "Instruction to geologists for geologic assessments on the Edwards aquifer recharge/transition zones" in 2001, which included a literature review and interviews with Edwards and international karst experts (Hovorka, 2001a and b), it was found that: (1) geomorphic features listed by the Edwards Rules as potentially sensitive are, in general, well-supported by research and by anecdotal evidence as the areas that need the greatest protection during urbanization; (2) the details of the methodology for effective but rapid and low-cost identification of these sensitive features are the subject of debate, and (3) guidance on appropriate BMPs was inadequate for the diverse spectrum of karst features observed.

Stresses on both the Edwards aquifer system and on the regulatory framework for aquifer protection continue to be high. Urbanization and development continue over the recharge zone, demands on water usage continue to increase, and Federal Endangered Species Act pressures for habitat and environmental protection have increased. Strong technical justification is needed that demonstrates the effectiveness of the protection measures applied in response to the Edwards Rules.

Initial research for identifying sensitive features has been done for the Edwards recharge zone. Quantitative measurement of the hydrologic function of selected Austin – area larger scale features such as caves and sinkholes with drains has been conducted by Hauwert and others (2005). The work of Veni (1999) is focused on the problem of identification of sensitive features; however the published work is restricted to the Camp

Bullis area. George Veni (personal communication, 2001) believes that more regional evaluation of his 1999 methodology (unpublished written communication) is needed to make it regionally applicable. A revised version of "Instructions to Geologists" (Hovorka, 2001c), recommended simplification of the assessment procedure from the previous TCEQ method and from Veni's procedure. Geologists with knowledge and experience regarding recharge to the Edwards aquifer expressed general satisfaction with the revised assessment methodology (stakeholders meeting, June 22, 2001, written record), and a field test suggests that it can be applied rapidly and consistently (field office review meeting, November 7, 2001).

This follow-on study (Lindley, 2005) undertakes a quantitative assessment of the hydrologic function of some of the smaller features which traditionally have been considered "possibly sensitive". A separate study (Barrett) updates the BMP's

Linkage between groundwater protection and karst geomorphology

A geomorphic approach to assessment of recharge features is justified by an understanding of karst landform evolution. Groundwater flow in karst aquifers is genetically linked to the development of the landscape. Water is introduced to the aquifer from the surface through features that make up the karst landscape. The surface features and the aquifer evolve concurrently as fractures and conduits are enlarged by preferential dissolution increasing the overall aperture of fractures and conduits as well as the overall connectivity of the system. Surface features are able to transmit more water to the subsurface as they mature. Thus, the groundwater circulation system in karst aquifers is developed by the positive feedback from the dissolution within and at the surface of the host rock.

One of the main characteristics of karst aquifers is the open conduits that provide pathways for fast and direct recharge from the surface to the subsurface and discharge groundwater from the aquifer to the surface as springs. Conduits dominate flow through karst aquifers. Orders of magnitude difference in the hydraulic conductivity means that up to 90 % of the flow in a karst aquifer may be through conduits, with the matrix and other fractures providing only10% (White and White, 2001). Hovorka and others (1998) documented a similar relationship for the Edwards aquifer and published data on permeability from matrix samples, fracture properties and core diameters. Halihan and others (2000) modeled the permeability of fractures and conduits and found that conduit permeability is orders of magnitude greater than both fractures and matrix, thus, conduits most likely control flow in the Edwards aquifer. They also hypothesized that many wells intercept isolated voids that are unconnected with the regional conduit system and that well yields can be attributed to the intersection of fractures including bedding plane partings. With hydraulic conductivities of several orders of magnitude higher than the matrix or fractures, conduits provide a direct path to the aquifer for water or any contaminants contained in the water.

The vulnerability of karst aquifers to contamination is much higher than many other types of aquifers because of preferential flow paths from the surface to the aquifer

provide rapid recharge to the aquifer with minima opportunities for mitigation which can occur by contact with organic and soil. Preferential flowpaths include large-aperture karst features like caves and sinkholes in the uplands and open fracture zones and swallets in river and streambeds.

The most common karst feature in karst landscapes, including the Edwards aquifer recharge zone, are sinkholes. Edwards sinkholes are commonly subtle, soil-floored depressions that lack large-aperture open drains. Typically they are small (less than 3 meters in diameter) and shallow (less than 25 centimeters in depth). Though Edwards sinkholes have little topographic relief, their karst origin through the feed back mechanisms described suggest the likelihood that they are interconnected with other karst features through the complex upper few meters of the soil and bedrock known as epikarst, and may have connection to larger karst conduits and to the aquifer at depth. Other types of small-aperture karst features that occur in the uplands include solution cavities and soil filled solutionally enlarged fractures.

Maintenance of depressions suggests that soil is removed as a result of transport from the bottom of the sinkhole, a process known as sapping. Soil removal is evidently more rapid than infilling of the depression, however, the implications of this soil transport for hydrologic function of small sinkholes was unknown prior to this study.

Geologic setting of the study area

The Edwards aquifer (figure 1) is separated into the Barton Springs segment on the north and the San Antonio segment by a groundwater divide in Hays County. Flow trends to the northeast in the Barton Springs segment and discharges into Barton Springs. In the San Antonio segment, flow is generally east in counties west of San Antonio, then northeast, discharging in Comal and San Marcos Springs.

The Edwards aquifer of south-central Texas is developed in the Lower Cretaceous Kainer and Person Formations of the Edwards Group along the Balcones Fault Zone, and significant influence of the stratigraphy and structure is noted The Edwards Group consists of generally thick bedded limestones and dolostones, with minor beds of argillaceous limestone and calcareous shale. The Balcones Fault Zone, is a zone of extension with a width of 50 kilometers (30 mi.), which has displaced the top of the aquifer downward more than 1965 meters (6450 ft.) (Collins, 1987; Collins and Hovorka, 1997) Throws on individual faults are as much as 260 meters (850 ft.) and a down-to the coast displacement is prevalent, though grabens are common. Faults and associated fractures are high angle. Opening mode fractures associated with regional faults are parallel to the regional fault trend.

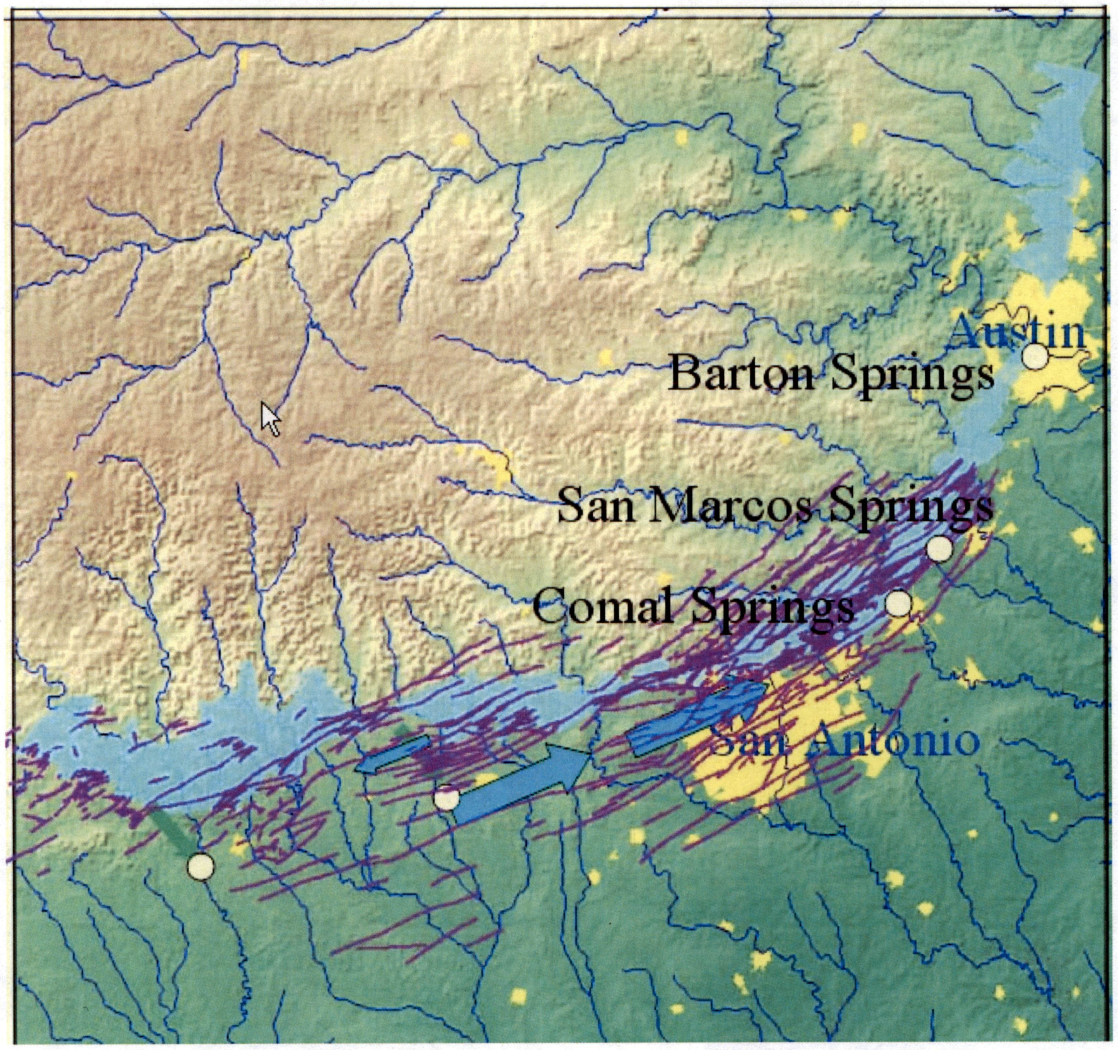

Figure 1. Map of the Edwards Aquifer showing recharge zone, Balcones fault system, major urban areas, and major springs.

Uplift on the Balcones Fault Zone has created a regional topography, which gives the name Balcones to the principle escarpment. Outcrop of the Edwards Group forms the recharge zone, which occurs at 490 meters (1600 ft.) in the northwest. In the southern and eastern parts of the recharge zone, the Edwards aquifer is overlain by weak, low transmissivity rocks, creating artesian conditions in the aquifer, and freshwater flow through a highly transmissive karst conduit systems extends to depths of more than 915 meters (3000 ft.) below sea level. Karst piracy has diverted flow in the whole aquifer system from western highlands toward eastern spring discharge points (Woodruff and Abbott, 1986).Deep dissection along major eastward flowing rivers has intersected pathways which supply to major springs that discharge at low elevation. Upland plateaus and moderately hilly areas lie between major streams (figure 1).

Regional orientation of lineaments studied on aerial photographs in the southern Edwards Plateau show lineaments related to two fractures sets, one of short incidence, up to 4.5 km, and one of long incidence, up to 160 km (Wermund and others, 1978). Approximately 400 lineaments were identified in each of the almost 200 aerial photo mosaics of the Balcones Fault Zone and the Edwards Plateau. The Balcones Fault Zone is an area of extensive faulting with associated fractures. Caves in the Edwards and underlying Glen Rose in this region were found to have passage segments that are oriented in a direction similar to that of both short and long fracture sets. Veni (1994) studied the bearings of 40 joint-guided passage segments in 23 caves in the southwestern Edwards Plateau to determine the orientations more prone to development. Though two trends showed the greatest development, the values were not high enough to be considered statistically significant.

The geologic setting described here was used as context to describe karst features at the site scale.

Recharge in the Uplands

The majority of recharge in the Edwards aquifer occurs via karst features in creek bottoms and streambeds. Water balance studies Barton Springs segment (Slade and others, 1989) estimate that 85% of recharge occurs in creeks and streams. The remaining recharge can be focused as discrete points or diffuse. A year-long water balance study for an internally drained microbasin in the Barton Springs segment showed that 42% of the precipitation that fell within the microbasin recharged the aquifer, 33.5% as diffuse recharge and 8% as discrete recharge. With internal drainage microbasins comprising 10% of the area of two subsegments and assuming all microbasins recharge 42% of precipitation, it was estimated that these features contribute the equivalent of 5% of the total discharge of Barton Springs (Hauwert, and others, 2005) Similarly, field tests using simulated rainfall over two caves in the San Antonio segment (Gregory and others, 2005) show that recharge via caves, while variable, may still account for a significant amount of recharge. One of the caves tested showed that nearly 4% of the total water applied to the cave footprint recharged through the cave, while the other cave tested showed that under natural conditions, a minimum of about 64% of the rain calculated to fall over its footprint recharged the cave.

The uplands of the Edwards aquifer recharge zone are currently undergoing development. Houses, streets, water and sewer lines associated with this development may introduce water quality risks to the aquifer if they bring poor quality water to recharge features. Figure 2 shows typical development in the uplands in which a housing development, Circle C Ranch, has been built in the recharge zone, in green, near a karst preserve, J17 Fortune Tract. This type of upland development is currently underway near the large urban areas of San Antonio, Austin, San Marcos, and New Braunfels on the Edwards aquifer recharge zone in central Texas. Urban development near karst features may present risks to water quality if degraded quality water from houses, streets, and water and sewer lines is rapidly introduced into the aquifer.

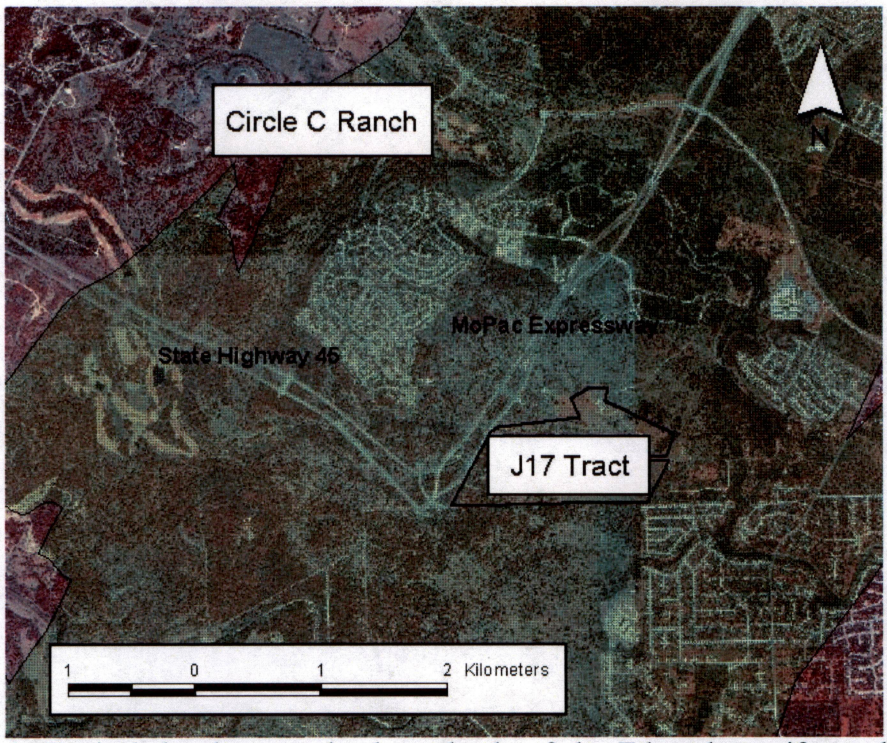

Figure 2. Typical development in the uplands of the Edwards aquifer recharge zone (green area). Note the proximity of developed areas to the karst preserve J17 Fortune Tract which was part of this study.

Large-scale features and those with clear hydrologic function such caves and sinkholes with obvious drains can be protected from development by Edwards Rules. This study is focused on the hydrologic function of the abundant but small sinkholes are protected under the Edwards Rules. These small soil lined features have previously been classified as by geologic assessments as "possibly sensitive" leaving doubt about the need for a BMP or if needed what the appropriate BMP should be.

Experimental Methods

Out test method to assess the hydrologic function of karst features was to directly measure the infiltration. Because the microtopographic features of interest are small, we elected to use a large-diameter single ring infiltrometer to enclose the sinkhole. In order to determine if infiltration was “rapid”, defined as an order of magnitude above background, we also measured the permeability of the background areas showing no geomorphic evidence of local karst features. Higher-than-background infiltration is evidence that the geomorphology is linked to recharge function. If these features indicate similar or lower infiltration characteristics than background, then at the present stage in their development, these features lack the high vertical permeability zone or the fractures or conduits that make up this zone are effectively clogged by clay soils.

Field Sites

Four field sites were selected in this study representing the Barton Springs and San Antonio segments of the Edwards aquifer: J-17Fortune Tract, Rutherford Ranch, Honey Creek Natural State Area, and Camp Bullis (Figure 3). These sites were selected because (1) they are representative of the recharge zone (2) previous geologic assessments had located a typical number of sensitive and possibly sensitive features (3) they are public for which access (including limited excavation) could be gained, (4) they had roads so that the water needed for the test could be delivered, and (5) they were in normal pre-development conditions (previous land use was ranching).

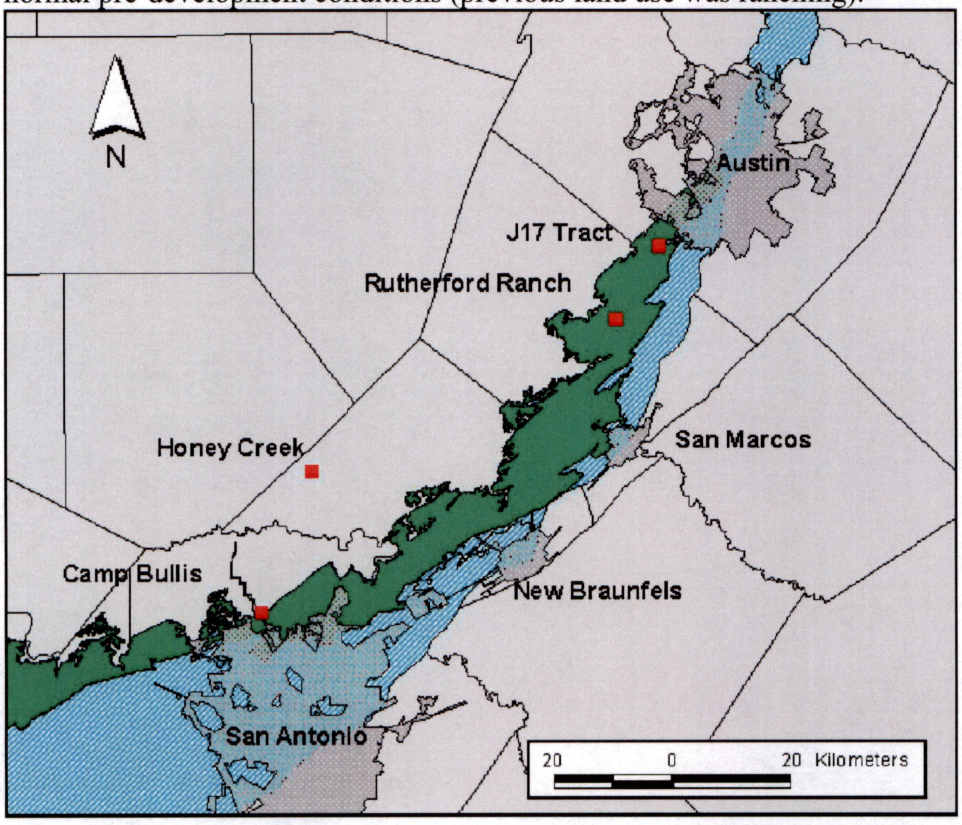

Figure 3. Site location map. The J17 tract and Rutherford Ranch are located within the Barton Springs segment of the Edwards aquifer, while Camp Bullis is located in the San Antonio segment. Honey Creek Natural State Area is not located within the recharge zone.

Rutherford Ranch and the J-17 Tract are part of the Water Quality Protection Lands Program managed by the City of Austin Water Utility. J-17 is located in southwestern Travis County and Rutherford Ranch is located in northern Hays County. Outcrops at both locations are both Kainer and Person Formation outcrop. Five upland

sinkholes were tested at the J-17 tract with four background plots. One solution cavity excavated by cavers shortly before the survey was also tested at the J-17 Tract. Four upland sinkholes and their associated control plots were tested at Rutherford Ranch. Both the J-17 tract and Rutherford Ranch are situated within the Barton Segment of the Edwards aquifer.

Honey Creek Natural State Area is located along the border of Comal and Kendall Counties adjacent to the Guadalupe River State Park. One sinkhole, one control plot, and the area around a juniper tree were tested. Although not in the Edwards aquifer recharge zone, studies at the Honey Creek Natural State Area were conducted in order to test the feasibility that vegetation may be a more influential factor than karst features in enhancing recharge over a broad area. Studies here also help assess possible scale effects by comparing ring infiltrometry results with data from a nearby large-scale rainfall simulation infiltration project conducted by the Biological and Agricultural Engineering Department at Texas A&M.

Camp Bullis is a 1,200-acre military base located north of San Antonio in Bexar County. Kainer Formation crops out in approximately 300 acres in the southeastern portion of the base, and are located within the San Antonio segment of the Edwards aquifer. One sinkhole and one control plot were tested. At each of the sites included in the study there are numerous large and small aperture karst features. The most common large aperture karst features encountered at the sites are caves. Most of these caves have little or no drainage area, though a few with large (multi-acre) closed drainage areas in the uplands or located in the streambeds do occur; which may capture a significant amount of recharge to the aquifer.

The dominant soil types at the field sites, Speck stony clay loam (SsC) and the Rumple-Comfort association (RUD), are described in the Travis County and Comal and Hays County Soil Surveys as having a permeability range of 0.1524 – 0.508 cm/hr (or 0.06 – 0.20 in/hr). The Soil Conservation Service estimates these permeability ranges for based on the structure and porosity of the soil. Typically these soils are thin, generally 35 to 50 cm, with 35% to 85% rock fragments (Werchan and others, 1974). The Speck stony clay loam is described as slow saturated transmissivity, or slow infiltration rates when wetted. Permeability for the Rumple-Comfort association is described as moderately slow in the Rumple and slow in the Comfort, yet is well drained, with a medium amount of surface runoff (Batte, 1984).

Identification of Sinkholes

Initial surveys of potential sites were conducted by walking transects across the property to identify potential geomorphic features for study, the same method used for geologic assessment. Although some sites had undergone previous assessments, we started fresh, so to provide a baseline. We focused only on the small features, and excluded from this test program large features such as caves, into which one could discharge large volumes of water and which be clearly assessed as sensitive following the "Instructions to Geologists". Candidate small features are identified by their closed bowl

shape, though in many cases they are difficult to see due to vegetation. Some features were discovered when they were walked into, and the shape and extent of the depression was determined by feel. Potential features were inspected more closely for more organics in soil and indicators of flow into the depression to determine whether they might have hydrologic significance. The setting was examined to attempt to screen out any depressions that are the product of previous land management, for example excavated animals, livestock, tree removal, or other human activities. Features and their associated control plots were given a feature identification number that included an abbreviation of the site name, feature type, and number. For example, RRSH4 indicates the site, Rutherford Ranch, the feature type, sinkhole, and identifying number 4. Basic descriptive characteristics of the candidate features were cataloged including their location, obtained using GPS, dimensions, diameter and depth, soil cover, type and color, and setting.

J-17 tract Barton Springs segment

The five sinkholes studied at the J-17 Tract are small soil-lined features with little topographic relief. J17SH1, J17SH2, and J17SH6 and their control plots are developed in the Person Formation, while J17SH3 and J17SH4 and their associated control plots and J17SC1 are developed in the Kainer Formation.

A contrast in the vegetation initially prompted a closer inspection of the area where J17SH1 was discovered. J17SH1 is approximately 6 feet by 5 feet, with a depth of 4 inches. It is elongated in to the northwest and is one of three sinkholes that form a complex that trend N38W. No evidence of rapid recharge, i.e. vegetation bent towards the sinkhole or an abundance of leaf litter, was observed upon initial inspection of the feature. The soil in and around J17SH1 consists mainly of a grayish brown clay loam with some organic detritus.

J17SH2 is 5 feet in diameter and 10 inches deep. A large prickly-pear cactus growing in the sinkhole was subsequently removed so infiltration tests could be conducted without complication by vegetation. The loose clay loam soil has an abundance of organic detritus, and there was no direct evidence of flow into the sinkhole. Few rounded, fist-sized cobbles were found at the surface of the sinkhole and around the feature in the immediate subsurface.

J17SH3 is 6 by 5 feet and 6 inches deep, with soil consisting of clay loam and organic detritus. Fist-sized, rounded cobbles were observed around the rim and base of the bowl at the surface and in the immediate subsurface.

J17SH4 is 5 by 4.5 feet and 8 inches deep. It is elongated in the NNE direction.

J17SC1 is a solution cavity with an opening that is 4.5 by 3 feet, elongated along a N55W trend. Photographs taken by cavers prior to this study show that before excavation, this solution cavity was completely filled with a silty clay loam soil. At the time water was applied to the feature, it had been excavated to a depth of 4 feet that resembled a cylindrical shaft. Further excavations have increased its depth to approximately 6 feet, and have revealed a more horizontal component as the cavity widens on the east side.

J17SH6 is 7 by 4.5 feet, elongated in the east-west direction, and is 6.25 inches deep. Several large rocks are present at the surface around the rim of the bowl. No open drain or any evidence of rapid flow to the sinkhole was detected.

Rutherford Ranch Barton Springs segment

Four sinkholes and their associated control plots were studied at Rutherford Ranch. RRSH1, RRSH3, and RRSH4 are developed in the Grainstone Member of the Kainer Formation, Edwards Group limestone, while RRSH2 is developed in the Leached and Collapsed Member of the Person Formation, Edwards Group limestone.

RRSH1 is a broad, 8 by 8.5 foot shallow, 5.75 inch deep, sinkhole that was initially identified by a contrast in vegetation. Within the sinkhole, low grasses and lush green plants were common and desiccated algae were observed, while the surrounding area consisted mainly of waist-high plants and less lush grasses and no algae.

Two larger features are located approximately 20 meters southeast of RRSH1, both distinguished by the vegetative contrast. RRSH2 is a relatively large sinkhole with a diameter of approximately 25 feet. A large prickly pear cactus was removed from the sinkhole to facilitate the initial survey and infiltration tests. The base of the bowl contains an obvious drain filled with fist-sized angular cobbles. A three-foot-long soil probe was inserted into the drain to a depth of 2 feet. Leaf litter accumulated near the drain and vegetation bent in the direction of the drain indicate rapid flow into the feature. It was previously identified in a 1999 Geologic Assessment by SWCA, Inc., Environmental Consultants and given the identification S-13, however, it will be referred as RRSH2 in this report.

RRSH3 and RRSH4 are two of a complex of four sinkholes that trend WNW. RRSH3 is 7.5 by 6 feet and 7 inches deep and has fist-sized cobbles in the base of its bowl. RRSH4 is 7 by 5.5 feet and 6 inches deep with weathered rocks at the surface and in the subsurface. Soil for both of these features is dominated by clay loam with some organic detritus.

HCSH1 is 7 by 4 feet and 6 inches deep. It is elongated to the NNE along a fracture zone that trends in the same direction and has several well developed solution cavities and many solution enlarged fractures. There were several 2 to 3 inch diameter rocks near the base of the bowl and the dominantly clay loam soil is between 2 and 8 inches thick over solid bedrock.

HCJP1 is the area enclosed by the ring that surrounds a 20-foot tall ashe juniper. A mat of juniper leaf litter 4 inches thick surrounds the tree above the loose very dry clay loam soil. Roots and large rocks are common in the subsurface.

One sinkhole and its associated control plot were tested at Camp Bullis. This sinkhole was identified previously by Joe Ivy and George Veni in 1993 and was named 11B-83. It is 6.5 feet in diameter and 8 inches deep. In this report, this sinkhole is referred to as CBSH1 for consistency.

Hydrological Examination of Sinkholes

To determine the local recharge characteristics of sinkholes, a ring infiltrometer is the tool of choice. A ring infiltrometers consist of a cylinder constructed of impermeable material, i.e. metal, which is driven into the ground in order to ensure that water applied will infiltrate the area enclosed. The volume of water added to maintain a constant water level, and the time are recorded in a constant head test, while in a falling head test the time required for a volume of water to infiltrate, thus an initial head and a final head, is recorded. Single ring infiltrometers include only one cylinder, while double ring infiltrometers require nested rings in order to control lateral spread of water.

In unsaturated soils, capillary pressure and gravity both influence the movement of water applied to an area enclosed by a ring infiltrometer. This causes the wetting front to move vertically downward as well as laterally (Dingman, 2002). When water is applied to the area enclosed by both rings, the area between the larger and smaller ring acts as a buffer, so the infiltration rate measured in the smaller inner ring describes the vertical component rather than infiltration due to capillary action horizontally. In a single ring infiltrometer, lateral leakage will occur, but the effects are minimized by increasing the size of the ponded area. Thus, using a large-scale ring reduces the error expected from horizontal flow.

Constant head and falling head are the two main methods used to determine the infiltration rates using ring infiltrometry. Falling head tests involve measuring the amount of time required for a volume of water applied to an area to infiltrate. In a constant head test, the amount of water required to maintain a set water level is recorded as well as the time of application.

Ring infiltrometers are used to measure infiltration in a wide variety of situations. Under normal circumstances, ring infiltrometers are used to determine the infiltration parameters in soils for effective soil, water, and crop management not to determine the infiltration characteristics of large areas. Common ring infiltrometers are small, which allows them to be transported easily in the field and require small amounts of water to conduct each test. It is likely that the logistical problems associated with transporting the large volumes of water required to conduct large-scale ring infiltrometry experiments to field sites is one of the reasons sinkholes have not been studied previously using this technique.

Guelph permeameters can also be used to determine the in-situ unsaturated hydraulic conductivity in soils. This type of instrument also uses the constant head method to determine infiltration characteristics. It is easily transported and operated by one person in the field and requires a small amount of water. The downside to using this type of permeameter is that the area where water is applied to the unsaturated soil is small; accordingly, it is more likely that many of the expected heterogeneities in the soil and bedrock in a sinkhole will not be observed.

There are a few differences between using a ring infiltrometer for testing soils versus karst features. First, the infiltration rate of the sinkhole is limited by the capacity

of any overlying soil to transmit water to the zone of high vertical permeability. That is, any soil that covers a drain in a sinkhole may effectively clog the preferred pathway and the infiltration rate for the feature will be the same as that of the soil. Second, though the infiltrometer gets an average infiltration rate for everything contained within the ring, there are likely to be a wide range of heterogeneities within the soil and bedrock that will dominate flow. To determine the function of sinkholes, it is necessary to test non-karst control plots to determine whether or not the heterogeneities found in the topographic depressions of sinkholes are unique to the sinkholes or if they are common all over the landscape. Therefore, comparing the infiltration per (L) unit head for sinkholes with that of control plots will lead to a relative understanding of infiltration in each scenario.

Infiltration is the process by which water enters the subsurface. An infiltration rate is the time required for a volume of water to enter the subsurface. Sinkhole infiltration is the process by which water enters the subsurface via features of a sinkhole, for example preferential flow through fractures or conduits, and can be defined as a rate, by the time required for a volume of water to enter the subsurface through these features. Infiltration is a function of the initial volumetric water content of the soil (volume of water in the soil/volume of soil). To ensure that the sinkhole infiltration rate is being accurately separated from the soil water content, the soil must be saturated, and the maximum rate of infiltration of the soil (infiltration capacity) exceeded. When sinkholes are not present, and the water input rate exceeds the infiltration capacity, ponding will occur. Where sinkholes are present, and the water input rate exceeds the infiltration capacity of the soil, infiltration via features associated with sinkholes will occur, and the rate of infiltration can be measured. Four factors that must be quantified in order to determine the sinkhole infiltration capacity include: the volume of water added V (L^3), the time required for infiltration to occur t, the area on which the water is added A (L^2), and the depth of ponding, or head h (L).

These four factors may be quantified by conducting a constant head ring infiltrometer test. The setup for this study is shown in figure 4.. The ring is inserted into the ground to minimize lateral leakage by digging a trench to match the circumference of the ring and packing it with bentonite. Water is then added to the enclosed area and is allowed to pond. Water is continually added to the area in the ring to maintain a continuous level of water within the ring, or constant head with reference to a fixed measurement point A paddlewheel flow meter (Omega model #1521) is used to determine the rate (V/t) that water is added to the ring, which is controlled by manually opening or closing a ball valve. The flow meter is connected to a datalogger that is programmed to record the volume of water introduced to the ring and the time at 10-liter intervals every 5 seconds. The area on which water is applied is the area of the ring, which is π times the square of the radius of the ring (L^2). Thus, by dividing the volume per time by the area, a sinkhole infiltration rate is achieved (L/t). This sinkhole infiltration rate is then divided by the head, resulting in an infiltration per (L) unit head that is normalized by the depth of ponding.

Figure 4. Typical ring infiltrometer installation.

IR = (Volume of water added (L^3) / Area of ponding (L^2) * *time*) / Depth of ponding (L)

It is necessary to conduct experiments that will test the entire feature as defined by topography, so that all of the local heterogeneities in the soil and bedrock of the feature are accounted for. Conducting large-scale ring infiltrometer experiments determines the hydrologic properties of the whole system of soil and bedrock within the ring, which is necessary to determine the function of karst features whose fractures, conduits or preferential flowpaths are concealed by the overlying soil and may cover broad areas. Thus, a 9-foot or 12-foot diameter ring is used to ensure that the whole feature is being tested. Experiments are generally several hours in duration, which limits the impact caused by disturbances in the soil where the ring is inserted as well as the effects of lateral leakage, resulting in a more accurate infiltration rate for the area tested.

Two different set ups are used to conduct the ring infiltrometer experiments. Both systems are designed to ensure constant head on the feature/area of interest; the only difference is in how the water is supplied to the ring. The first setup uses an 1800-gallon water truck as the water supply reservoir, while the second involves pumping water from a 1000-gallon collapsible water tank to an elevated 55-gallon drum. Water supplied from

either of these two reservoirs is ultimately gravity fed through a flow control section, where the paddle wheel flow meter is affixed, and into the ring. The flow control section is required to reduce turbulence and maintain laminar flow both up and down gradient from the paddle wheel, and is a 10-foot length of 2-inch diameter PVC up gradient and an 18-inch length of 2-inch diameter PVC down gradient from the flow meter.

Morphological Examination of Sinkholes

Microtopography and soil thickness surveys were conducted for tested sinkholes and soil thickness surveys were conducted for control plots in order to better characterize the epikarst system at each location. These surveys were conducted by laying out a grid with a one-foot by one-foot spacing and taking elevation and soil depth measurements at the intersections of rows and columns within the grid. String wrapped around four posts that mark the boundaries of the grid were leveled using a line level, creating a datum from which topographic information could be measured. Soil thickness measurements were obtained by measuring the depth a soil probe could be pushed into the soil along the one-foot intervals of the grid. Microtopography and soil thickness measurements were transferred to a spreadsheet as Z coordinates with X and Y coordinates obtained from their respective positions in the grid. This information is then imported to Surfer 7.0, a software package that displays topography as a three dimensional wire frame surface and creates contour maps of the soil thickness that is then draped over the three dimensional surface.

Ground Penetrating Radar

The use of GPR has been used extensively in areas of karst to detect major structural and solution-formed features in the subsurface. Bedrock, cave, medium and large sinkhole detection and mapping studies have proven GPR a quick and inexpensive method for determining the degree and extent of karstification in the subsurface (Chamberlain and others , 2000; Collins and others, 1994; Barr, 1993; and Benson and Yuhr, 1987). Ground penetrating radar surveys across sinkholes and control plots at the J17 tract were conducted during wet and dry conditions, to explore the geometry of the soil and bedrock as well as the distribution of water during artificial recharge. GPR data was collected for J17SH6 both before and 24 hours after water was applied. A SIR3000 GPR transmitter and 200Hz antenna was drug over the surface of features and along perpendicular transects using the geology scan function. The data obtained from the GPR surveys were processed using two software packages: Seismic Processing Workshop and RADAN, which allowed the data to be viewed graphically.

Dye Tracing

The introduction of dye to the subsurface allows preferential flowpaths to be identified after excavations. Dye was allowed to infiltrate two sinkholes at the J17 Tract - J17SH2 and J17SH6. Initially, 200 gallons of water were used to wet the feature of

interest. FD&C Blue No. 1 (referred to as dye) is a FDA certified colorant commonly used as a food coloring. One and a half pounds of powered dye was mixed in a 100-gallon water tank with an attached agitator. Once mixed completely, the dye was pumped into the ring and allowed to infiltrate with an additional 200 gallons of water to help flush the dye into the soil. The excavation of dyed features entailed the removal of soil and loose rock down to the bedrock in the area previously enclosed by the ring. These subsequent excavations of these sinkholes allow the identification of preferential flowpaths where the blue dye is most visible.

Hydrometer Tests

The percent clay content of the soils at selected sinkholes and control plots was determined Soil samples were collected at several sinkholes and control plots to determine the percent clay content grain-size analysis.

Results

A few assumptions were made about the nature of sinkholes and single ring infiltrometers to simplify the experiments. The first assumption is that the region of highest vertical permeability in a sinkhole is located in the lowest part of the sinkhole bowl. The expectation is that there are solutionally enlarged fractures or conduits across the bedrock surface throughout the recharge zone, but sinkholes will form only in areas where these features are concentrated, and where the maximum transport of sediments and solutes occur, the greater the topographic relief. The second assumption is that the vertical permeability is greater than the horizontal permeability in the subsurface, and that lateral leakage under the ring is minimized with the use of bentonite.

Hydrological results

The results for ring infiltrometery for ten small sinkholes and their associated control plots using the ring infiltrometery method are presented in Table 1. J17SH2 and J17SH6 share a control plot due to their close proximity to one another. The miscellaneous feature results and their associated control plots tested using the ring infiltrometer method, including one medium sinkhole, one solution cavity, two excavated small sinkholes, and one juniper plot are presented in Table 2.

Table 1. Ring infiltrometry results. Infiltration rates normalized for depth of ponding.

Feature name	*feature type*	*Head (cm)*	*infiltration per (cm) unit of head (1/hr)*
J17BG1	Background	12.70	0.31
J17BG2	Background	10.16	0.24
J17BG3	Background	12.70	0.06
J17BG4	Background	10.16	0.21
RRBG1	Background	10.16	0.40
RRBG2	Background	10.16	0.18
RRBG3	Background	10.16	0.43
RRBG4	Background	10.16	0.25
HCBG1	Background	12.70	0.19
CBBG1	Background	9.53	0.89
J17SH1	Sinkhole	13.97	0.06
J17SH2	Sinkhole	30.48	0.15
J17SH3	Sinkhole	20.32	0.11
J17SH4	Sinkhole	22.23	0.20
J17SH6	Sinkhole	20.32	0.35
RRSH1	Sinkhole	16.51	0.08
RRSH3	Sinkhole	19.05	0.24
RRSH4	Sinkhole	20.32	0.29
HCSH1	Sinkhole	17.78	0.44
CBSH1	Sinkhole	17.78	0.35

Table 2. Ring infiltrometry results of miscellaneous features.

Feature name	*Feature type*	*Average infiltration rate (cm/hr)*
J17SH2	exc. Sinkhole	0.16
J17SH6	exc. Sinkhole	0.42
RRSH2	med. Sinkhole	5.69
J17SC1	solution Cavity	3.44
HCJP1	juniper plot	6.31

Morphological measurements

Sinkhole microtopography and soil thickness maps are presented in Appendix A. Soil contour maps created from soil thickness surveys has been draped over the three-dimensional wireframes to show the distribution of soils relative to elevation. Statistical information collected on each feature includes the average depth and average soil depth for sinkholes (Table 3), and the average soil depth for control plots (Table 4). The maximum topographic relief and the average depth of each sinkhole were used to calculate the infiltration per unit (cm) of head. One sinkhole, J17SH6, was not surveyed

and one sinkhole, CBSH1, was partially excavated prior the beginning of the study and therefore was not included in the table.

Table 3. Physical characteristics of sinkholes obtained by microtopographical and soil thickness surveys. Note: sinkhole J17SH6 was not surveyed.

	dimensions						
Feature Name	x (m)	y (m)	z (cm)	Average Soil Thickness (cm)	Average Depth (cm)	max length/max depth	Ratio (length:depth)
J17SH1	1.83	1.52	13.335	9.18	6.18	29.61	30 : 1
J17SH2	1.52	1.52	21.59	10.87	6.88	22.09	22 : 1
J17SH3	1.83	1.52	17.15	10.26	5.95	30.76	31 : 1
J17SH4	1.52	1.37	17.15	10.61	9.31	16.33	16 : 1
J17SH6	2.13	1.37	15.88			13.41	13 : 1
RRSH1	2.59	2.44	19.05	32.92	11.29	22.94	23 : 1
RRSH2	7.62	7.62	43.18	11.96	14.15	53.85	54 : 1
RRSH3	2.29	1.83	24.13	14.18	14.95	15.32	15 : 1
RRSH4	2.13	1.68	19.69	24.15	6.99	30.47	30 : 1
CBSH1	1.98	1.98	55.88	19.48	25.74	7.69	8 : 1
HCSH1	2.13	1.22	16.38	11.03	4.43	48.08	48 : 1

Table 4. Control plot average soil thickness.

Feature Name	Average Soil Thickness
J17BG1	12.28
J17BG2	13.72
J17BG3	19.85
J17BG4	17.55
RRBG1	22.48
RRBG2	10.92
RRBG3	17.78
RRBG4	31.07
CBBG1	8.19
HCBG1	4.67

Geophysical measurements

Processed radar profiles from one sinkhole at the J17 Tract are presented in Figure 5. All other sinkhole and control plot transects are presented in Appendix B. In each radar profile, the vertical scale is a time scale, and the horizontal scale is distance along the surface. Using the RADAN software package, profiles were surface normalized, color transforms were applied, and he range gain was set to one. The Seismic Processing Workstation software package was used to only to display the data with simple red and blue color transform.

Many of the perpendicular transects run over each of the sinkholes at the J17 Fortune tract have strongly attenuated signal and show no heterogeneities that might be interpreted as karst voids, with the exception of the north to south transect for J17SH1, shown in Figure 5. In this transect, the center of the sinkhole is located at the 20 ft. tick

mark, and the surface expression of the sinkhole extends three feet to either side of the center. The color transform selected using the RADAN software package shows areas of high dielectric contrast where white and gray are adjacent to one another. The high contrast shown in this transect signifies an abrupt change in the material in the subsurface which may indicate the presence of a void.

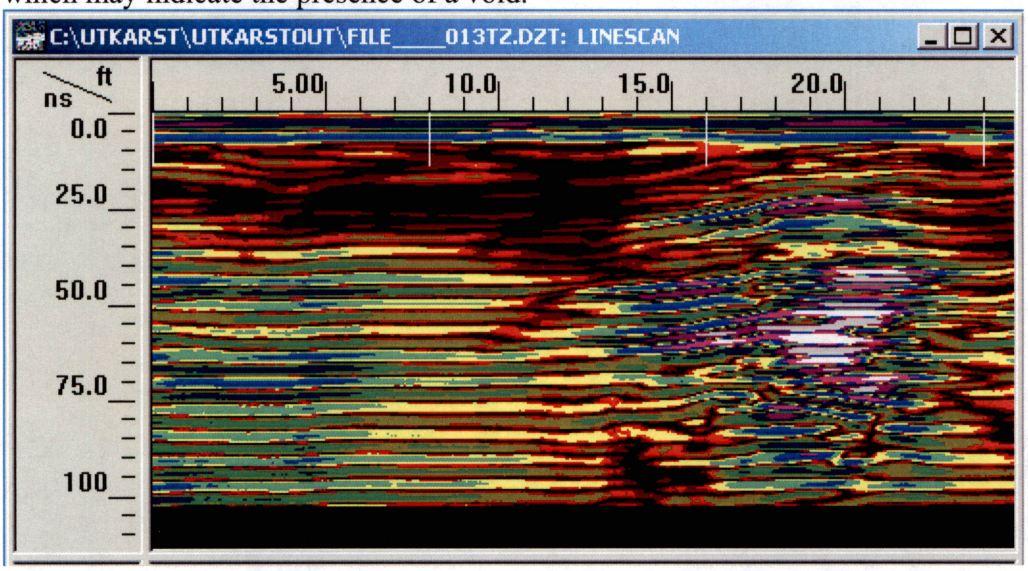

Figure 5. GPR image of the subsurface beneath J17SH1. Center of sinkhole is 20 ft. from left. High contrast in the dielectric is represented by white and gray, which may indicate a soil/air interface, indicating possible void.

Discussion

Many of the control plots have a somewhat higher infiltration per (cm) unit of head than their associated sinkholes when the variation in topography is ignored and the maximum depth of ponding is assumed as the base elevation from which head is measured. With this in mind, the results have been plotted in Figure 6 comparing the infiltration per (cm) unit head ($1/t$) of small sinkholes with paired control plots. The one to one line that bisects the graph separates the pairs of features as those in which sinkhole infiltration is higher than control plot, above the line, from those in which the infiltration of the control plot is higher than its paired sinkhole, lower than the line. The different symbols, diamond, square, triangle, and circle, represent the different field sites.

However, this may not represent infiltration under natural conditions. Under natural conditions, water will pond in the small soil-lined sinkholes. The variable topography between the flat lying land and the bowl of the sinkhole generates a continuum of head values within the bowl. For this reason, the average depth for a sinkhole is may be used to determine more natural representative infiltration

characteristics (figure 6). The average depth is calculated using data collected from the microtopographic survey and Surfer 7.0.

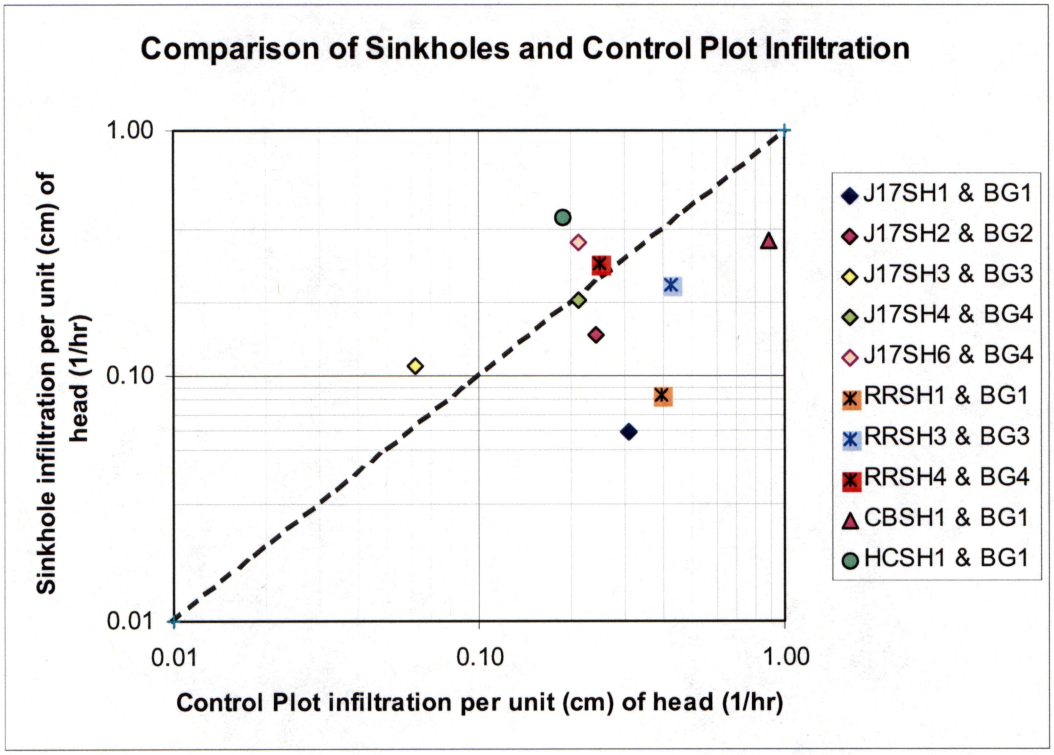

Figure 6. Infiltrometry results using maximum depth as applied head.

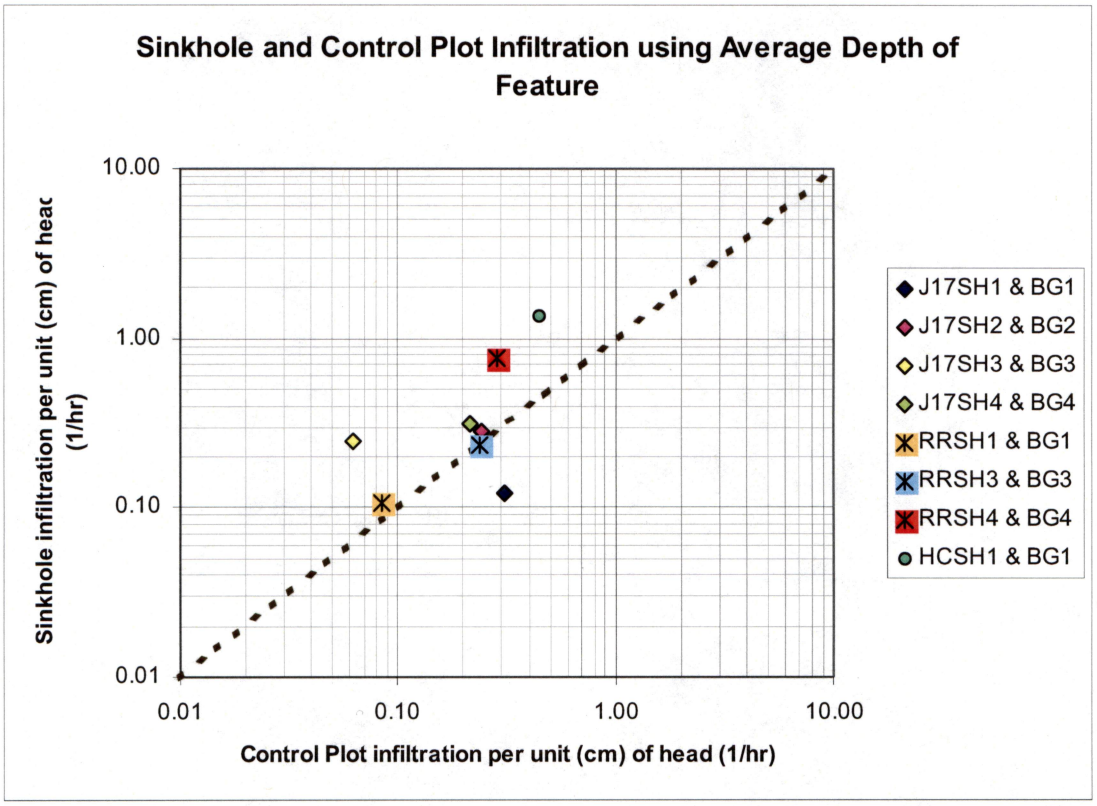

Figure 7. Infiltrometry results using average depth as applied head.

Using the average depth of sinkholes as the base elevation to calculate the amount of head applied seems to show a more normal distribution of infiltration values. These infiltration values more closely follow the one-to-one line, yet the sinkhole infiltration is slightly higher than paired control plots.

Miscellaneous features tested all had infiltration rates higher than their control plots (figure 8) thus; the one to one line is not displayed on the graph. It is important to note that the solution cavity tested had been partially excavated prior to ponding water on the feature. It is likely that the infiltration per (cm) unit of head would be lower if the feature had been tested prior to excavation, and it is also likely that the infiltration per (cm) unit of head would be higher if a cave is revealed after further excavations. Similarly, the medium sinkhole tested had a drain choked with small rocks and plant debris when tested. After a limited amount of excavation, a large open fracture was revealed and it is unlikely that water could be ponded over the feature using the ring infiltrometer method.

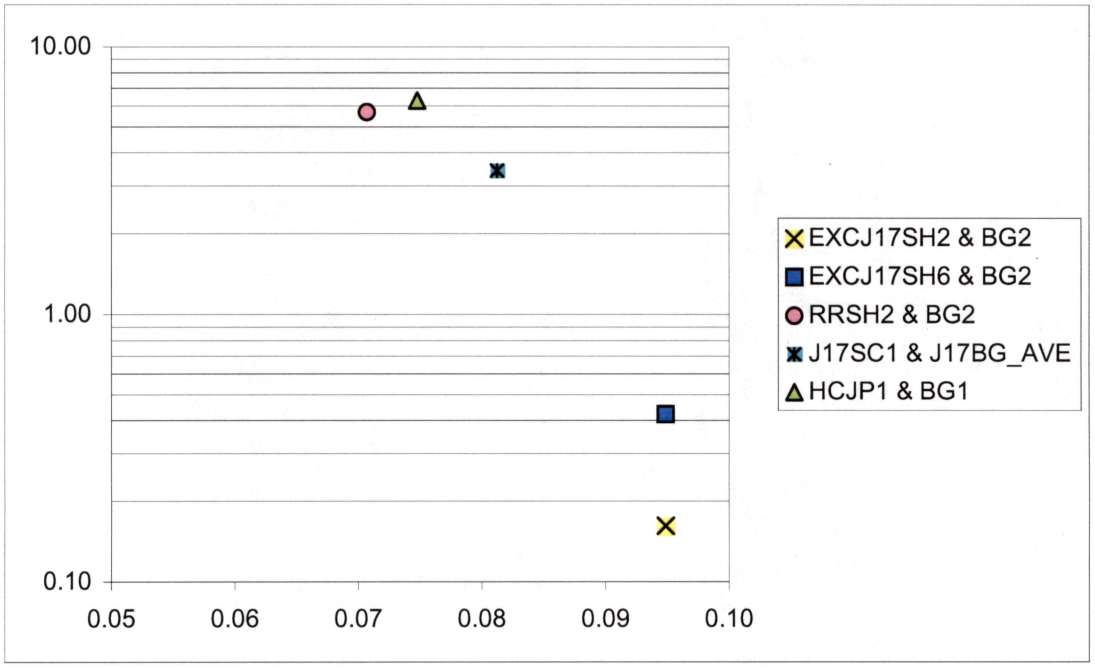

Figure 8. Miscellaneous feature infiltrometry results.

Although not in the Edwards recharge zone, features at Honey Creek Natural State area were tested. Rainfall simulation studies conducted by Clyde Munster and other A&M students indicated that recharge rates were significantly higher than the permeability range for the soils in the area (Gregory, L., July 2005: personal communication). Small sinkholes, solution cavities, and caves are common in the area. If soil is the factor that dominates the infiltration of small sinkholes in a karst terrain, then a similar relationship should be visible in the rainfall simulations. Rainfall simulations were conducted over a 7 by 14 meter area that contained several ashe juniper trees. The infiltration rates obtained by varying the intensity of simulated rain events over the juniper test plot ranged between 1 and 9.25 cm/hr.[1] These values are orders of magnitude higher than those obtained with the ring infiltrometer, thus it was deemed necessary to determine the reason for the large discrepancy. A nearby small sinkhole and control plot was tested using the ring infiltrometer to compare the infiltration characteristics obtained by the two methods. The resulting infiltration per (cm) unit head obtained for the sinkhole (0.44) and control plot (0.19) is comparatively low. Using the ring infiltrometer on an area that contained an ashe juniper tree revealed the source of the discrepancies. The infiltration rate obtained for the juniper plot using the ring infiltrometer method included a maximum value of over 10 cm/hr during the initial addition of water and an average sustained value, after the initial wetting of 6.31 cm/hr. Severe lateral leakage was observed 20 minutes after the experiment was initiated. Water began upwelling several

1

feet outside of the juniper plot around the ring. This may be the ponded water flowing through preferential flow paths created by the tree roots.

Dye tracing experiments and subsequent excavations of sinkholes served three purposes. First, observations of dye in the soil and on the bedrock provided clues as to what the dominant types of flowpaths exist in the near surface. Dye was observed mainly along plant roots small, grass roots, and large, cacti and small brush, and along the interface between rocks and soil in the subsurface. Second, due to low infiltration rates from ring infiltrometer tests, concerns arose that the depressions observed were not in fact karst features, but were the product of previous land management (for example depressions where stumps were pulled or pits dug.. Excavating sinkholes in order to look for the zone of high vertical permeability or drains helped allay these concerns, as fractures and solutionally enlarged vertical conduits were observed. After excavation of soil on the surface of the bedrock, dye was observed along fractures and around solutionally enlarged fractures and conduits (figure 9).Third, excavating these two sinkholes allowed further infiltration tests to be conducted with the soil removed. The resulting infiltration per unit heads is only slightly higher than when soil is present, which indicates drains that are plugged by soil in the subsurface. This may also indicate that active soil piping is occurring.

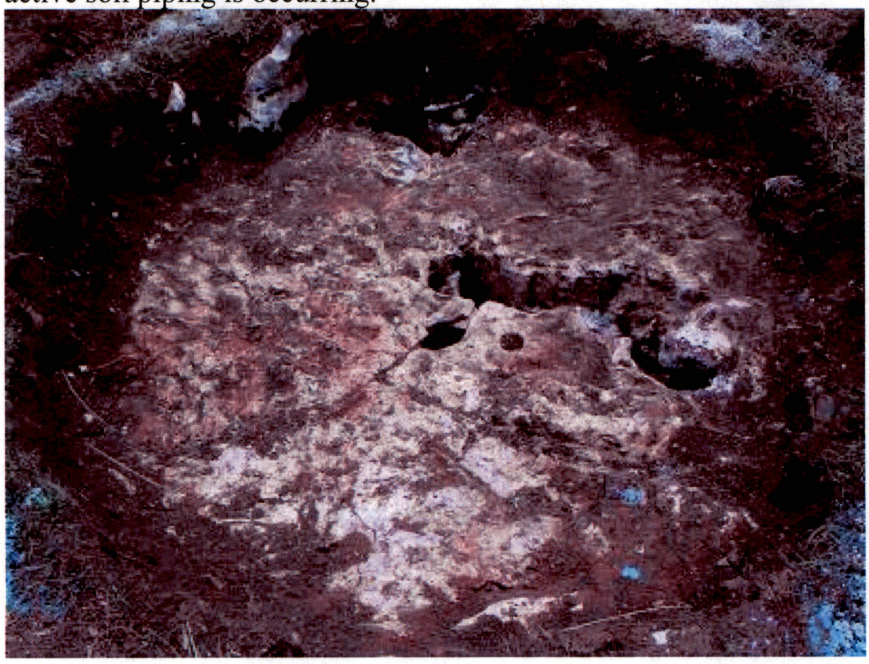

Figure 9. After completion of the GPR, infiltration, and dye tracing, soil was removed from beneath a sinkhole. Solutionally enlarged fractures and conduits document karst origin of small soil lined sinkholes and show the pathways where infiltration and soil sapping likely occur.

Ground penetrating radar results were somewhat mixed. One void is interpreted for the GPR data, and though there may be some evidence of karst features in the subsurface, much of the data shows banded areas where the radar signal has been attenuated. This attenuation of signal may be due to saturated conditions in the subsurface or reflect to the clay content in the soil.

Small karst features, like subtle sinkholes and fracture zones are ubiquitous across the Edwards recharge zone. Though they do not have large drainage areas, they exist in such numbers that collectively they may impact recharge in the uplands. In an assessment of recharge in arid environments, Scanlon and others (1999). concluded that, despite being clay filled, small subtle topographic depressions are the locus of high mean water fluxes based on mean chloride concentrations and high water potentials found in these features. We observe that during rainfall these small depressions pond water. Maintenance of the depression shows that soil remove focused in the depression is greater than soil erosion. Dye shows that recharge is focused in soil-filled solution-enlarged fractures within the sinkhole bedrock floor. Vegetation also suggests that small sinkholes are effective in focusing recharge. However, it is not clear if under natural conditions the recharge form the small sinkholes is a significant part of the water budget. One scenario worth considering is the effect of a spill or otherwise very degraded water introduced as a result of development, for example if a bar ditch was constructed through the features. Even if a feature naturally had a small function in terms of recharge, it might need protection from such an artificial introduction of pollution. Even when the surface soil was removed, infiltration was not enhanced at the two features tested. The clay soil plug in the solution enlarged cracks continued to retard infiltration, suggesting that these features at least would not serve as conduits even after the surface soil was modified.

Conclusions

Small sinkholes are ubiquitous in the uplands of the Edwards aquifer recharge zone where much of the urban development is currently taking place. These incipient features are examples of the early steps in the evolution of karst terrains.

Infiltration experiments conducted at a representative set of small soil-filled sinkholes show that these features do not provide rapid recharge to the aquifer, and therefore do not qualify as "sensitive features" under the Edwards rules. Even thin soil reduces hydraulic conductivity and recharge rate of the soil/bedrock system... Some of the tested small, soil-lined sinkholes recharge somewhat more quickly than background, and somewhat more sustained when ponding occurs, so they may be significant in upland recharge.. Excavation of the test features shows that although solution-enlarged karst features exist in the subsurface below small sinkholes, these fractures and conduits are plugged by the clay soil common in the uplands of the recharge zone. GPR over tested features did not locate significant voids in the subsurface.

The results of this test program should not be overextended to imply that these small soil-lined sinkholes are completely irrelevant with respect to transmission of contamination into the aquifer. Maintenance of numerous small sinkholes suggests that

active karst processes such as soil sapping are focused by karst and epikarst development. It is likely that these features experience cycles of soil-dominated infiltration when plugged and rapid infiltration when the plug is removed, only to become plugged once again when a choke develops further down in the drainage network. Experience of local karst experts shows that the excavation of some of these subtle features will lead to the discovery of more extensive karst features, including potentially enterable caves.

Subtle karst features are significant for recharge because of their maintained microtopography. Under natural conditions, small sinkholes pond water during rain events. As ponding occurs, the increase in head from ponding increases the infiltration per unit (L) head, allowing a larger volume of water to infiltrate to the subsurface. As there is little runoff and ponding rarely occurs at non-depressed areas, areas of little relief do not benefit from this increase in head.

It is also important that the results of this study for small soil lined sinkholes not be overextended to larger features and to those that have open (non-soil filled) drains, Documentation of the role of caves and closed basins in focusing recharge continues to grow. Karst connection between the land surface, the subterranean drainage network and the aquifer supports rapid and high volume recharge. Two of the features tested in this study show high infiltration typical of karst. A medium sized sinkhole with a gravel-filled drain had infiltration rates 10 times background and should be considered sensitive because recharge was rapid. After testing, excavation of the gravel revealed a large open conduit that was partially blocked near the surface. We also measured high infiltration at partially excavated large solution cavity, or well-shaped sinkhole that after further excavation, showed horizontal openings.

The last caution to be expressed in that rapid and high infiltration may occur at locations with no geomorphic indication of karst. One test area with no geomorphic evidence of cave or sinkhole but that contained an ashe juniper tree within the ring. highest infiltration rate of all the features studied. Other studies inside caves have measured cave drips with no surface indication of focused recharge. The geomorphic method of locating sensitive features provides no protection for these karstic recharge mechanisms except regional preservation of water quality.

Acknowledgements

This project was funded by the Texas Commission on Environmental Quality (TCEQ) and much of the work was completed as part of as a MA Thesis at the Jackson School of Geoscience by Adrien Lindley. Fieldwork for this project was greatly facilitated by assistance from Kevin Thuessen, Ph.D. and the City of Austin's Wildland Conservation Division, Lucas Cooksey of the Essex Corporation, George Veni of George Veni and Associates, Dr. Clyde Munster of Texas A&M University and Honey Creek State Natural Area. Technical and logistical assistance were provided by Robert Reedy (BEG), Cynthia Burton (Exploration Instruments), James Donnelly (CRC), and Steven Kelley (PRC).Dr. John M. Sharp and Dr. Jay Banner served as reviewers for the thesis which provides the data for this report (Lindley, 2005) .

References

Barr, G. L., 1993: Application of ground-penetrating radar methods in determining hydrogeologic conditions in a karst area, West-Central Florida. USGS Water Resources Investigations Report. 92-4141, p. 26.

Batte, C., 1984: Soil Survey of Comal and Hays Counties Texas. United States Department of Agriculture, Soil Conservation Service in Cooperation with Texas Agricultural Experiment Station, 136 p.

Benson, R. C., Yuhr, L., B., 1987: Assessment and long term monitoring of localized subsidence using ground penetrating radar. *In* Beck, B. F. and Wilson, W. L., eds., *Karst Hydrogeology: Engineering and Environmental Applications*. Proceedings of the Second Multidisciplinary Conference on Sinkholes and the Environmental Impacts of Karst. A. A. Balkema Publishers, Rotterdam, The Netherlands, 467 pp.

Chamberlain, A. T., Sellers, W., Proctor, C., Coard, R., 2000: Cave detection in limestone using ground penetrating radar. Journal of Archaeological Science, v. 27, p. 957-964.

Collins, E. W., 1987: Characterization of fractures in limestones, northern segment of the Edwards aquifer and Balcones Fault Zone, central Texas: Gulf Coast Association of Geological Societies Transactions, v. 37, p. 43-54.

Collins, E. W., and Hovorka, S. D., 1997: Structure map of the San Antonio segment of the Edwards aquifer and Balcones Fault Zone, South-central Texas: Structural framework of a major limestone aquifer: Kinney, Uvalde, Medina, Bexar, Comal and Hays Counties: University of Texas at Austin, Bureau of Economic Geology, Miscellaneous map 38.

Collins, M. E., Crum, M., Hanninen, P., 1994: Using ground-penetrating radar to investigate subsurface karst landscape in North-Central Florida. Geoderma, v. 61, p. 1-15.

Dingman, L. S., 2002: *Physical Hydrology*. Prentice Hall, Upper Saddle River. New Jersey, 646 pp.

Gregory, L., Veni, G., Shade, B., Wilcox, B., Munster, C., and Owens, K., 2005: Quantifying Recharge via Fractures in an Ashe Juniper Dominated Landscape. *In* Beck, B. F., and P. E. LaMoreaux & Associates, Inc. *eds. Sinkholes and the Engineering and Environmental Impacts of Karst*, Proceedings of the Tenth Multidisciplinary Conference: American Society of Civil Engineers, Geotechnical Special Publication No. 114, p.216 - 223.

Halihan, Todd, Mace, R. E., Sharp, J. M, 2000, Flow in the San Antonio segment of the Edwards aquifer; matrix, fractures, or conduits?: *in* Sasowsky, I. D. and Wicks, C. M., Groundwater flow and contaminant transport in carbonate aquifers, p. 129-146.

Hauwert, N. M., Litvak, M. E., and Sharp, J., M., 2005: Characterization and Water Balance of Internal Drainage Sinkholes. *In* Beck, B. F., and P. E. LaMoreaux & Associates, Inc. *eds.* Sinkholes and the Engineering and Environmental Impacts of Karst, Proceedings of the Tenth Multidisciplinary Conference: American Society of Civil Engineers, Geotechnical Special Publication No. 114, p.188-200.

Hovorka, S. D., Mace, R. E., and Collins, E. W., 1998: Permeability structure of the Edwards aquifer, South Texas—implications for aquifer management: The University of Texas at Austin, Bureau of Economic Geology Report of Investigations No. 250, 55 p.

Hovorka, S. D., 2001 a, Task 3 milestone: approaches for the recognition and management of sensitive features in the Edwards aquifer recharge zones: The University of Texas at Austin, Bureau of Economic Geology, milestone report prepared for Texas Natural Resource Conservation Commission, 42 p.

Hovorka, S. D., 2001 b, Task 1 milestone: draft bibliography on karst geomorphology and hydrology relevant to geologic assessment of recharge features in the Edwards aquifer interagency contract on evaluation of the geologic assessment of sensitive features: The University of Texas at Austin, Bureau of Economic Geology, milestone report prepared for Texas Natural Resource Conservation Commission, 10 p.

Hovorka, S. D., 2001 c, Task 5 milestone: instructions to geologists for geologic assessments on the Edwards aquifer recharge/transition zones: The University of Texas at Austin, Bureau of Economic Geology, milestone report prepared for Texas Natural Resource Conservation Commission, 34 p.

Lindley, Adrien, 2005, The hydrologic function of small sinkholes in the Edwards aquifer recharge zone; University of Texas at Austin, MS thesis, 111 p.

Scanlon, B., Langford, R., and Goldsmith, R., 1999: Relationship between geomorphic settings and unsaturated flow in an arid setting. Water Resources Research, v. 35, no. 4, p983 – 999.

Veni, George, 1987, Fracture permeability; implications on cave and sinkhole development and their environmental assessments, *in* Beck, Barry F., Wilson, William L. , Karst hydrogeology; engineering and environmental applications, University of Central Florida, Florida Sinkhole Research Institute, Orlando, FL: Proceedings Multidisciplinary Conference on Sinkholes and the Environmental Impacts of Karst, v. 2, p. 101-105.

Veni, George, 1994, Honey Creek Cave, Texas; in Elliot, W. R., and Veni, George eds, The caves and Karst of Texas; The National Speleologial Society 1994 convention guidebook, p. 175-187.

Veni, George, 1999, A geomorphological strategy for conducting environmental impact assessments in karst areas, Geomorphology, Volume 31, Issues 1-4, December 1999, Pages 151-180

Wermund, E. G., Cepeda, J. C., and Luttrell, P. E., 1978: Regional distribution of fractures in the southern Edwards Plateau and their relationship to tectonics and caves: The University of Texas at Austin, Bureau of Economic Geology Geological Circular, no. 2, 14 p.

Werchan, L., Lowther, A. and Ramsey, R., 1974: Soil Survey of Travis County Texas. United States Department of Agriculture, Soil Conservation Service in Cooperation with Texas Agricultural Experiment Station, 123 p.

White, William B., and White, Elizabeth L., 2001, Conduit fragmentation, cave patterns, and the localization of karst ground water basins: the Appalachians as a test case; Theoretical and Applied Karstology, 13-14, 9-24.

Woodruff, C. M., Jr., 1984: Water budget analysis for the area contributing recharge to the Edwards Aquifer, Barton Springs segment. *In* Woodruff, C. M., Jr. and Slade, R. M. Jr., *eds. Hydrology of the Edwards Aquifer-Barton Springs Segment*. Austin Geological Society Guidebook No. 6, Austin, Texas.

Woodruff, C. M., and Abbott, P. L., 1986: Stream piracy and evolution of the Edwards Aquifer along the Balcones Escarpment, Central Texas; in Abbot, P. L. and Woodruff, C. M., Jr. eds., The Balcones Escarpment, central Texas: Geological Society of America Annual Meeting, p 77-100.

Appendix A

Appendix A is the graphical representation of the microtopography for each sinkhole tested. All figures in appendix were created using the graphics software Surfer 7.0. Contour maps show the soil thickness obtained from soil thickness surveys and draped over wireframes depicting sinkhole microtopography indicate the distribution of soils over karst features. Contour maps for control plots are also included. All wireframes, contour maps and color scales are in centimeters.

SINKHOLES

J17SH1

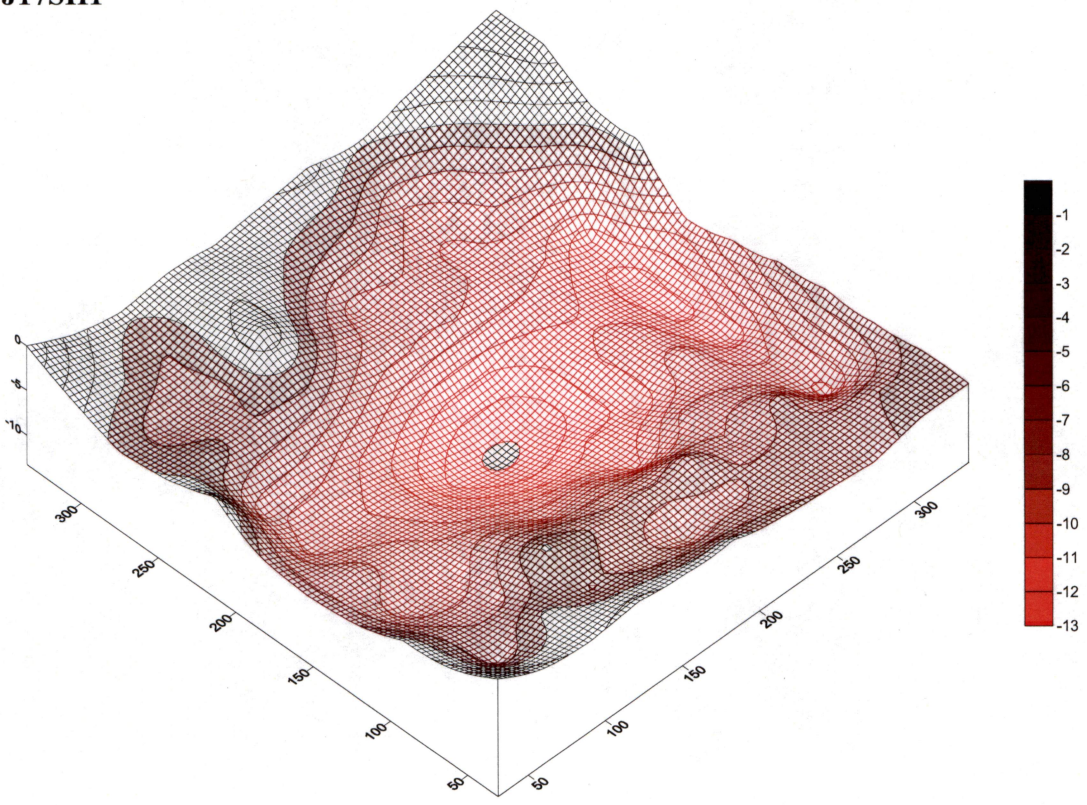

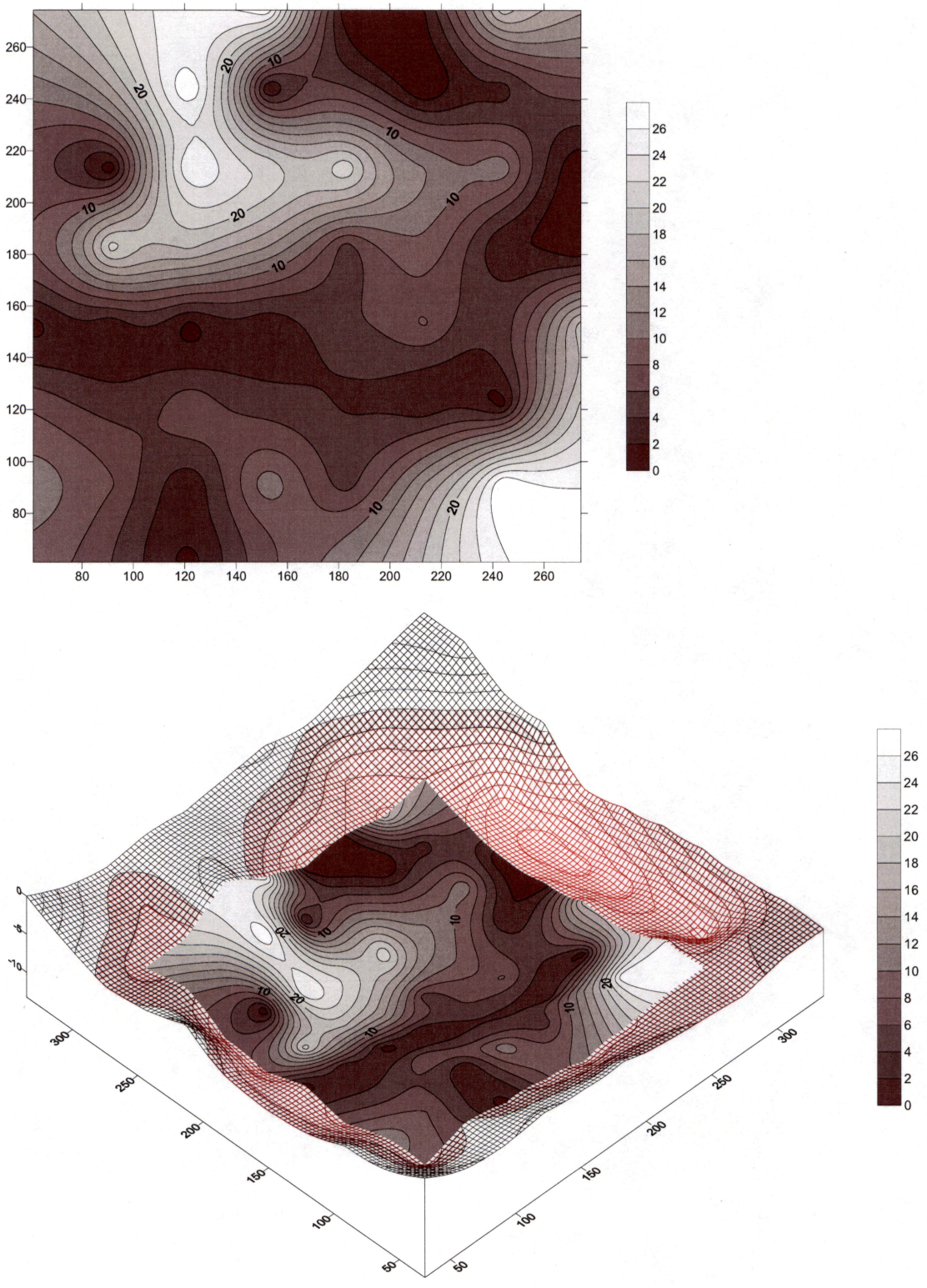
260
240
220
200
180
160
140
120
100
80
80 100 120 140 160 180 200 220 240 260
10
20
26 24 22 20 18 16 14 12 10 8 6 4 2 0
300 250 200 150 100 50

J17SH2

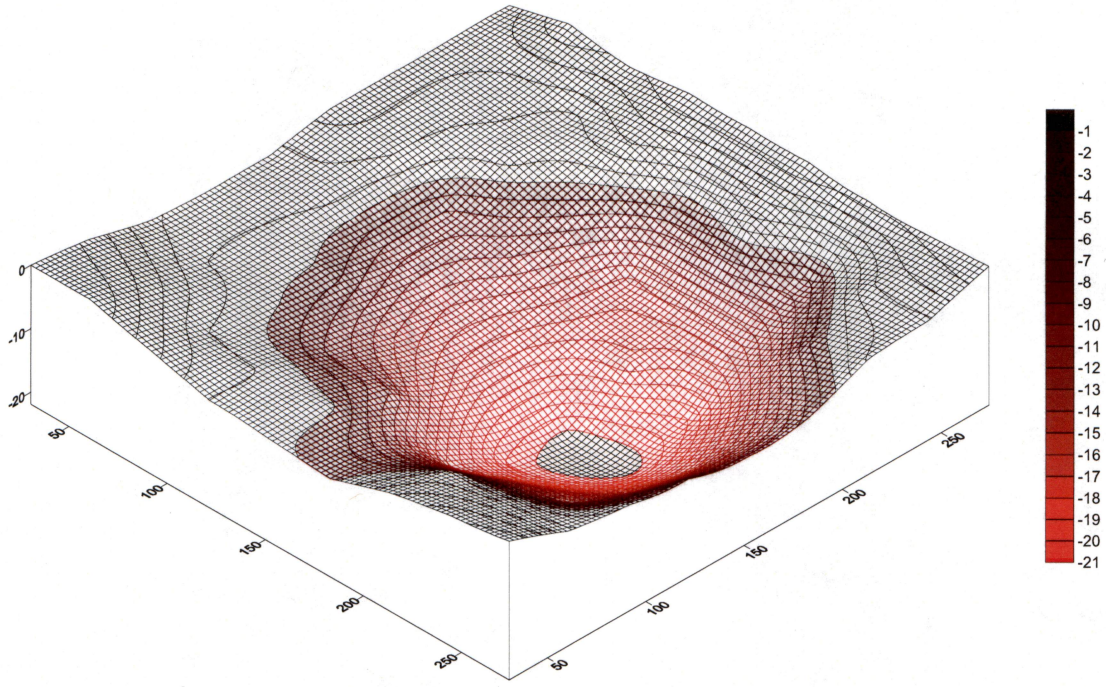
0
-10
-20
50
100
150
200
250
-1
-2
-3
-4
-5
-6
-7
-8
-9
-10
-11
-12
-13
-14
-15
-16
-17
-18
-19
-20
-21

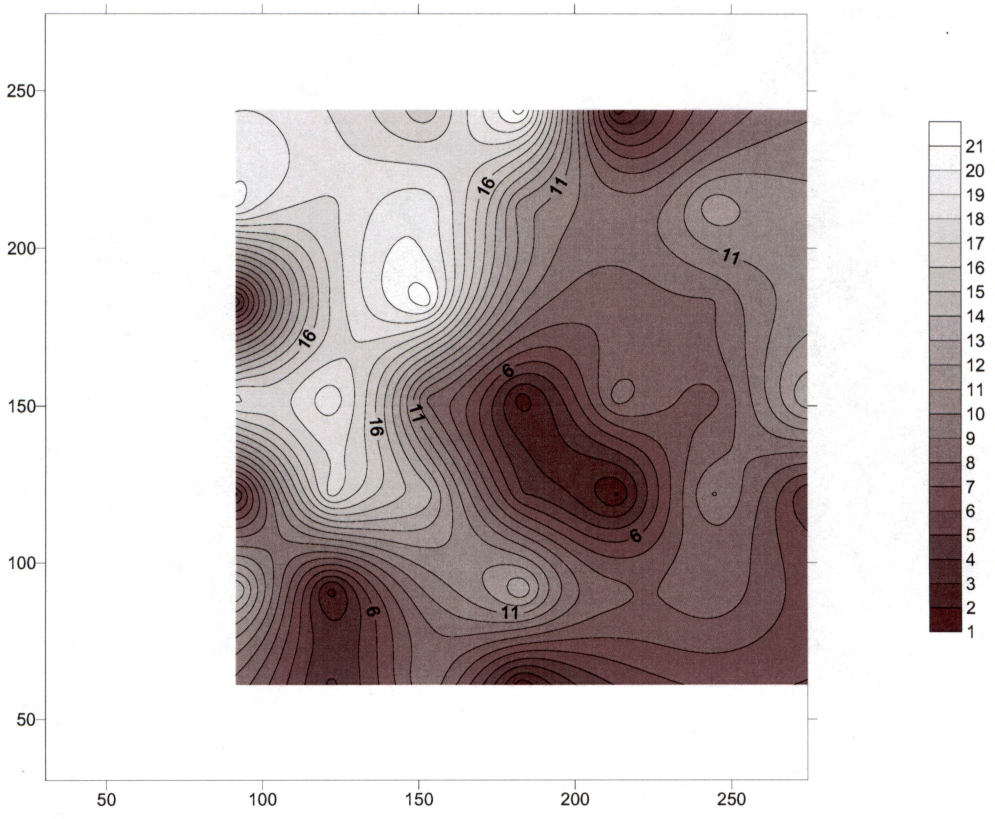
250
200
150
100
50
50
100
150
200
250
16
11
11
16
6
16
11
6
6
11
21
20
19
18
17
16
15
14
13
12
11
10
9
8
7
6
5
4
3
2
1

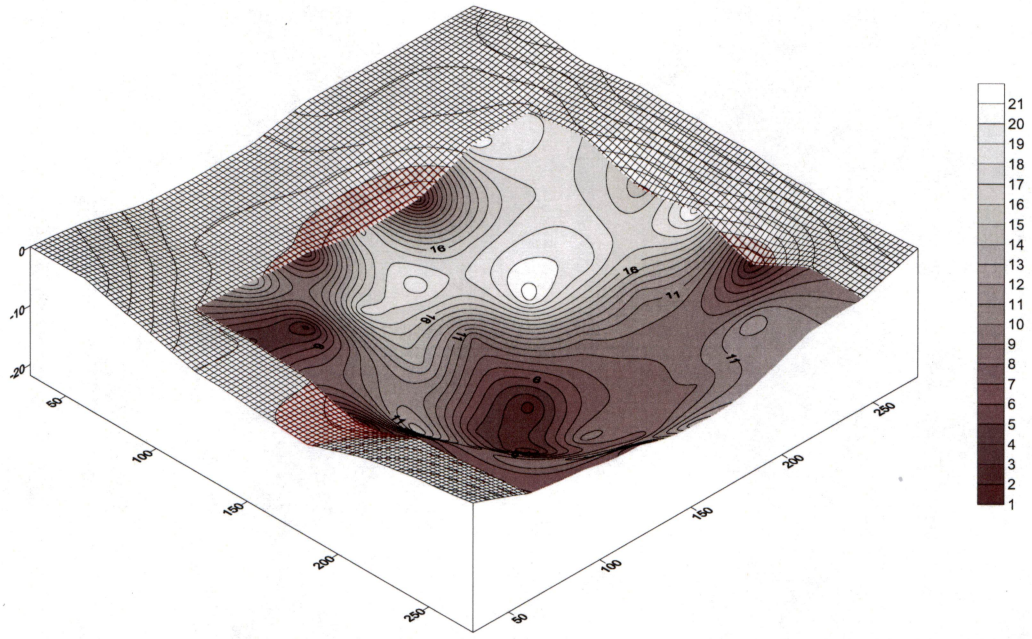
0
-10
-20
50
100
150
200
250
50
100
150
200
250
21
20
19
18
17
16
15
14
13
12
11
10
9
8
7
6
5
4
3
2
1

J17SH3

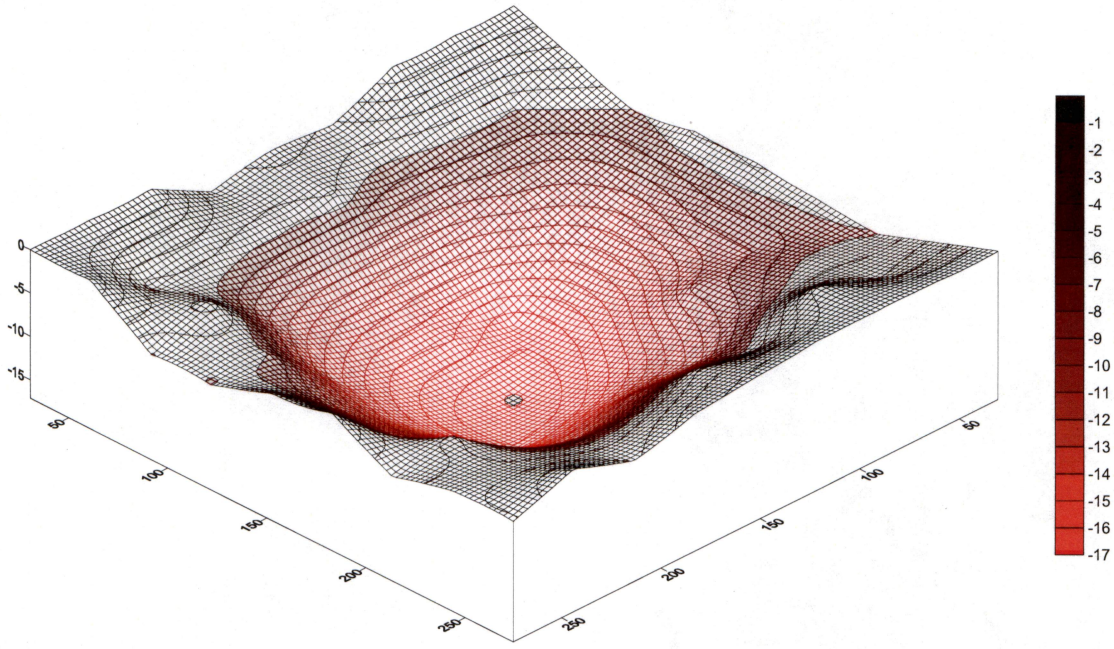
0
-5
-10
-15
50
100
150
200
250
-1
-2
-3
-4
-5
-6
-7
-8
-9
-10
-11
-12
-13
-14
-15
-16
-17

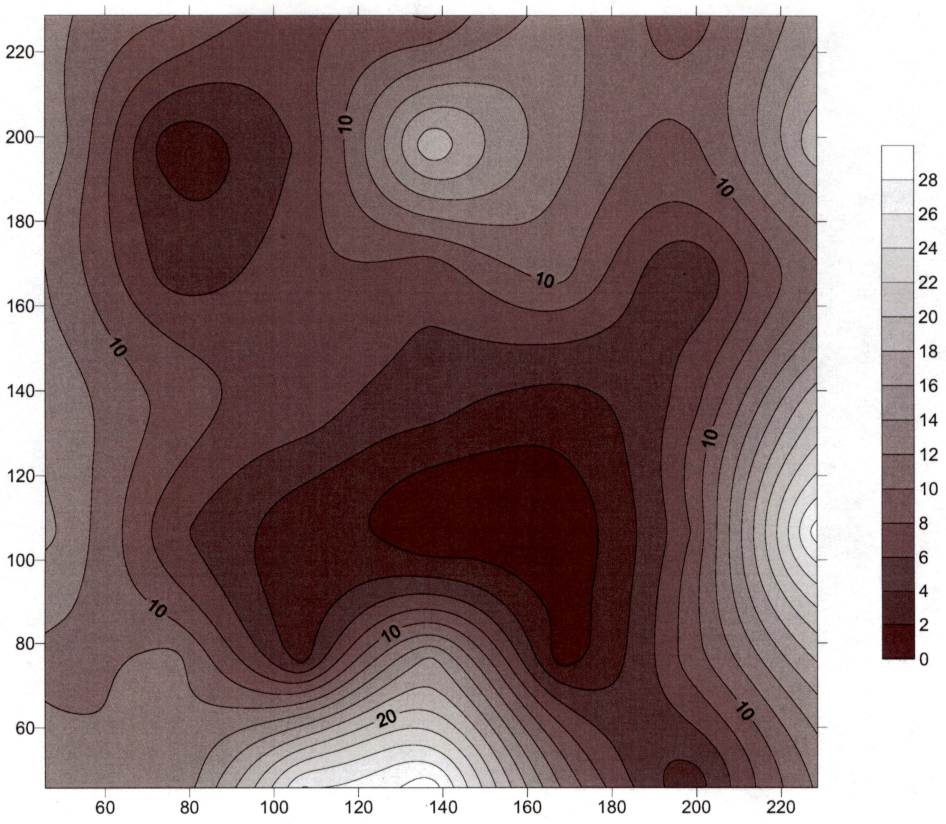
220
200
180
160
140
120
100
80
60
60
80
100
120
140
160
180
200
220
10
20
28
26
24
22
20
18
16
14
12
10
8
6
4
2
0

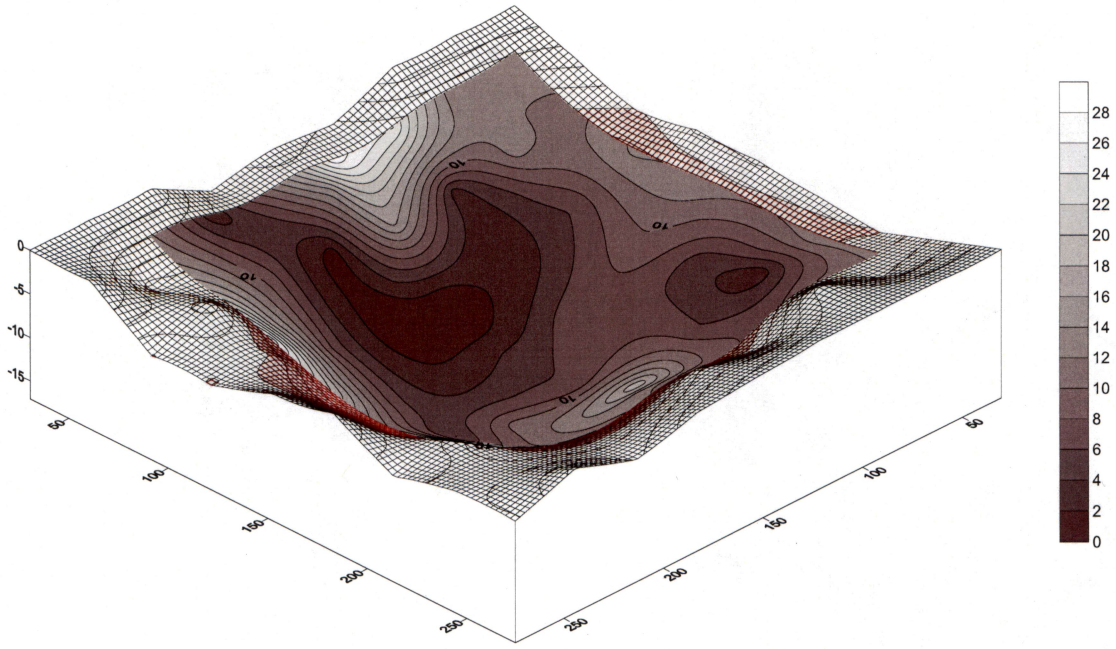
0
-5
-10
-15
50
100
150
200
250
10
10
10
10
28
26
24
22
20
18
16
14
12
10
8
6
4
2
0

J17SH4

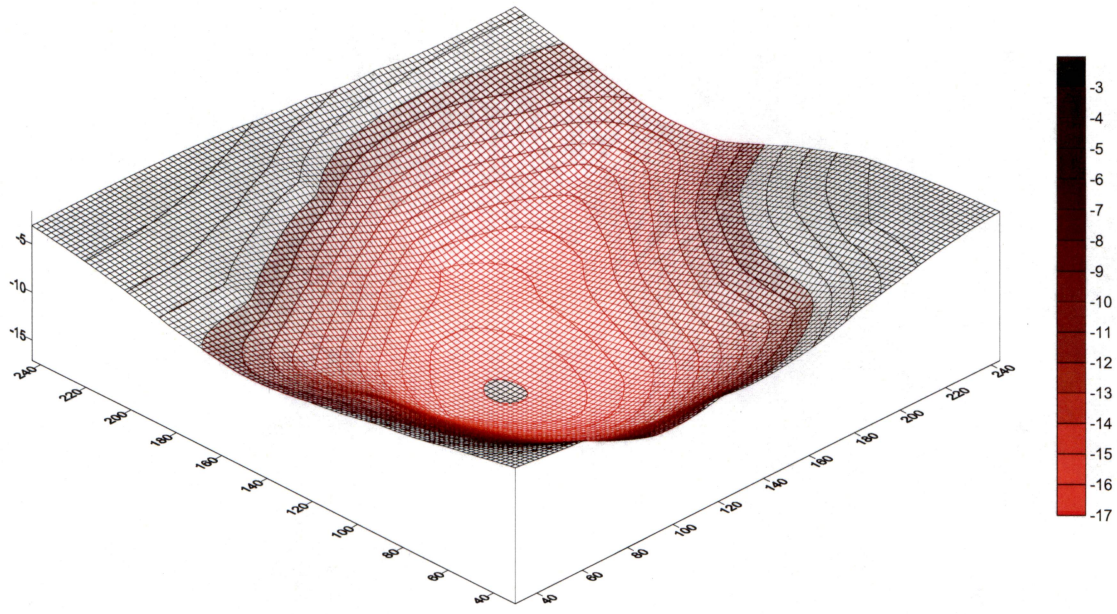
-3
-4
-5
-6
-7
-8
-9
-10
-11
-12
-13
-14
-15
-16
-17

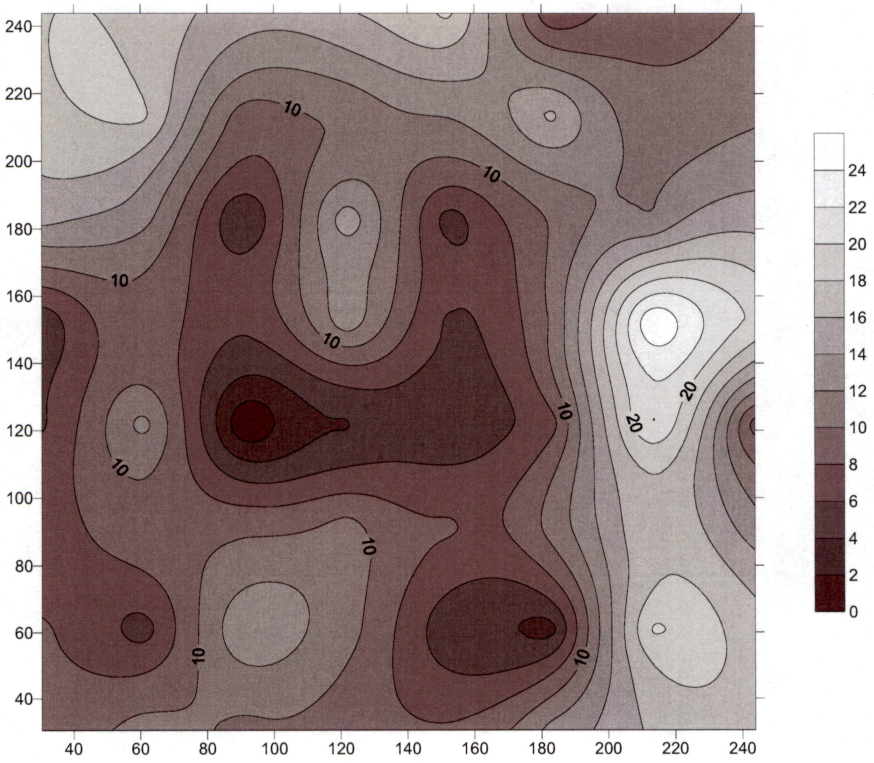
240
220
200
180
160
140
120
100
80
60
40
10
20
24
22
20
18
16
14
12
10
8
6
4
2
0

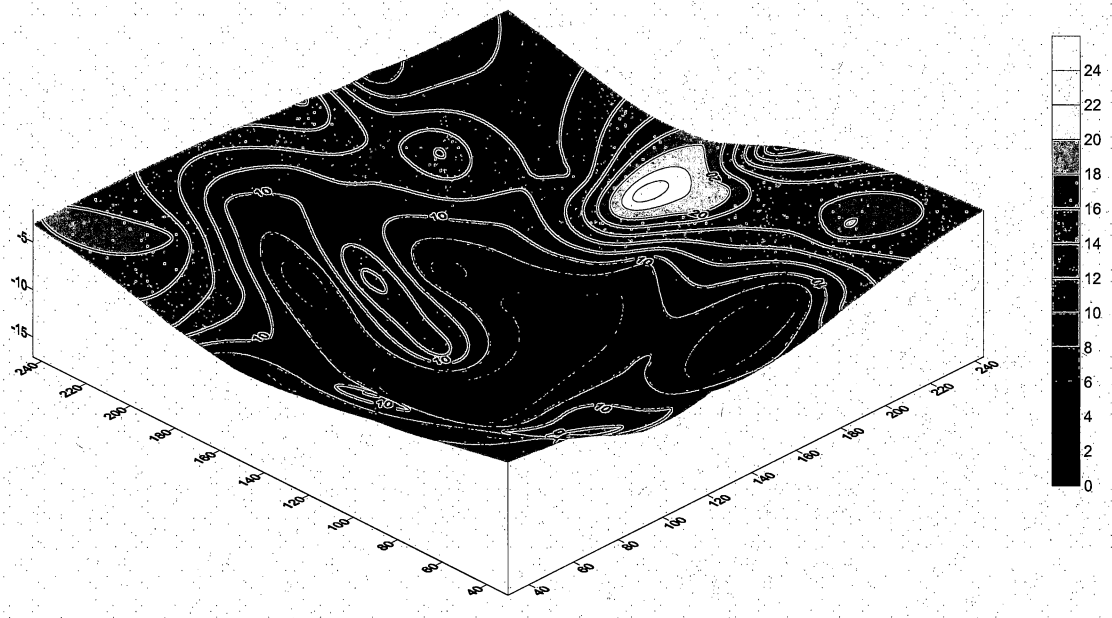
24
22
20
18
16
14
12
10
8
6
4
2
0

RRSH1

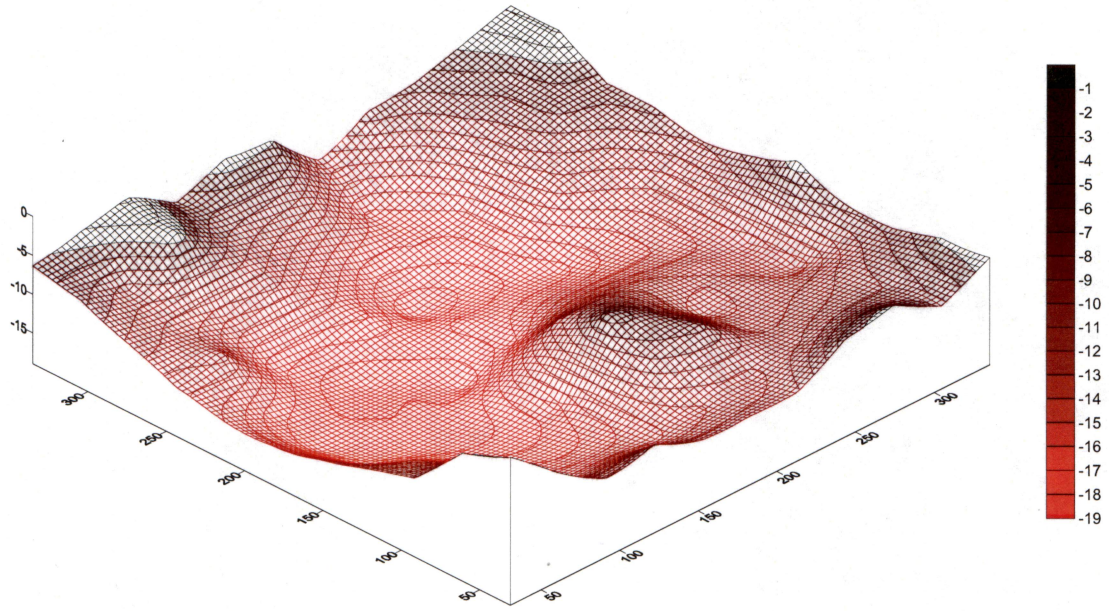
0
-5
-10
-15
300
250
200
150
100
50
-1
-2
-3
-4
-5
-6
-7
-8
-9
-10
-11
-12
-13
-14
-15
-16
-17
-18
-19

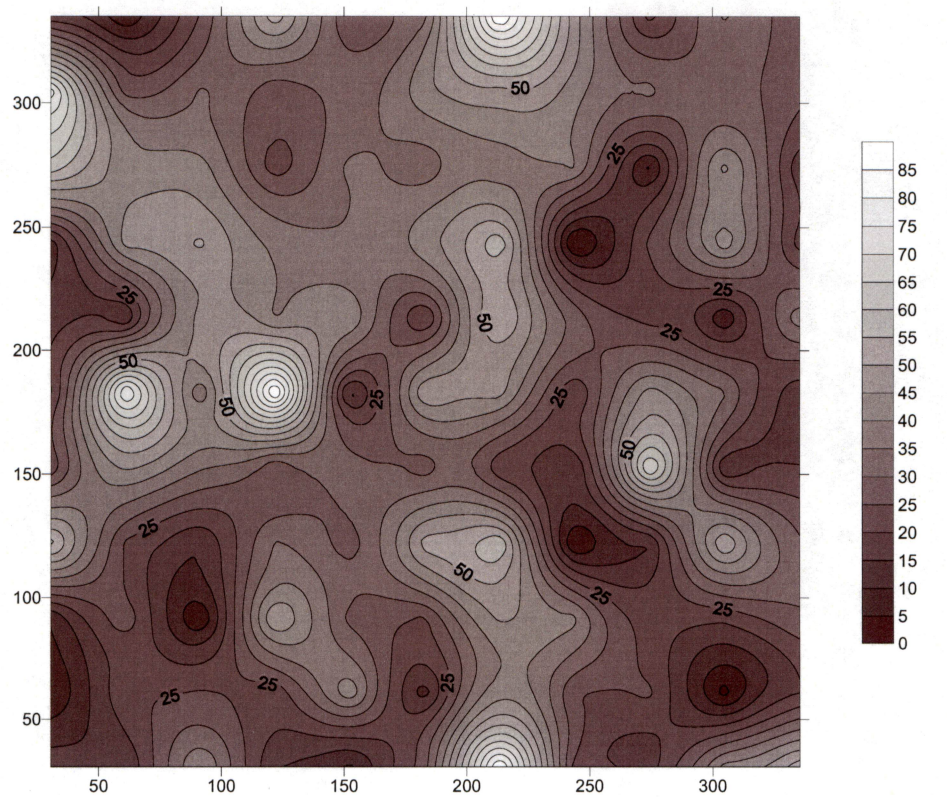
300
250
200
150
100
50
50
100
150
200
250
300
25
50
85
80
75
70
65
60
55
50
45
40
35
30
25
20
15
10
5
0

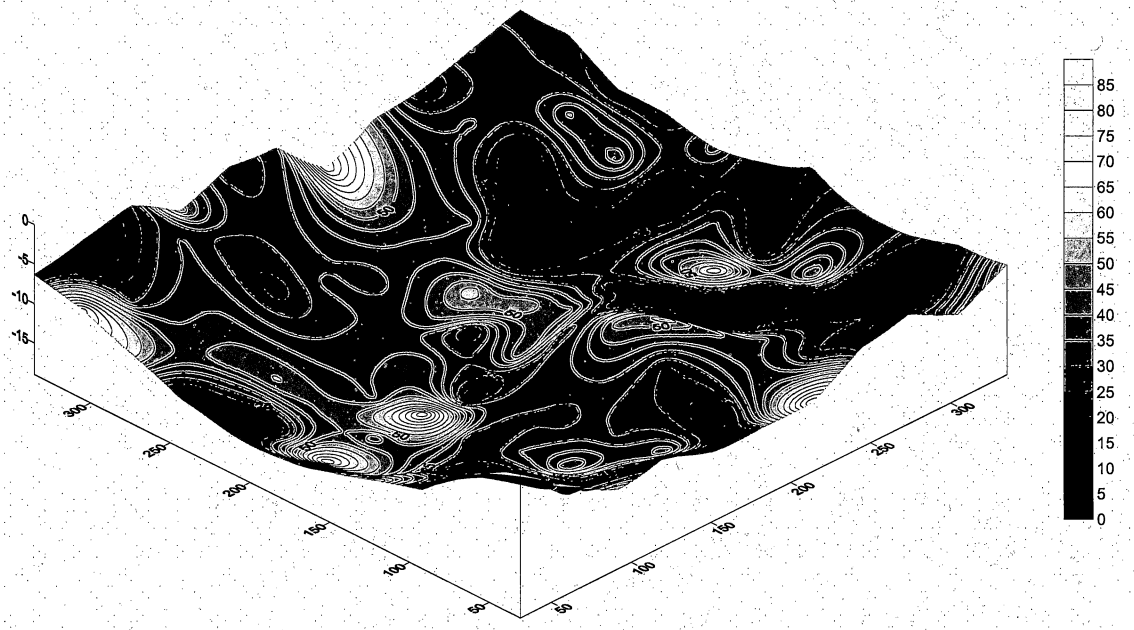
0
-5
-10
-15
300
250
200
150
100
50
50
100
150
200
250
300
85
80
75
70
65
60
55
50
45
40
35
30
25
20
15
10
5
0

J17SH2

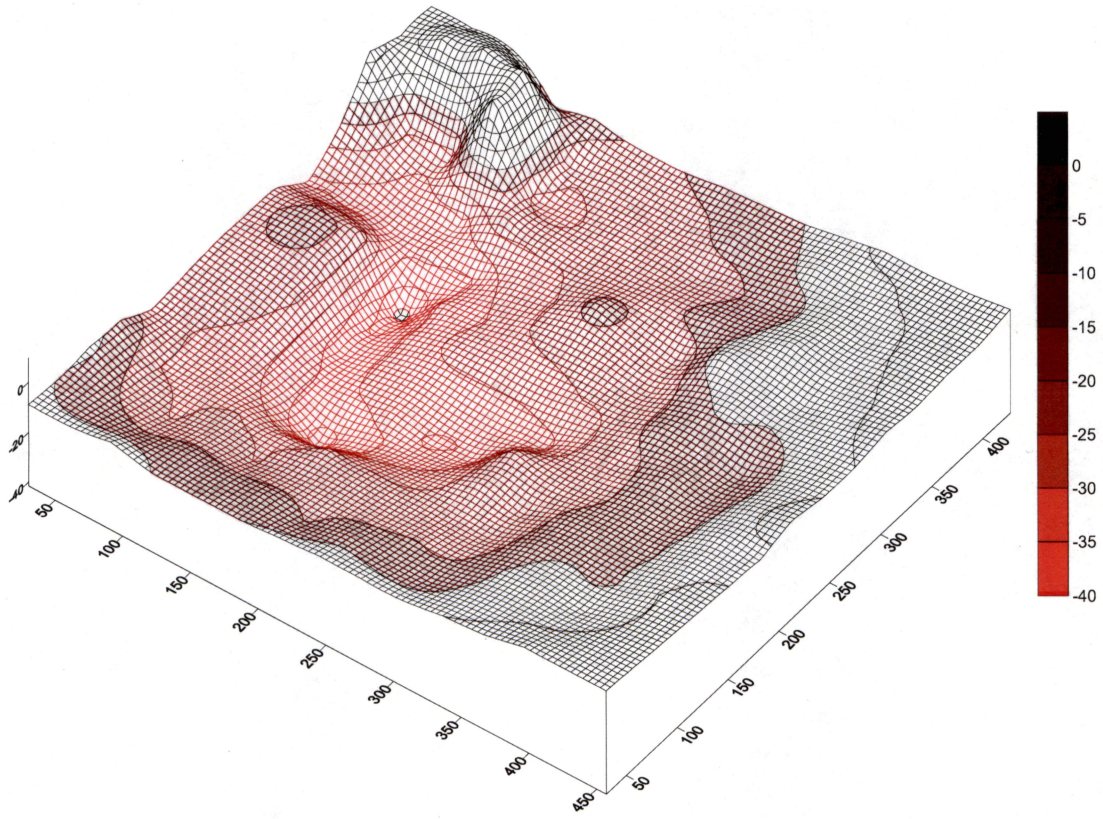
0
-5
-10
-15
-20
-25
-30
-35
-40
0
-20
-40
50
100
150
200
250
300
350
400
450
50
100
150
200
250
300
350
400

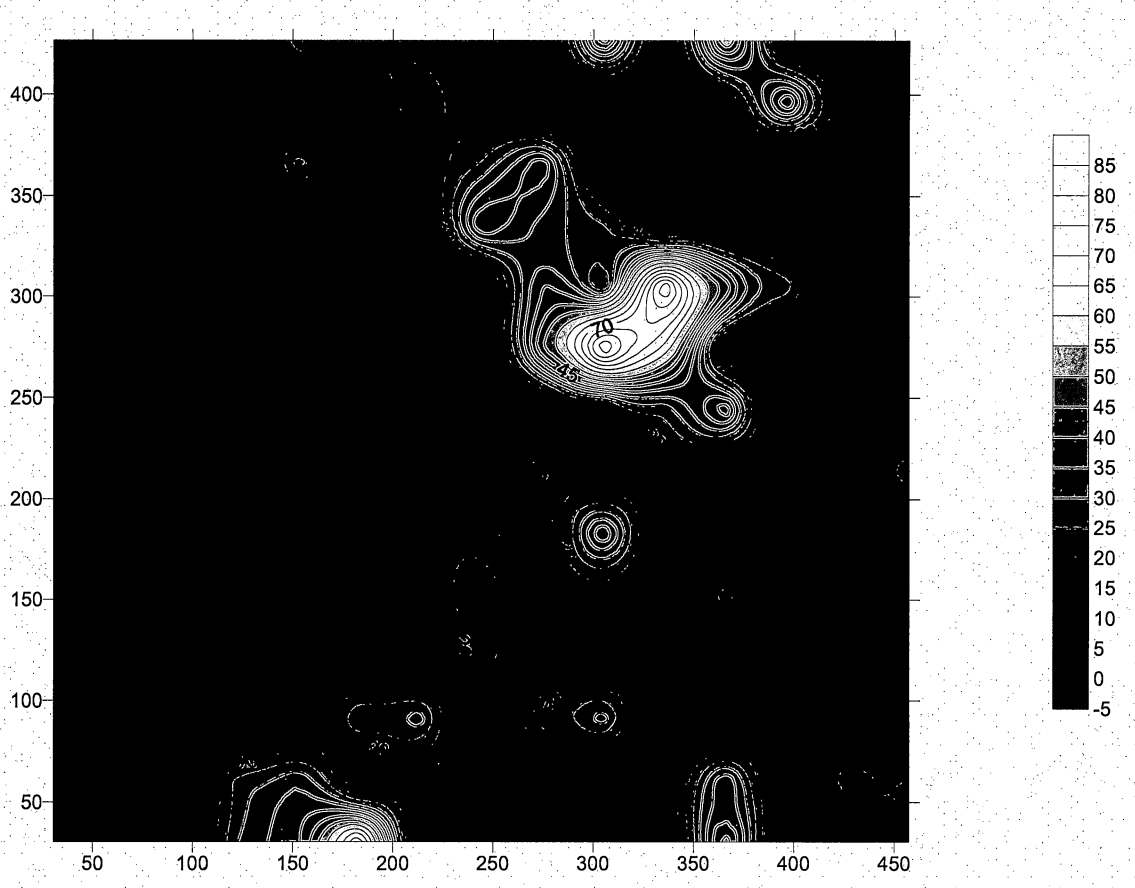
400
350
300
250
200
150
100
50
50
100
150
200
250
300
350
400
450
10
45
85
80
75
70
65
60
55
50
45
40
35
30
25
20
15
10
5
0
-5

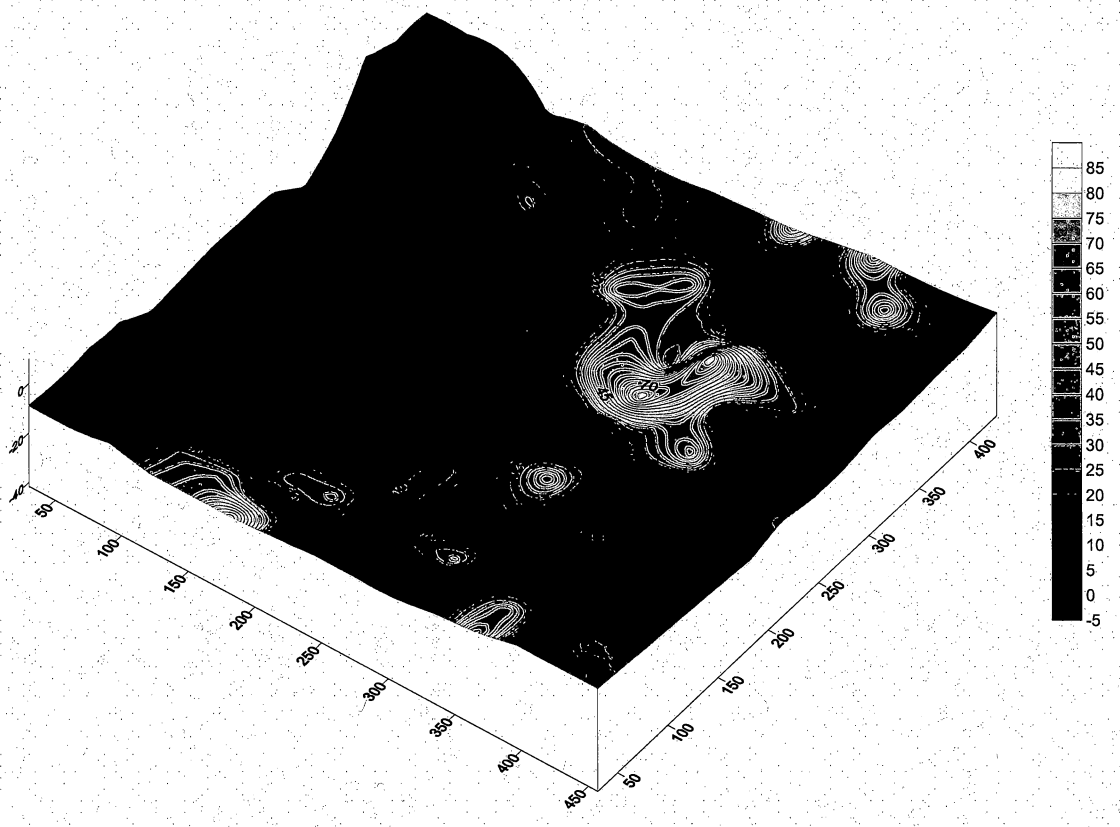
85
80
75
70
65
60
55
50
45
40
35
30
25
20
15
10
5
0
-5
0
-20
-40
50
100
150
200
250
300
350
400
450
50
100
150
200
250
300
350
400

RRSH3

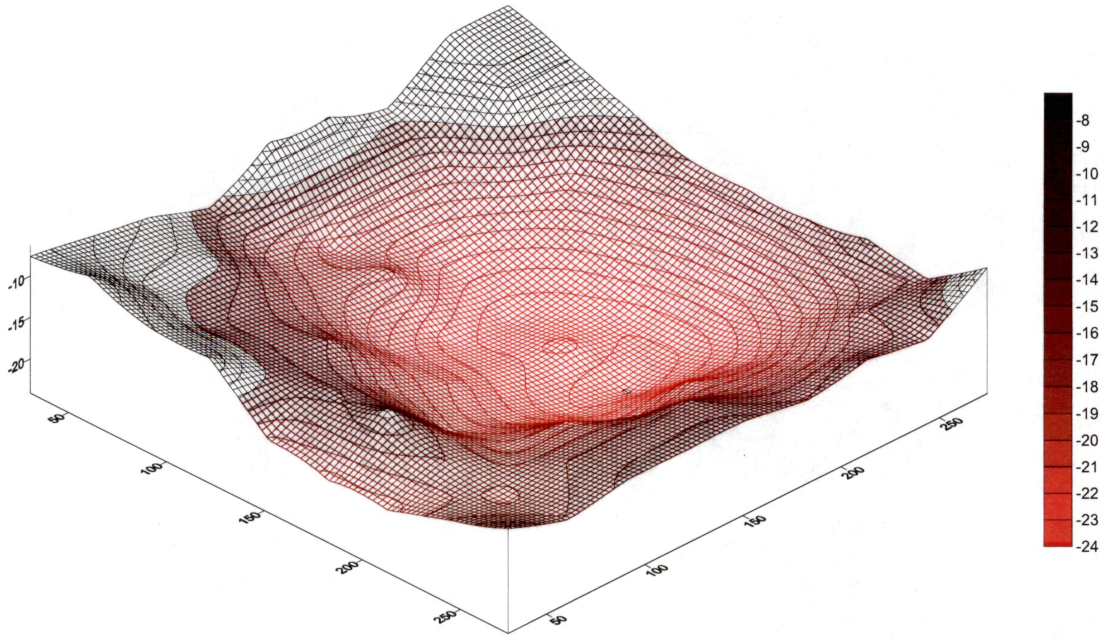
-8
-9
-10
-11
-12
-13
-14
-15
-16
-17
-18
-19
-20
-21
-22
-23
-24

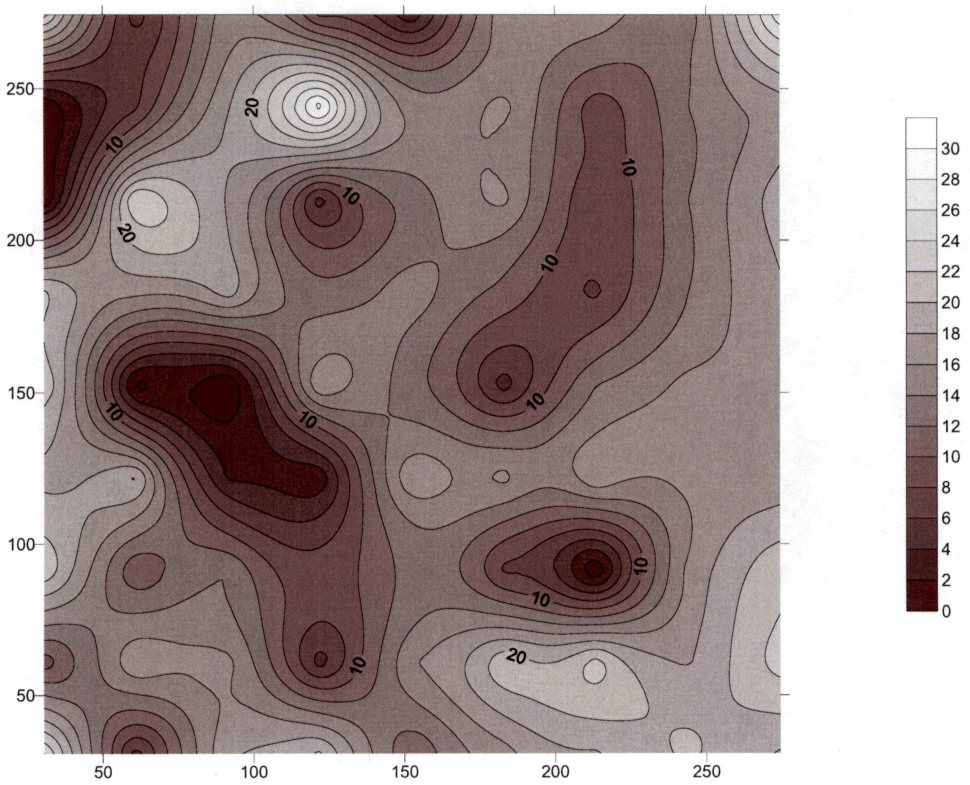
250
200
150
100
50
50
100
150
200
250
10
20
30
28
26
24
22
20
18
16
14
12
10
8
6
4
2
0

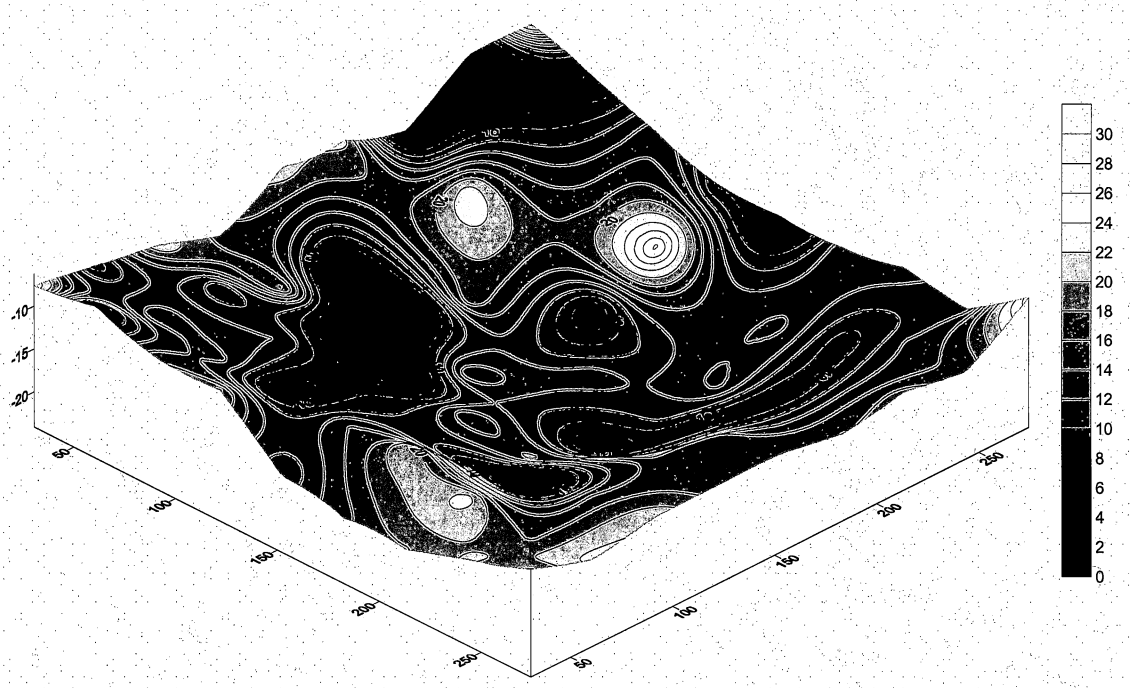
-10
-15
-20
50
100
150
200
250
50
100
150
200
250
30
28
26
24
22
20
18
16
14
12
10
8
6
4
2
0

RRSH4

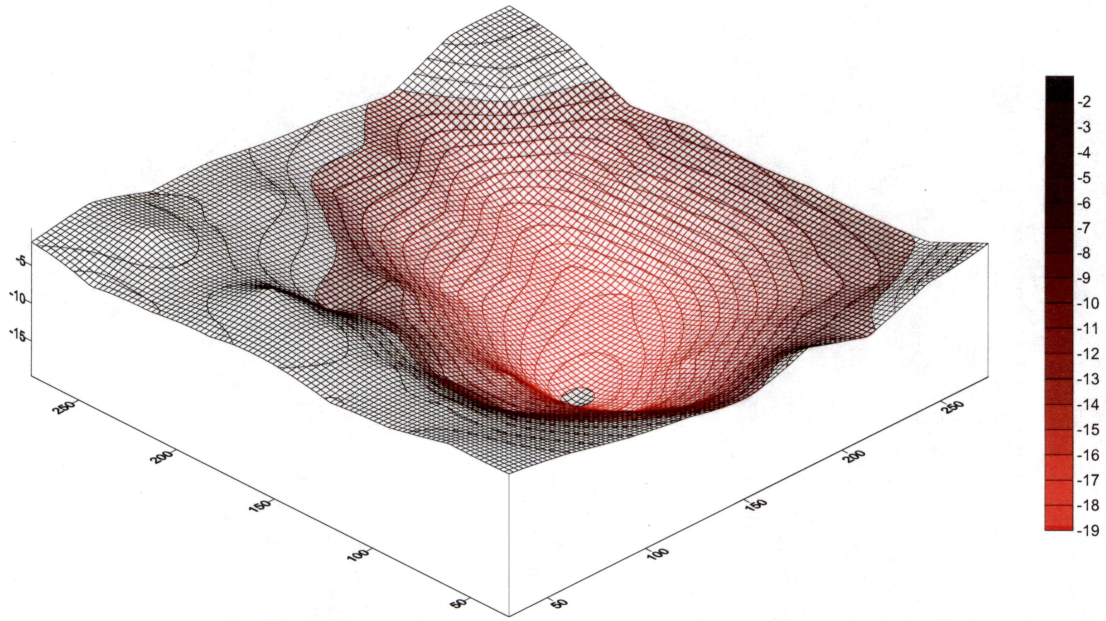
-2
-3
-4
-5
-6
-7
-8
-9
-10
-11
-12
-13
-14
-15
-16
-17
-18
-19

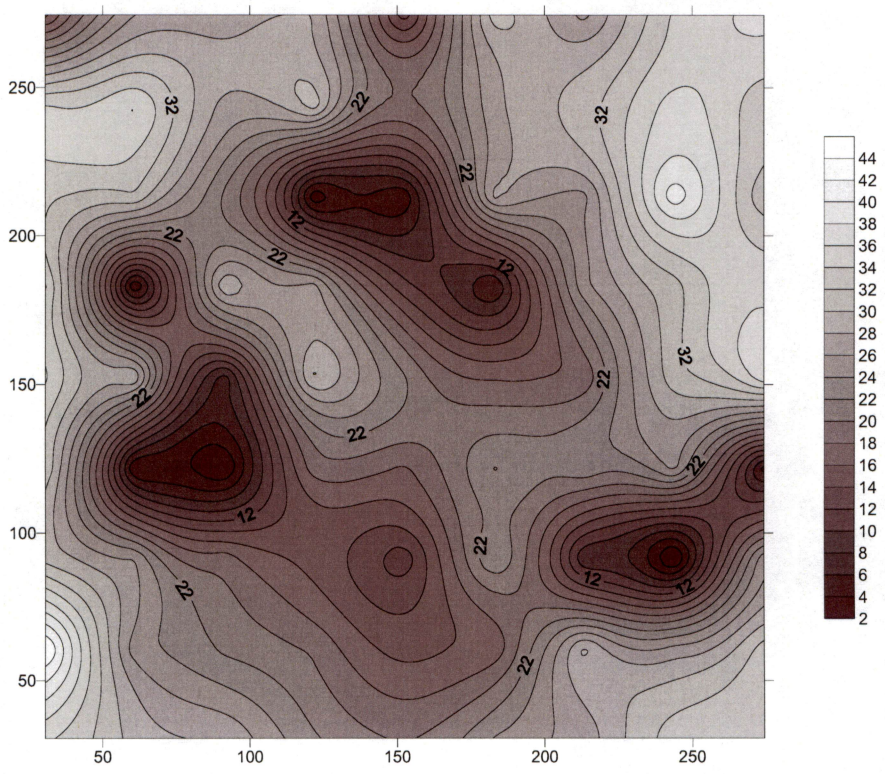
250
200
150
100
50
50
100
150
200
250
44
42
40
38
36
34
32
30
28
26
24
22
20
18
16
14
12
10
8
6
4
2

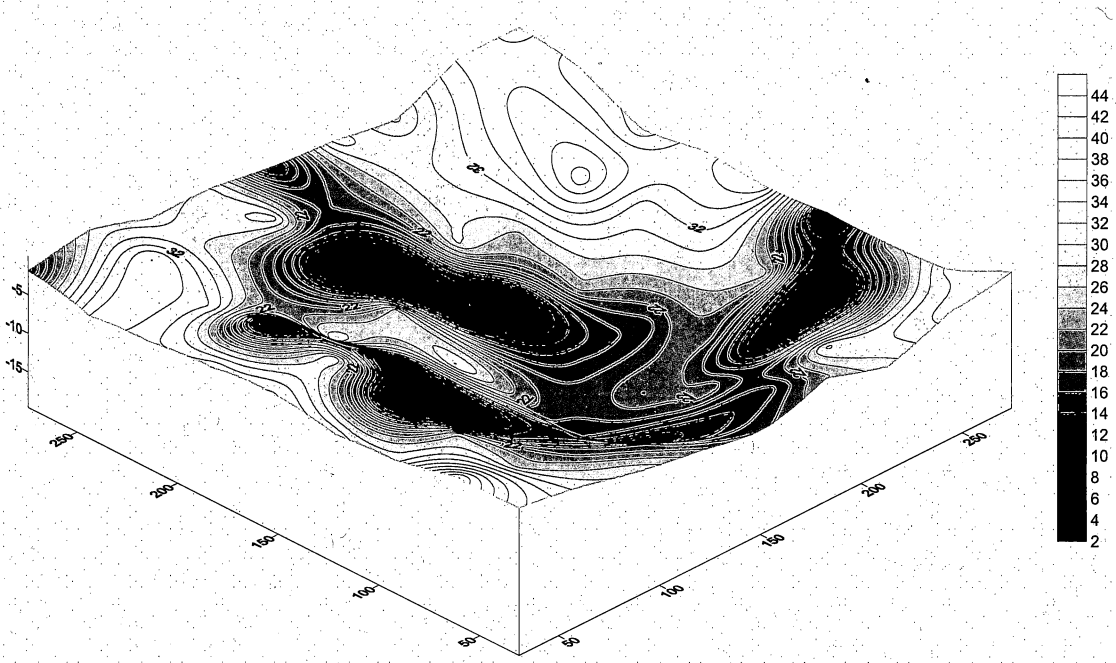
-5
-10
-15
250
200
150
100
50
50
100
150
200
250
44
42
40
38
36
34
32
30
28
26
24
22
20
18
16
14
12
10
8
6
4
2

CBSH1

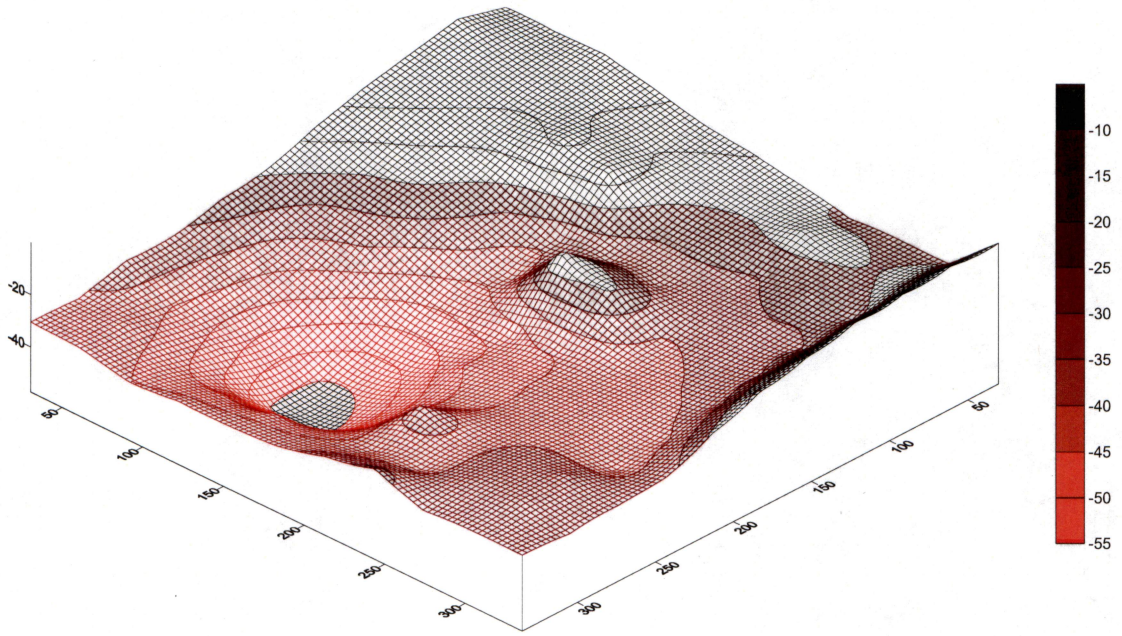
-10
-15
-20
-25
-30
-35
-40
-45
-50
-55

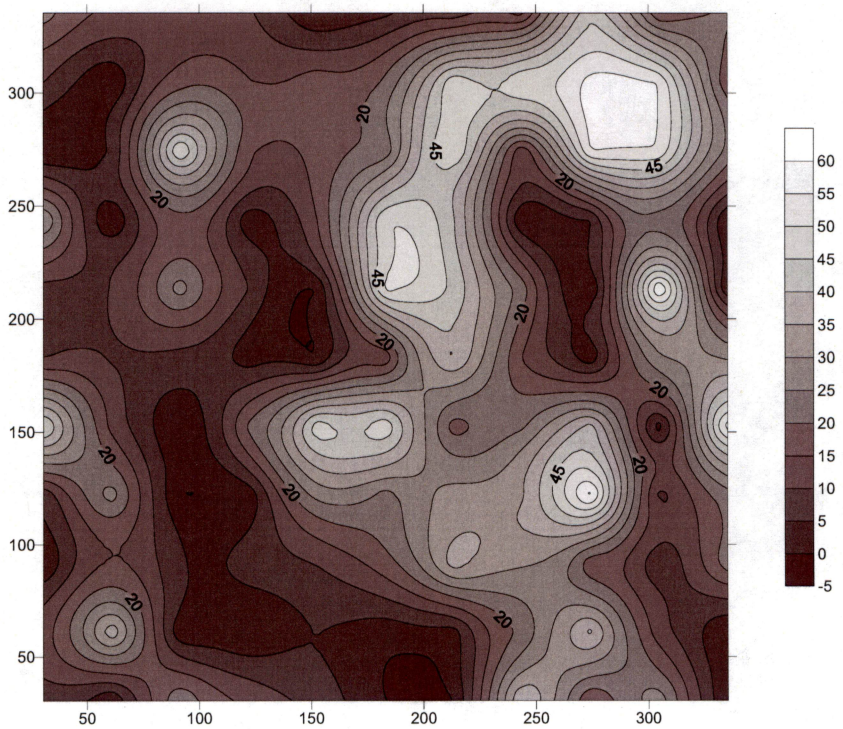
300
250
200
150
100
50
50
100
150
200
250
300
20
45
60
55
50
45
40
35
30
25
20
15
10
5
0
-5

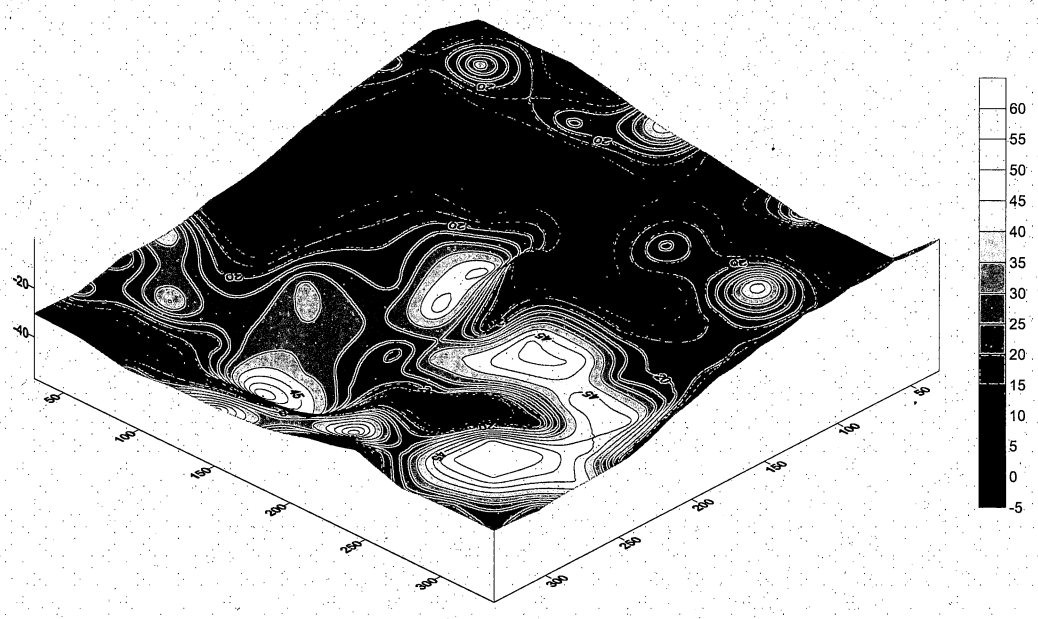
60
55
50
45
40
35
30
25
20
15
10
5
0
-5
-20
-40
50
100
150
200
250
300
350
250
200
150
100
50

HCSH1

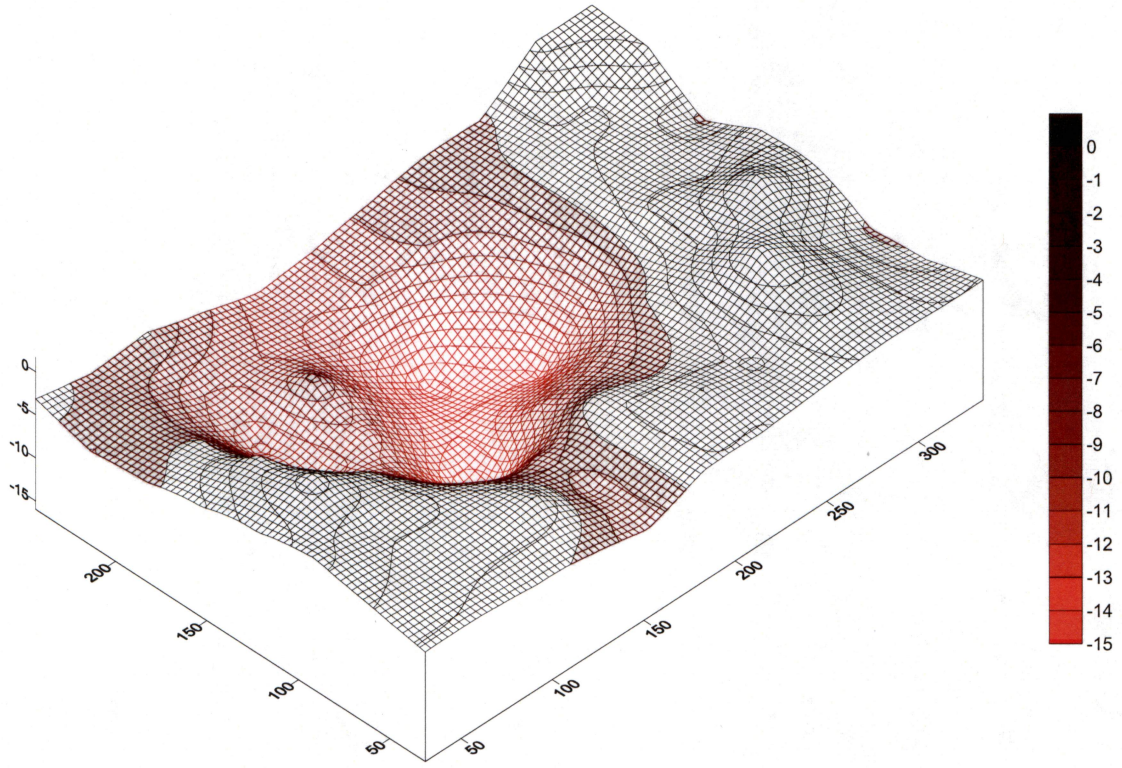
0
-1
-2
-3
-4
-5
-6
-7
-8
-9
-10
-11
-12
-13
-14
-15
50
100
150
200
250
300

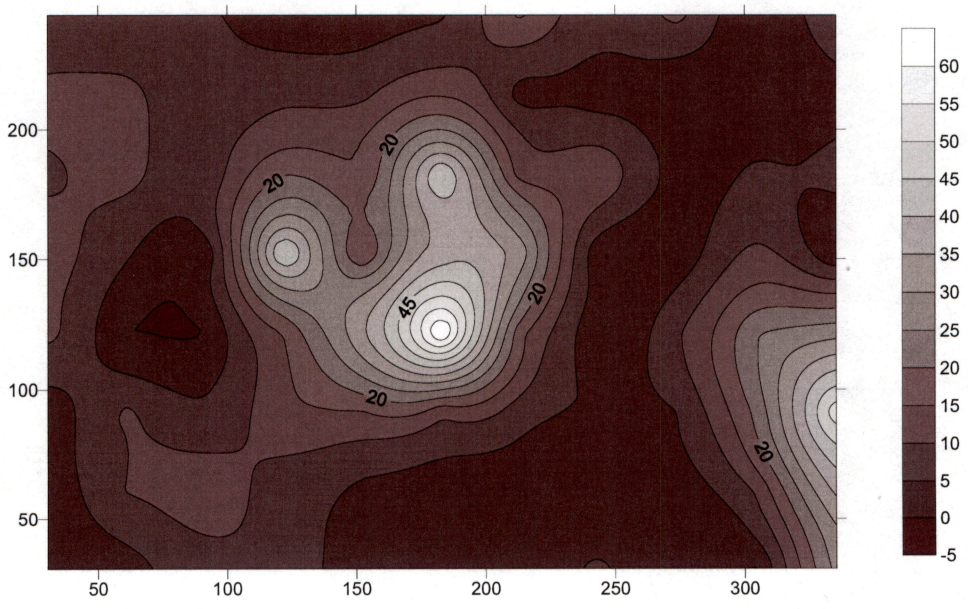
60
55
50
45
40
35
30
25
20
15
10
5
0
-5
20
45
50
100
150
200
250
300

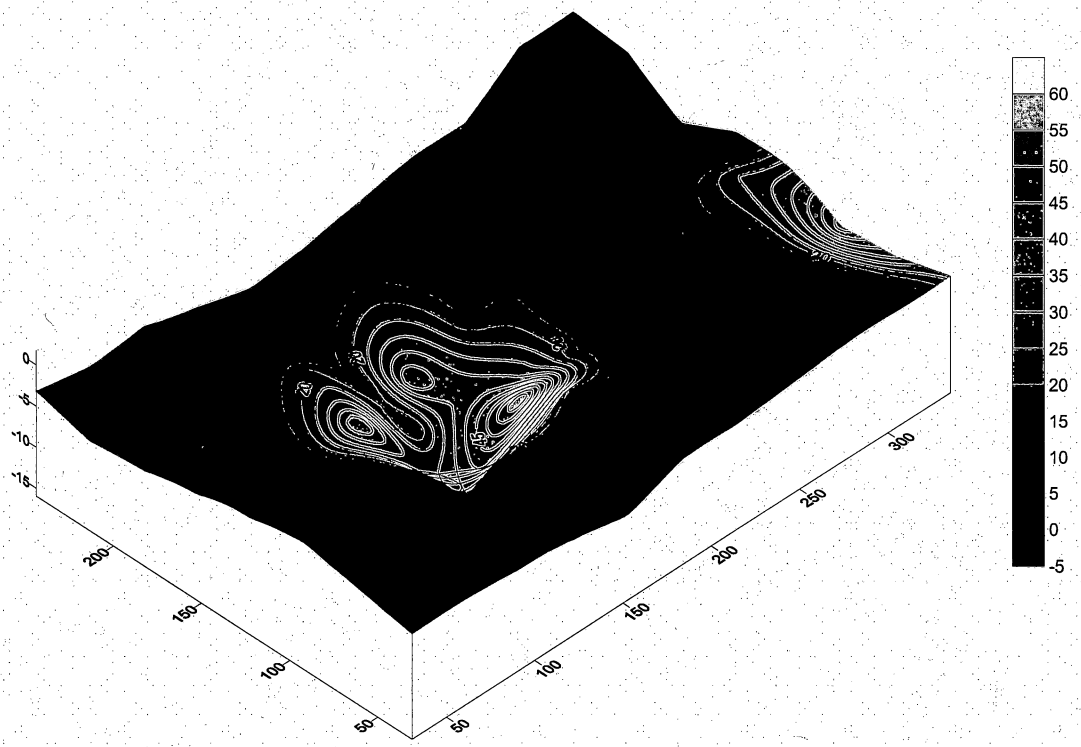
60
55
50
45
40
35
30
25
20
15
10
5
0
-5
50
100
150
200
250
300

CONTROL PLOTS

J17BG1

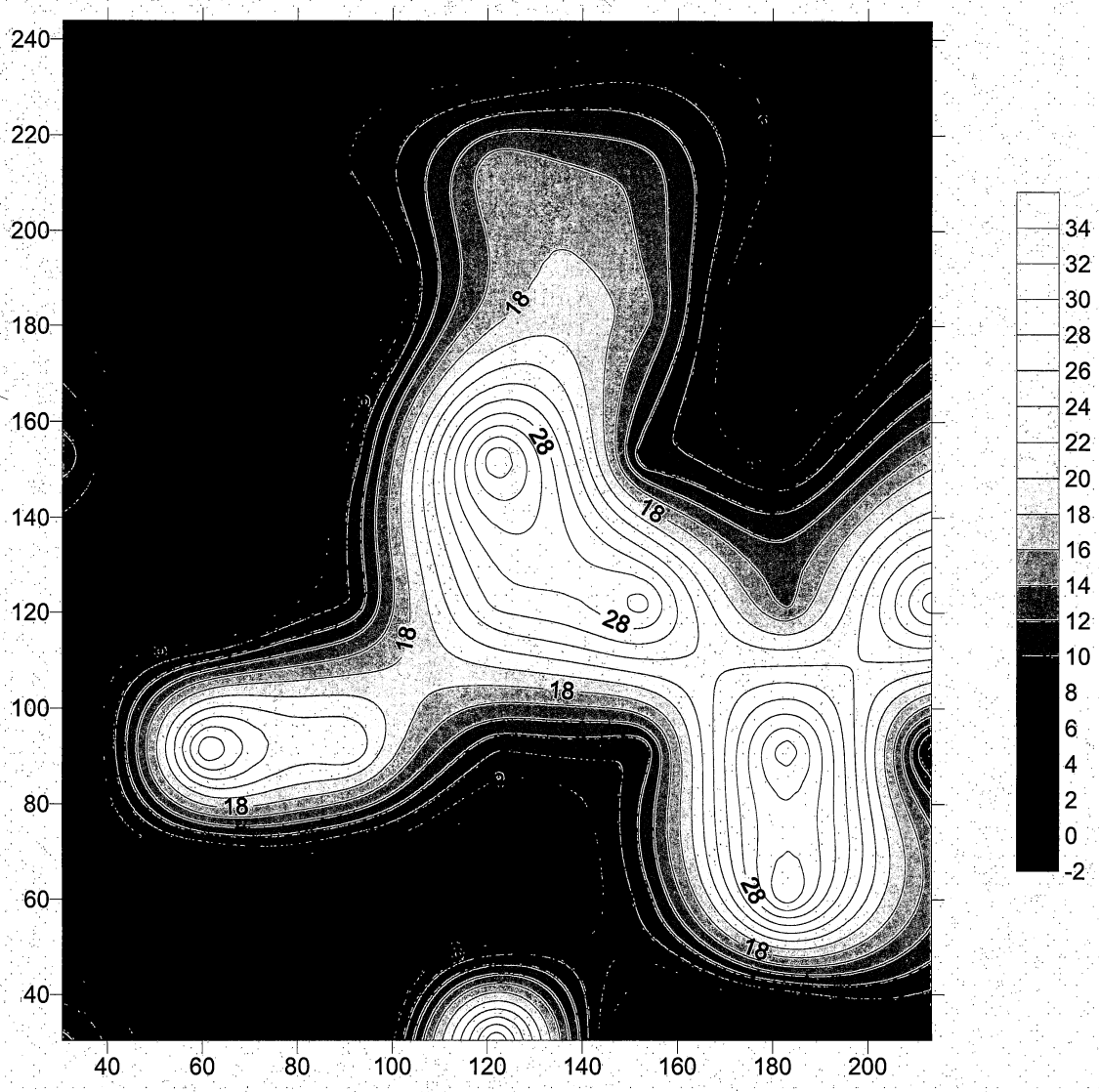

J17BG2

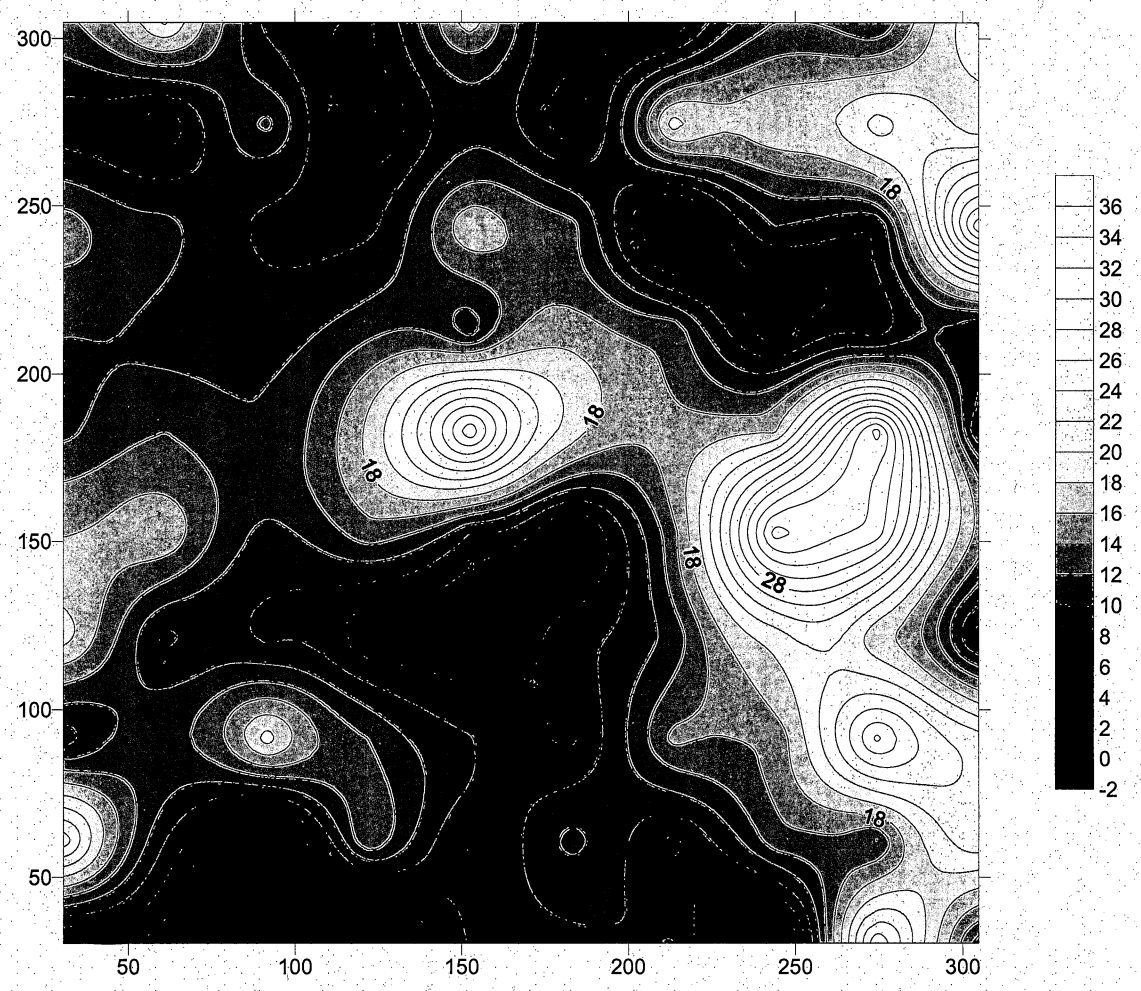
300
250
200
150
100
50
50
100
150
200
250
300
18
18
18
18
28
18
36
34
32
30
28
26
24
22
20
18
16
14
12
10
8
6
4
2
0
-2

J17BG3

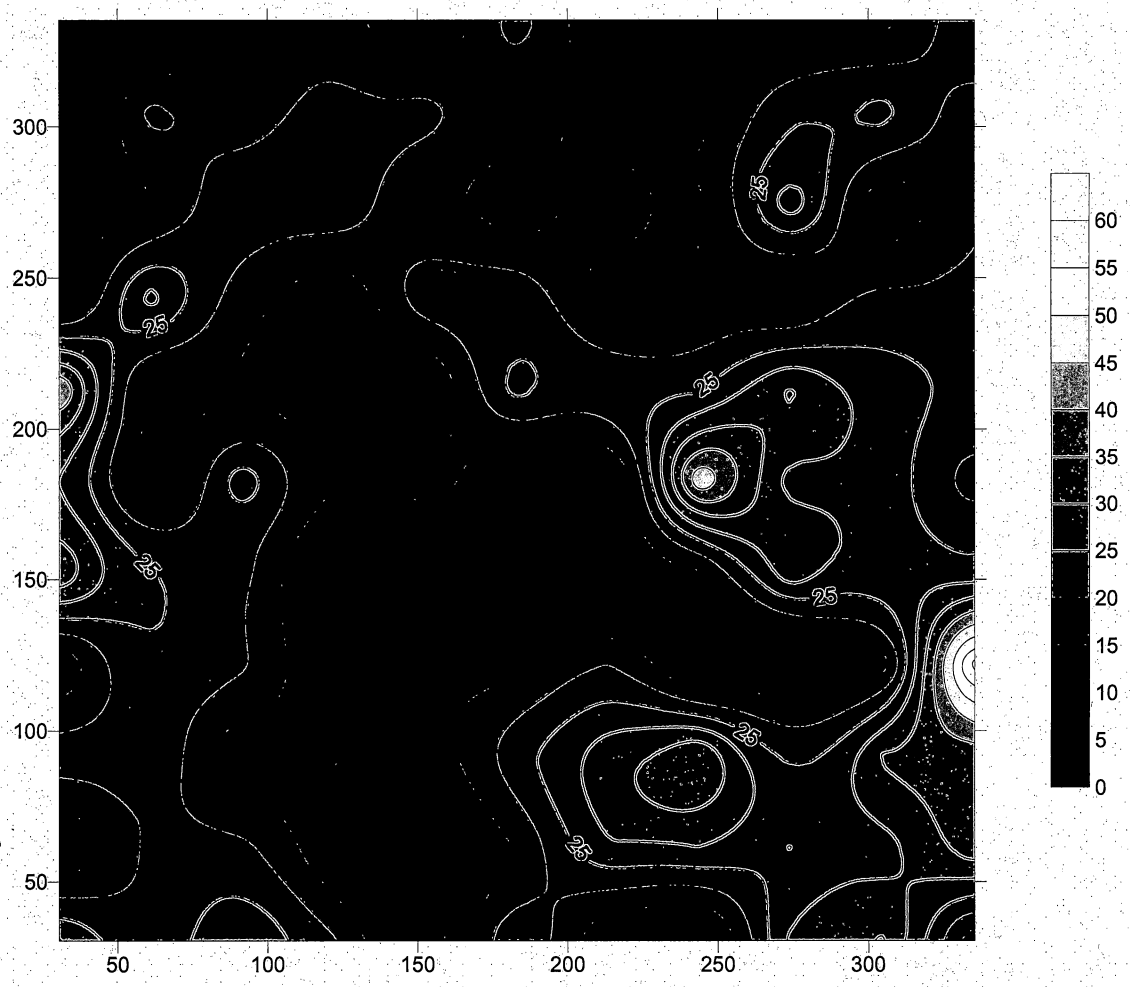
300
250
200
150
100
50
50
100
150
200
250
300
25
25
25
25
25
25
60
55
50
45
40
35
30
25
20
15
10
5
0

J17BG4

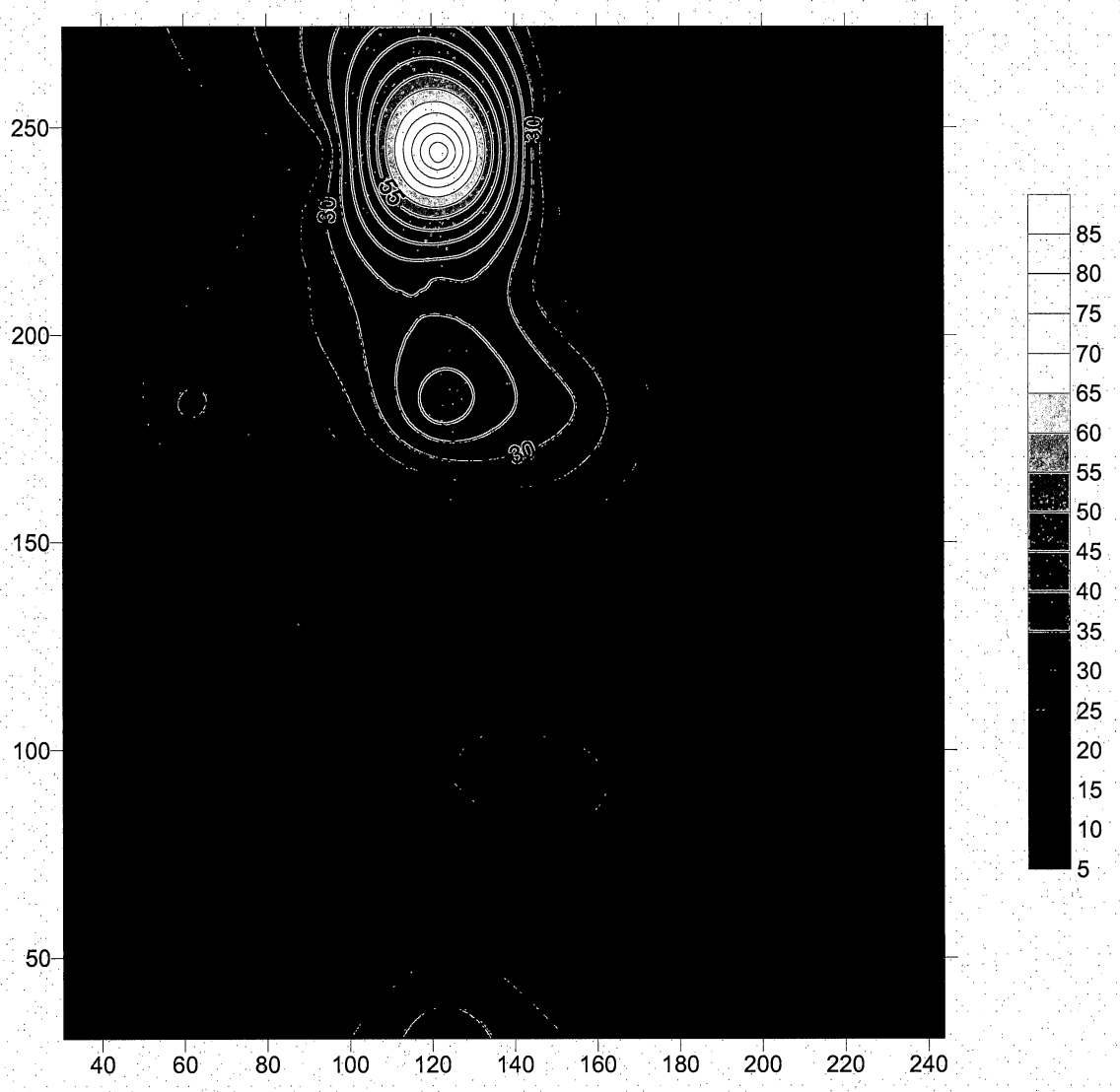
250
200
150
100
50
40
60
80
100
120
140
160
180
200
220
240
85
80
75
70
65
60
55
50
45
40
35
30
25
20
15
10
5

RRBG1

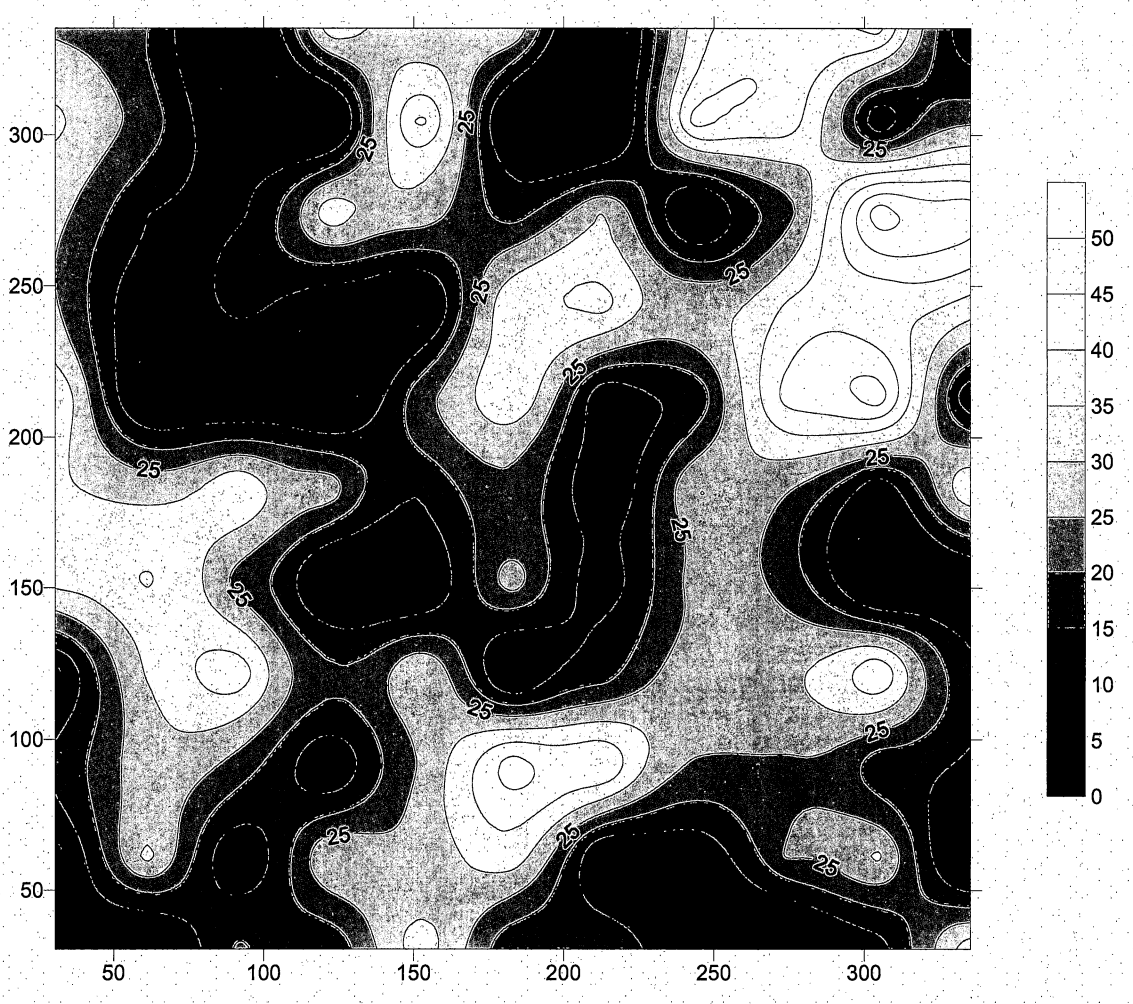
300
250
200
150
100
50
50
100
150
200
250
300
25
50
45
40
35
30
25
20
15
10
5
0

RRBG2

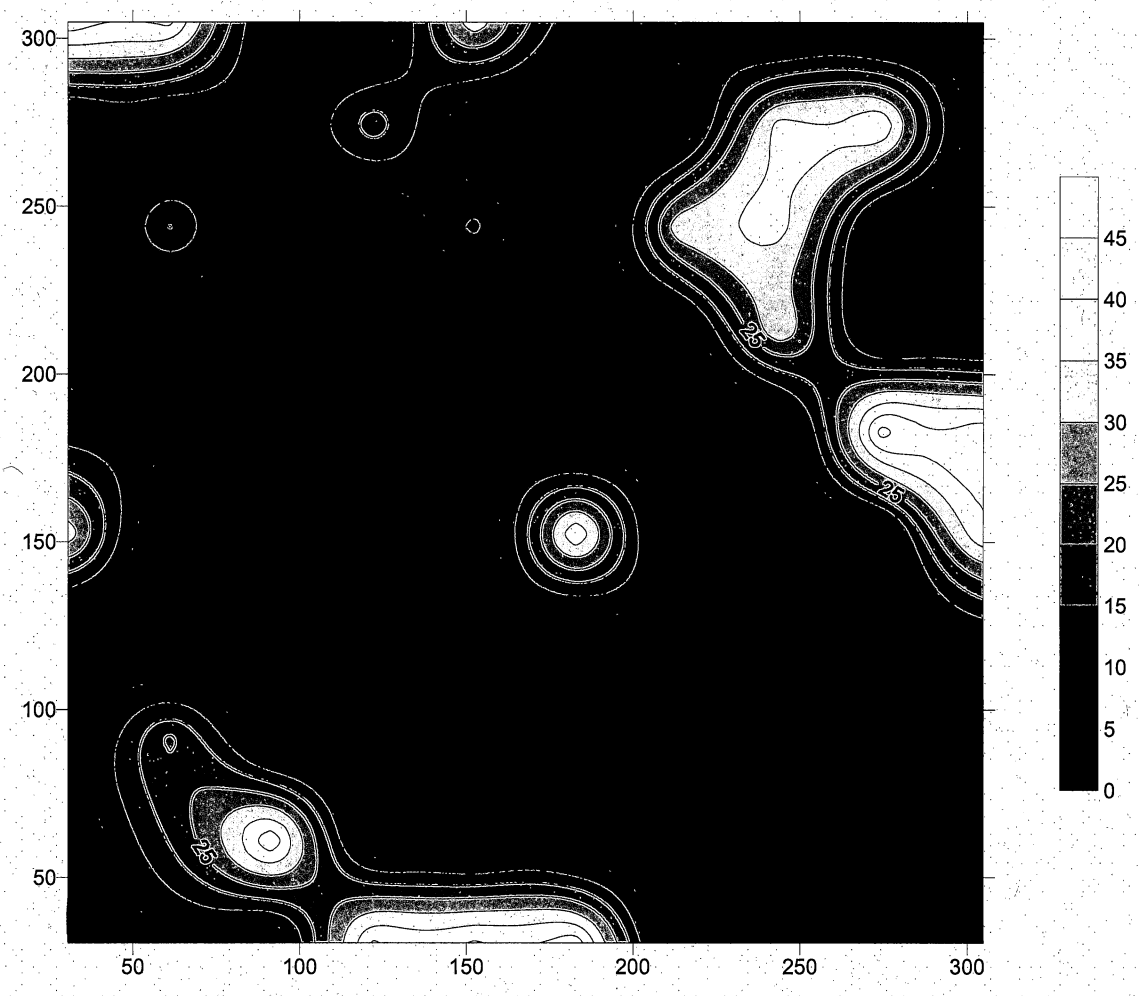
300
250
200
150
100
50
50
100
150
200
250
300
25
25
25
45
40
35
30
25
20
15
10
5
0

RRBG3

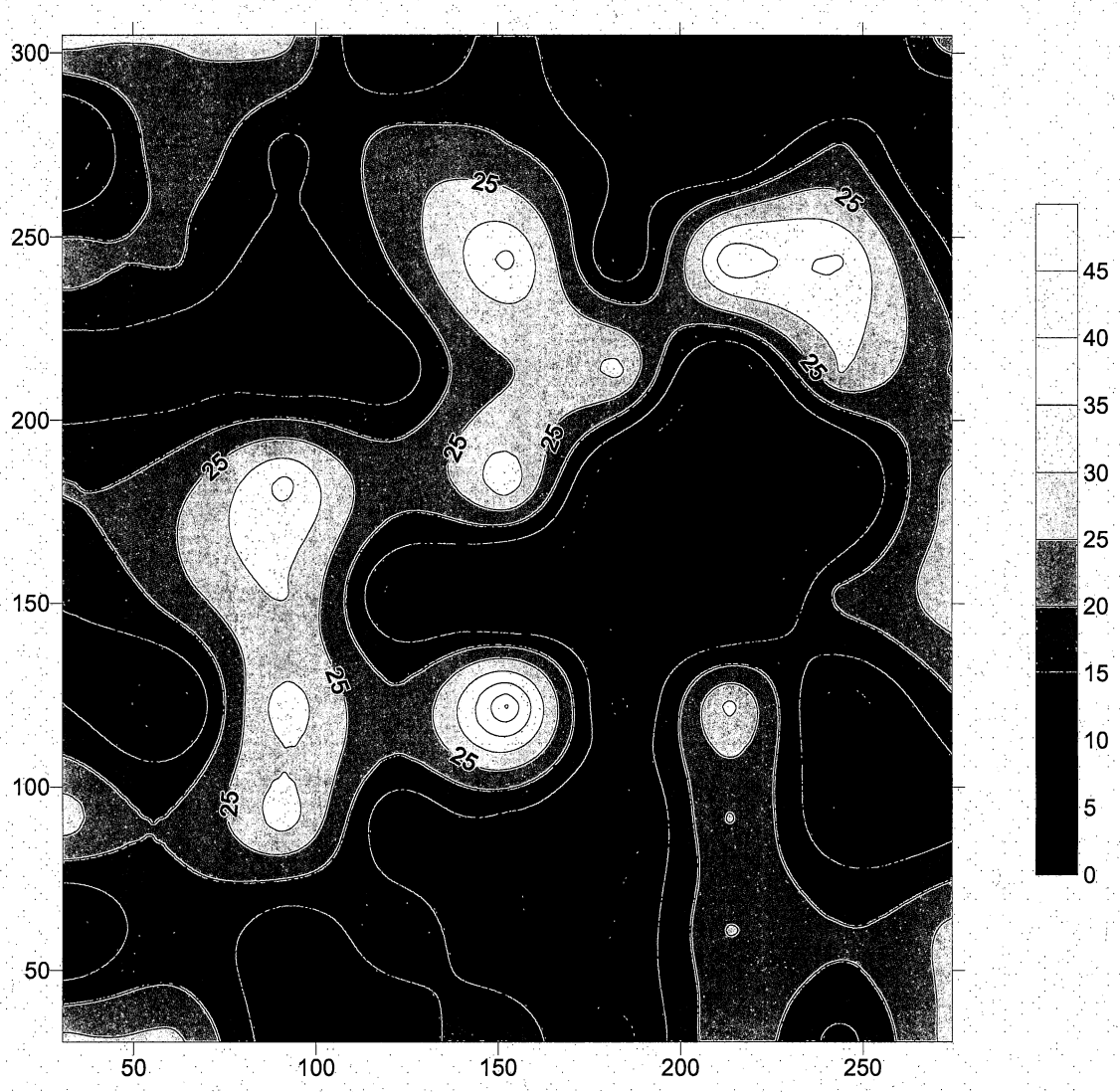
300
250
200
150
100
50
50
100
150
200
250
25
25
25
25
25
25
25
45
40
35
30
25
20
15
10
5
0

RRBG4

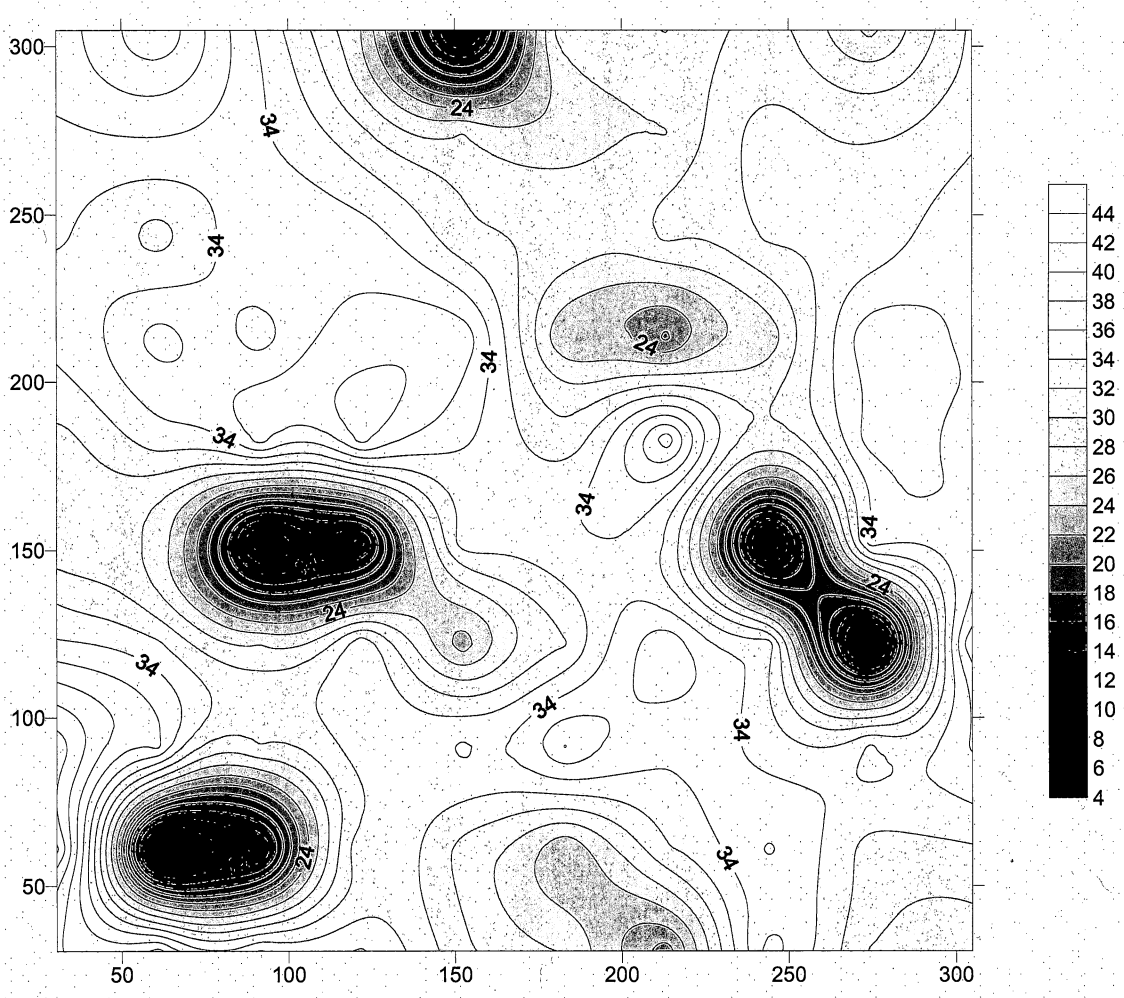
300
250
200
150
100
50
50
100
150
200
250
300
24
34
44
42
40
38
36
34
32
30
28
26
24
22
20
18
16
14
12
10
8
6
4

CBBG1

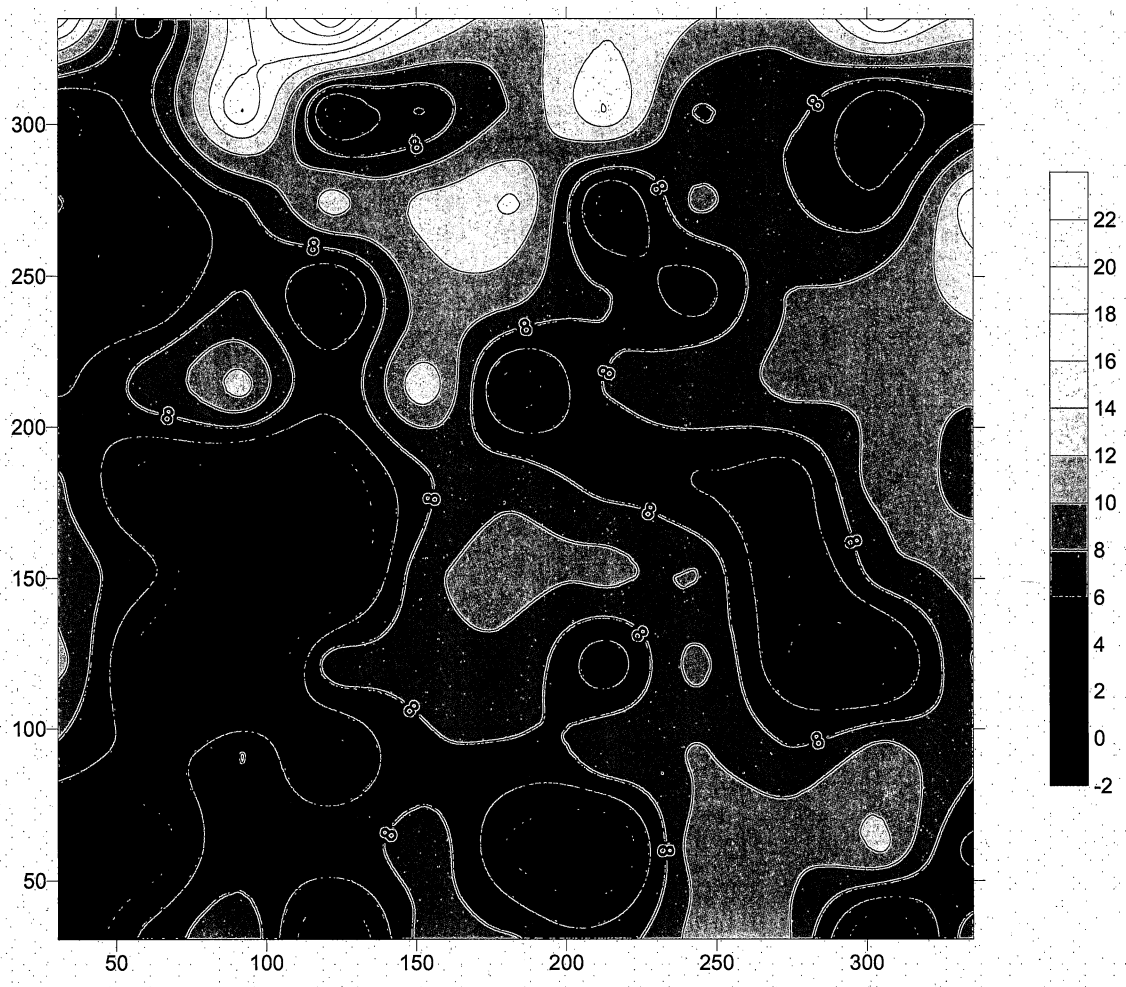
300
250
200
150
100
50
50
100
150
200
250
300
22
20
18
16
14
12
10
8
6
4
2
0
-2

HCBG1

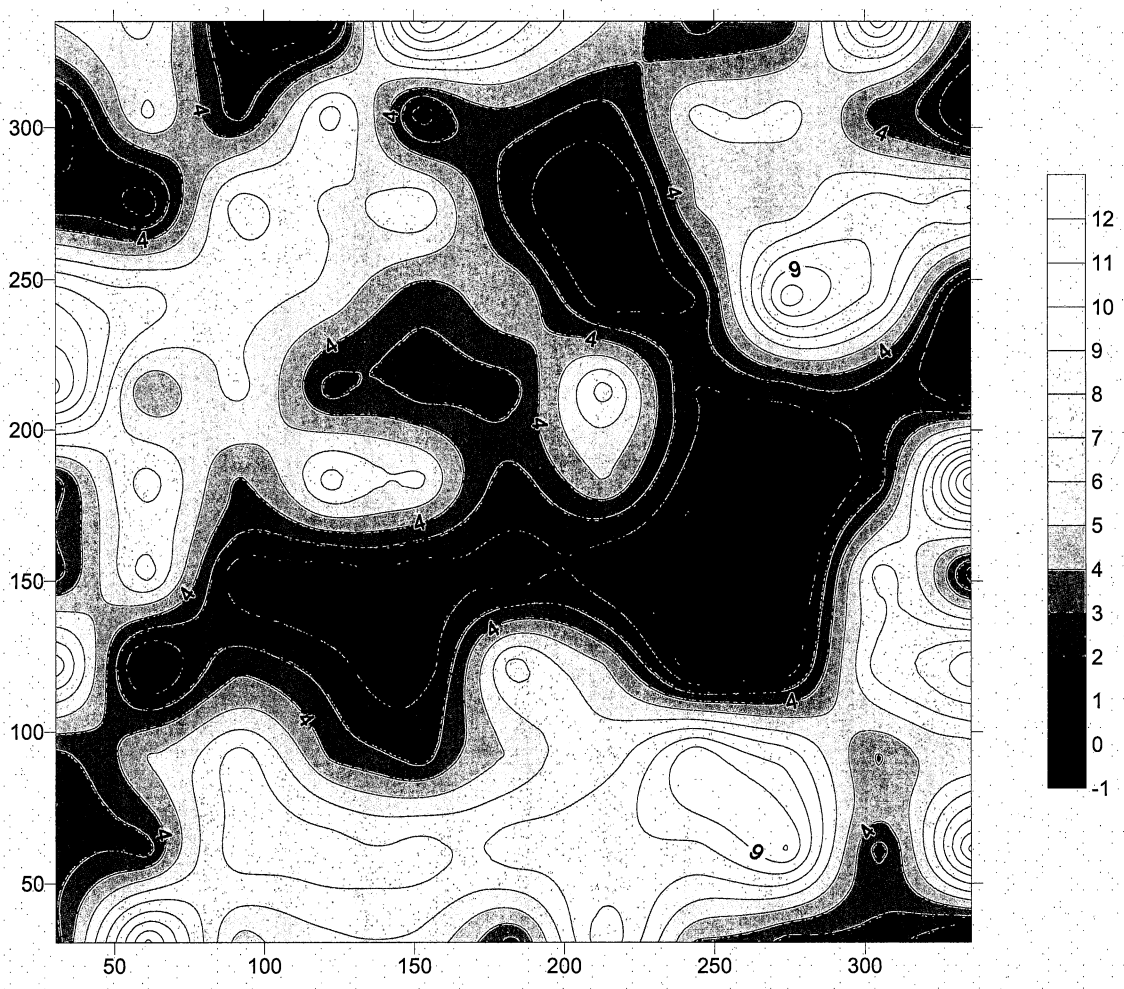
300
250
200
150
100
50
50
100
150
200
250
300
4
9
12
11
10
9
8
7
6
5
4
3
2
1
0
-1

Appendix B

The following are images representing the contrast in dielectric obtained using a ground penetrating radar (GPR) unit, SIR3000. The raw GPR data was processed using two software packages, Seismic Processing Workshop and RADAN. Data processed by Seismic Processing Workshop can be recognized by the red and blue color transform applied, while data processed using RADAN uses a multicolored color transform.

J17SH6

W – E

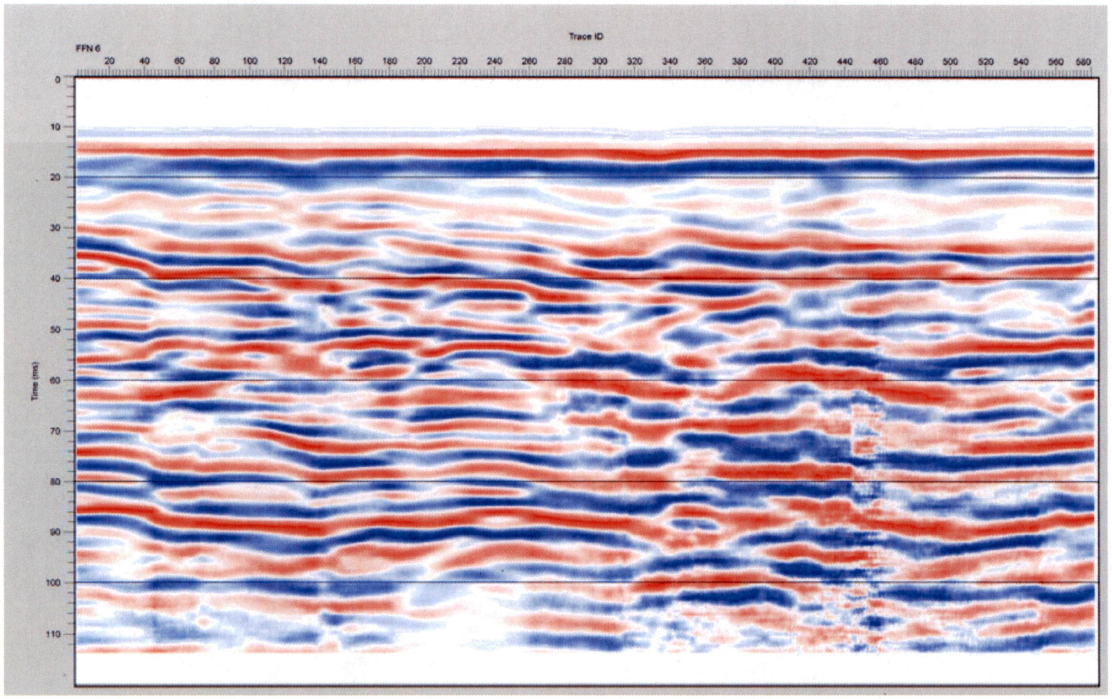

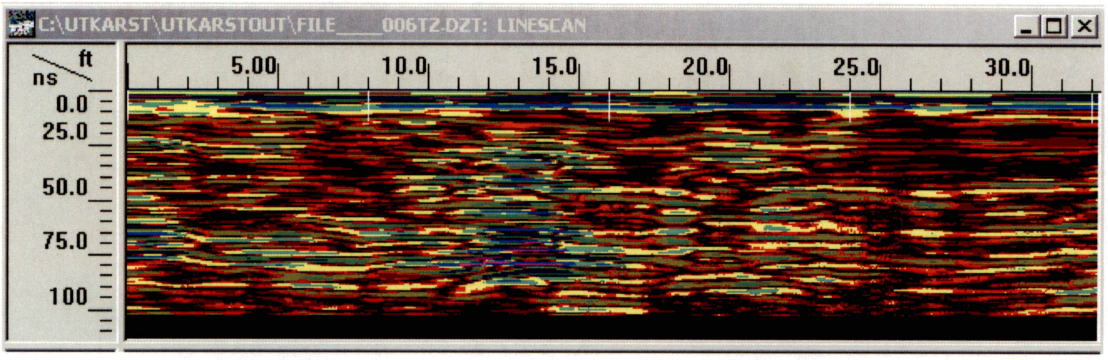
C:\UTKARST\UTKARSTOUT\FILE____006T2.DZT: LINESCAN
ft
ns
5.00
10.0
15.0
20.0
25.0
30.0
0.0
25.0
50.0
75.0
100

S – E

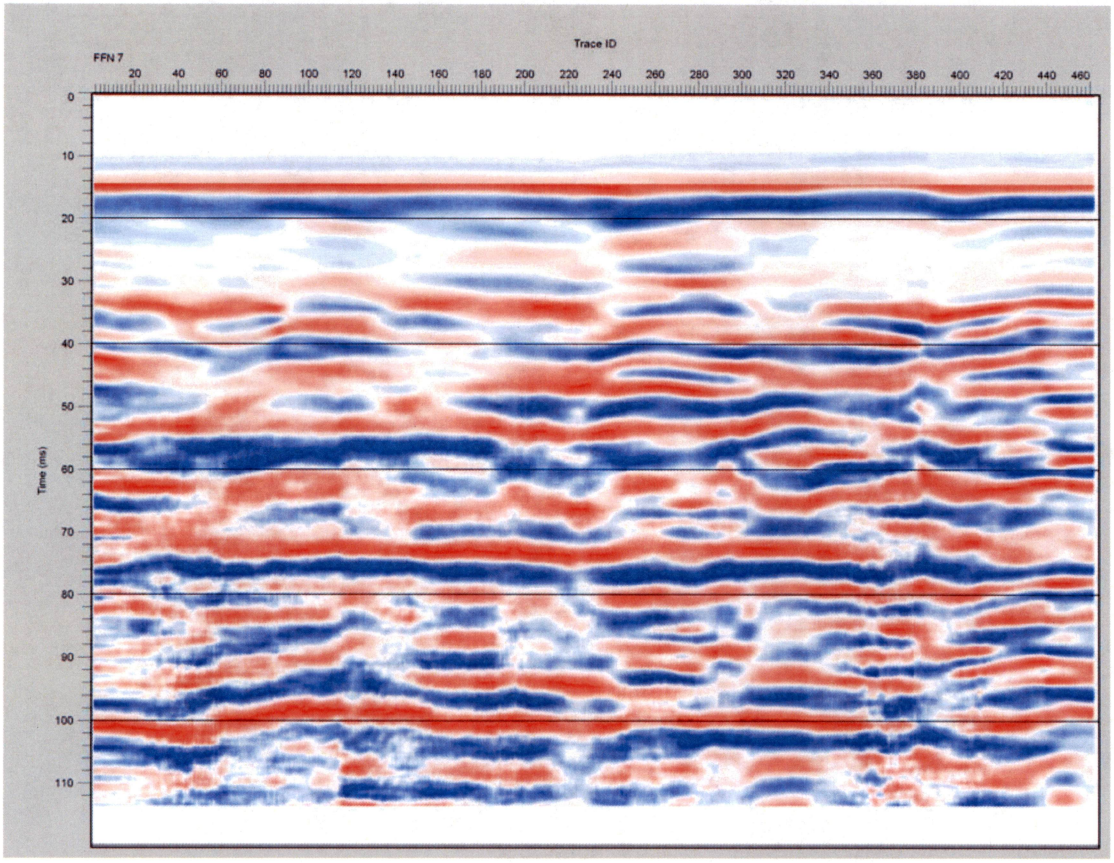
Trace ID
FFN 7
Time (ns)

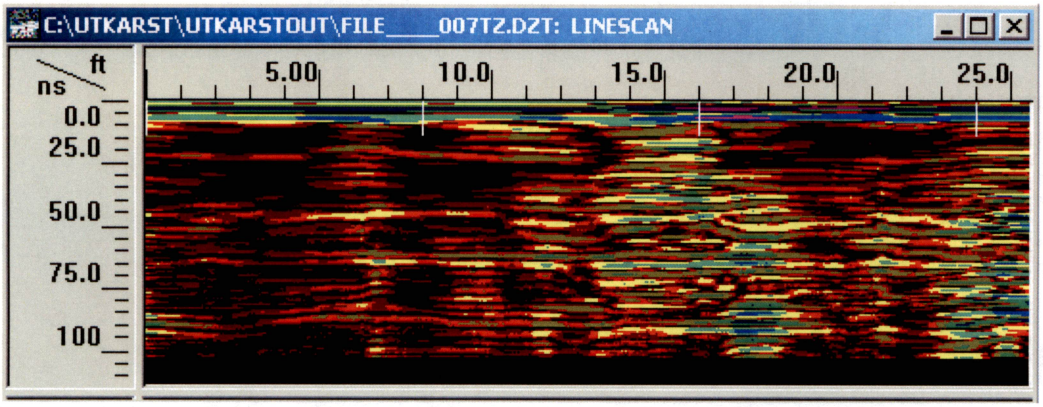
C:\UTKARST\UTKARSTOUT\FILE____007TZ.DZT: LINESCAN
ft
ns
5.00
10.0
15.0
20.0
25.0
0.0
25.0
50.0
75.0
100

J17BG2

S – N

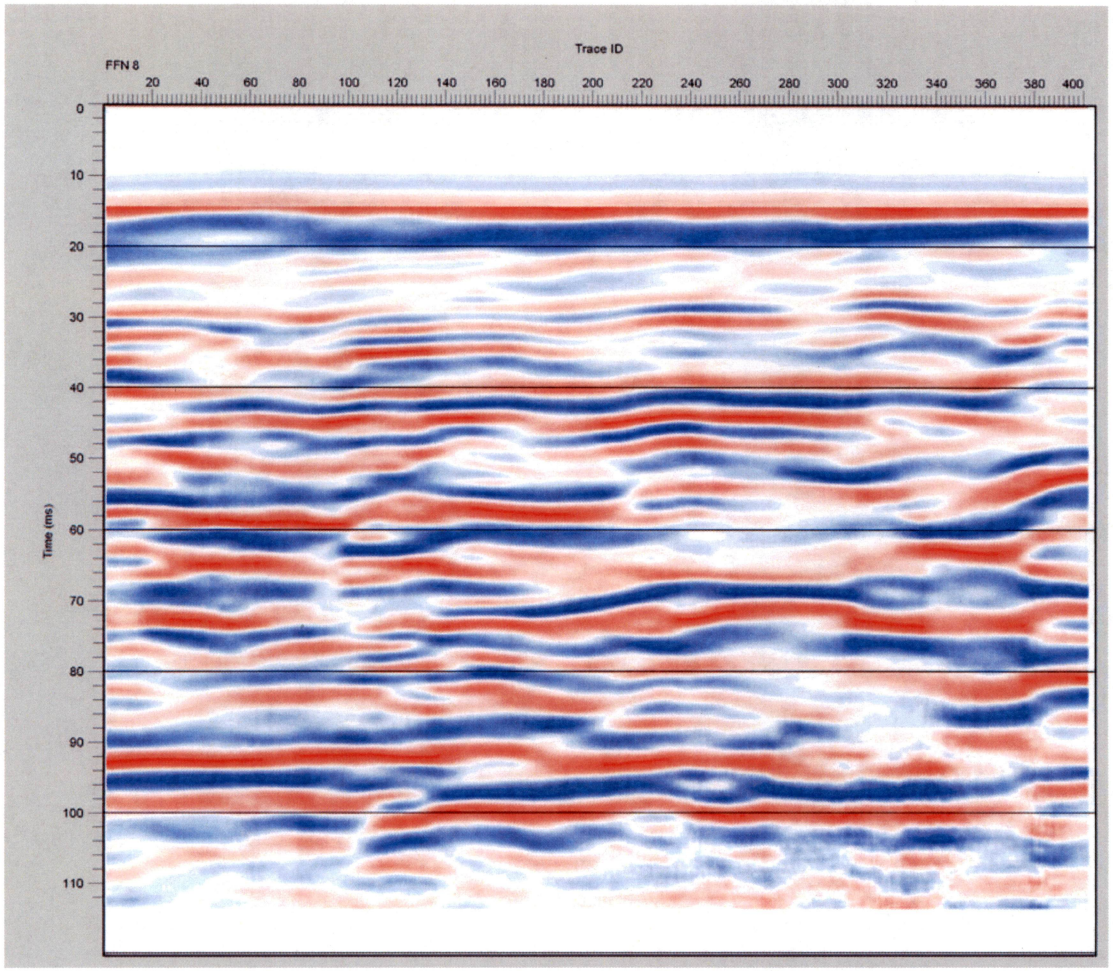
Trace ID
FFN 8
20 40 60 80 100 120 140 160 180 200 220 240 260 280 300 320 340 360 380 400
Time (ns)
0 10 20 30 40 50 60 70 80 90 100 110

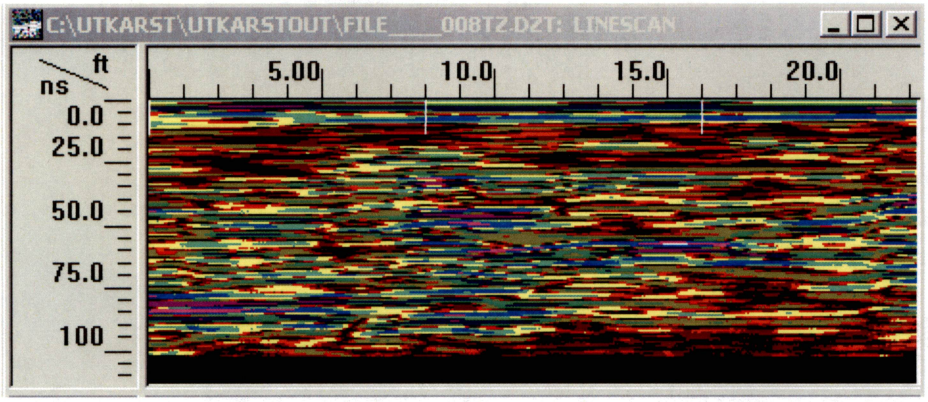

J17SH2

WSW – ENE

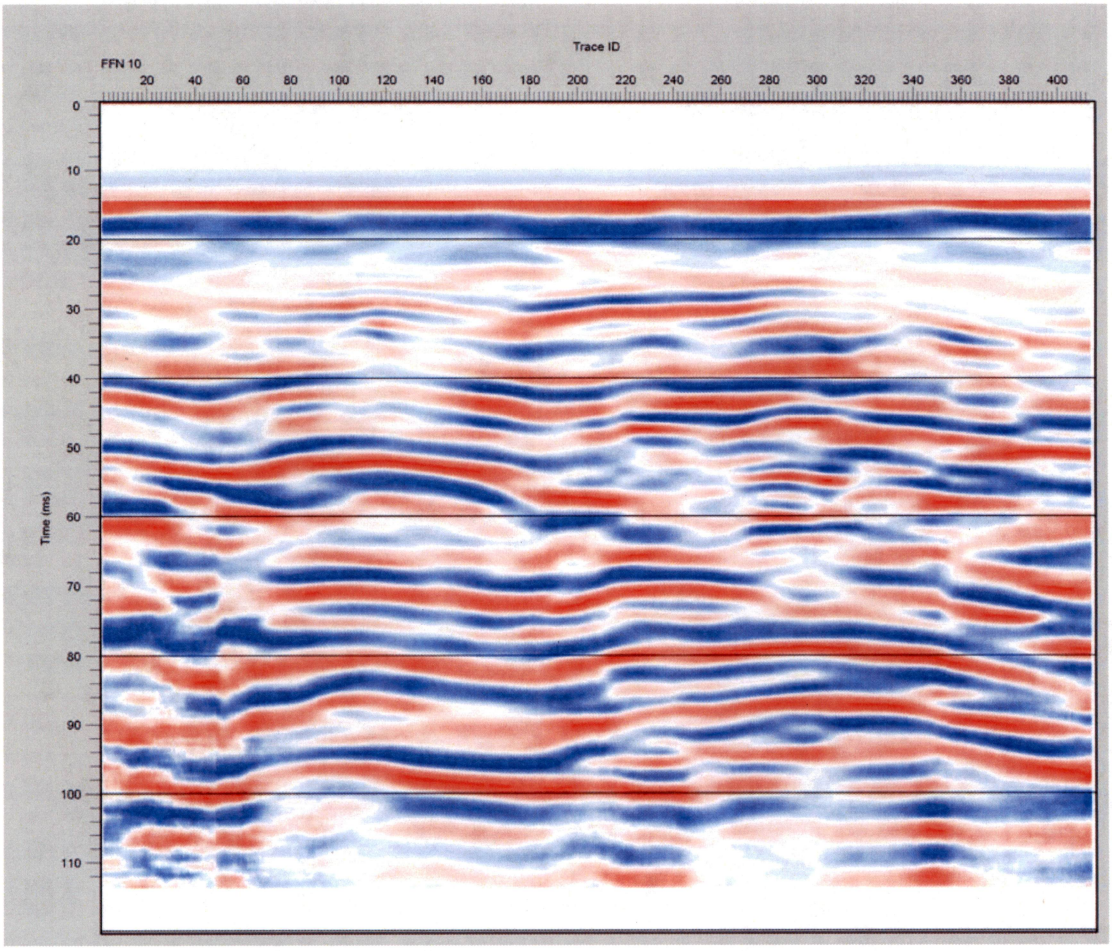

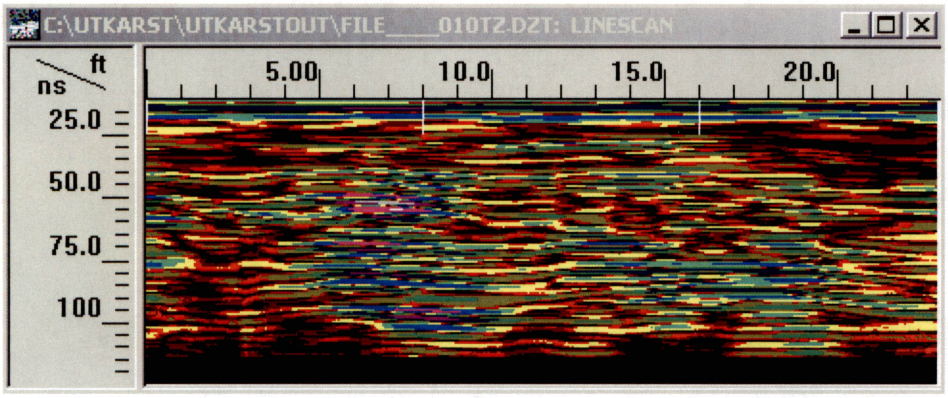
C:\UTKARST\UTKARSTOUT\FILE____010T2.DZT: LINESCAN
ft
ns
5.00
10.0
15.0
20.0
25.0
50.0
75.0
100

NNW – SSE

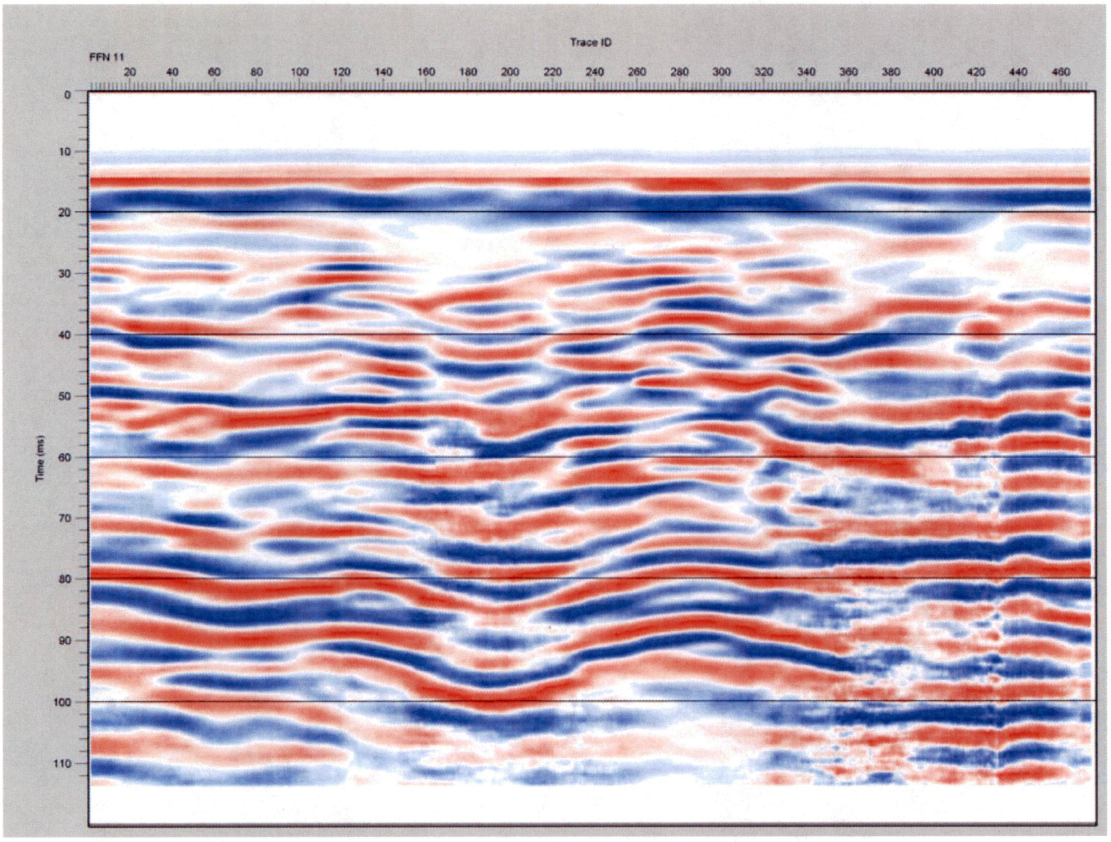
Trace ID
FFN 11
Time (ns)

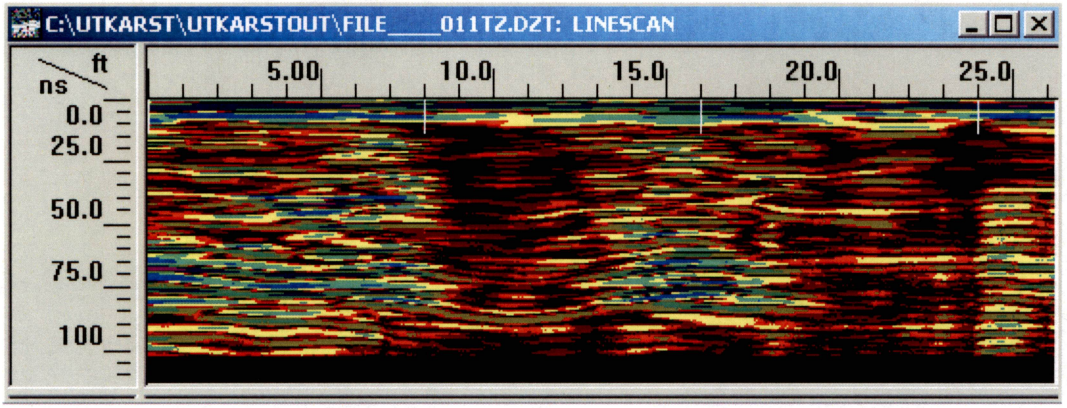

J17SH3

S – N

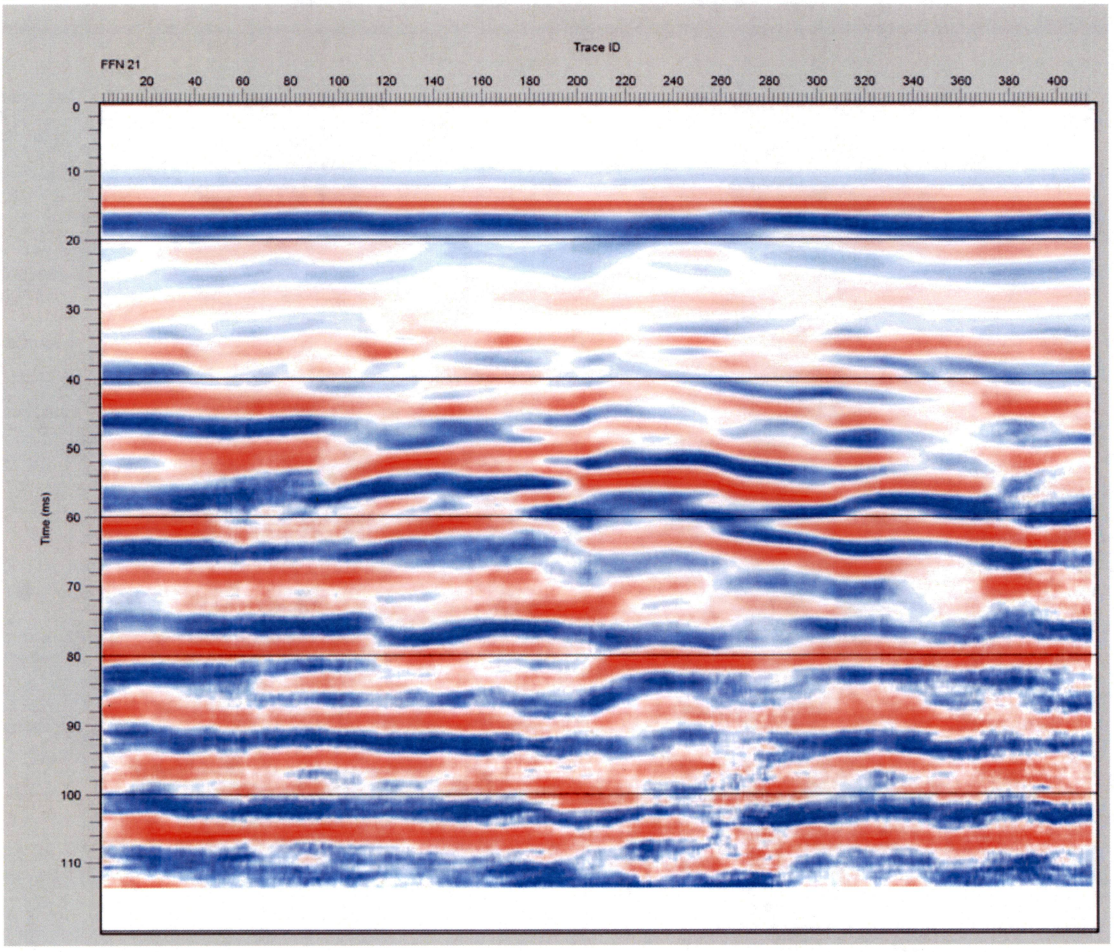

NE - SW

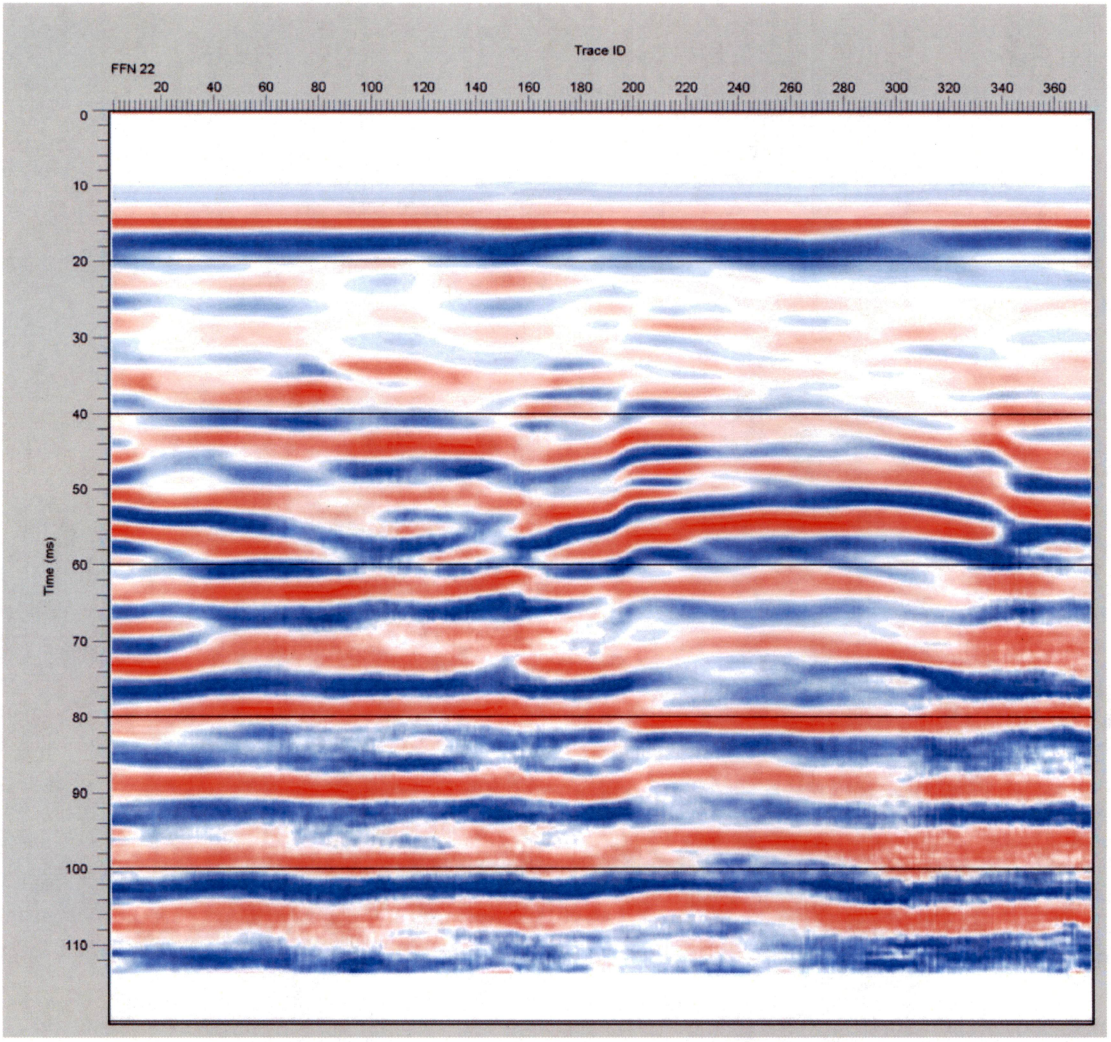
Trace ID
FFN 22
20 40 60 80 100 120 140 160 180 200 220 240 260 280 300 320 340 360
0 10 20 30 40 50 60 70 80 90 100 110
Time (ms)

J17BG3

SE - NW

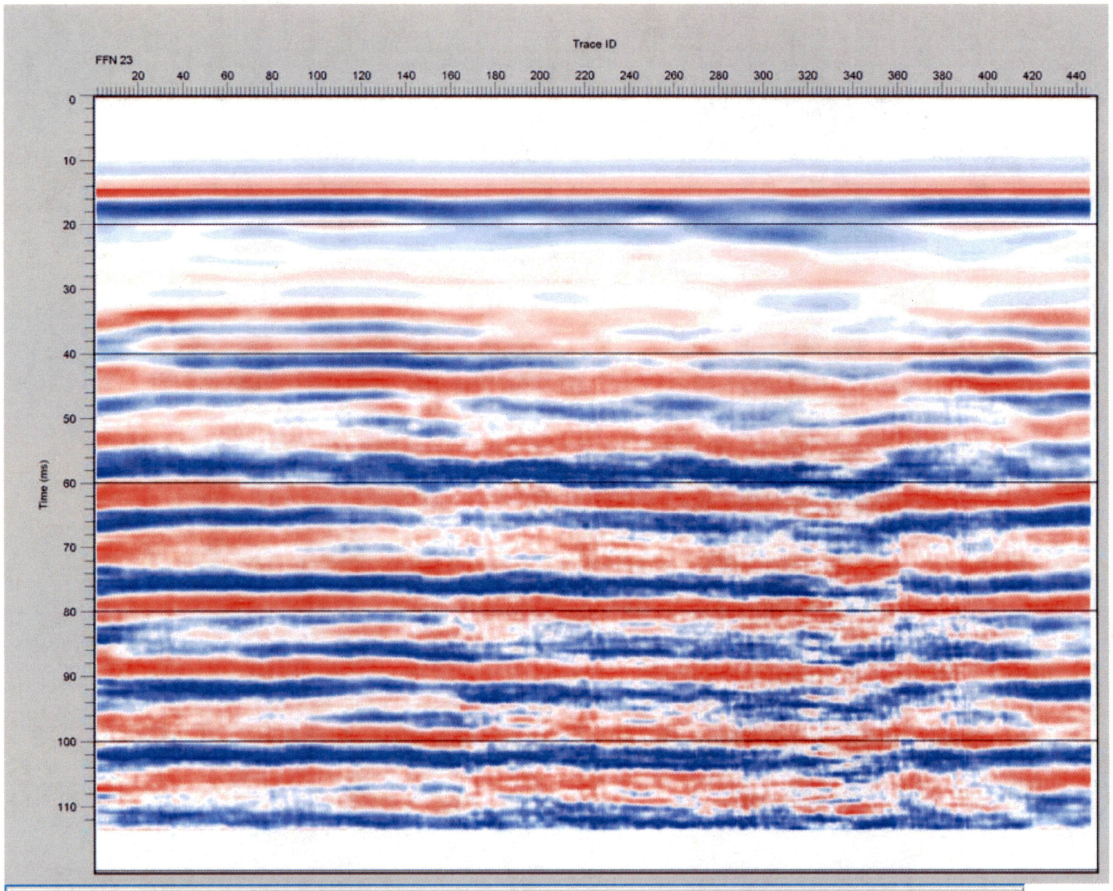
Trace ID
FFN 23
20 40 60 80 100 120 140 160 180 200 220 240 260 280 300 320 340 360 380 400 420 440
0 10 20 30 40 50 60 70 80 90 100 110
Time (ns)

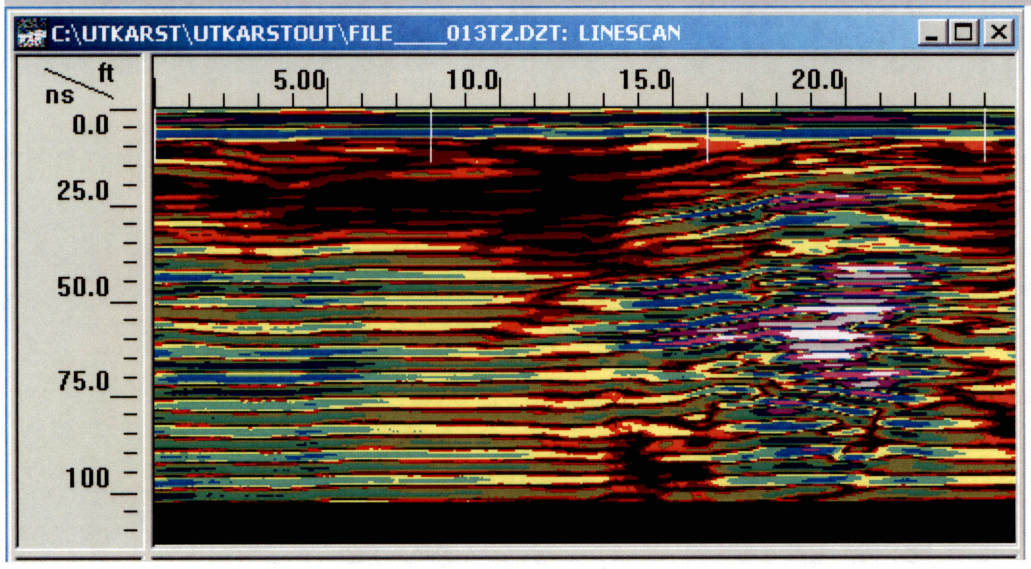
C:\UTKARST\UTKARSTOUT\FILE____013TZ.DZT: LINESCAN
ft
ns
5.00
10.0
15.0
20.0
0.0
25.0
50.0
75.0
100

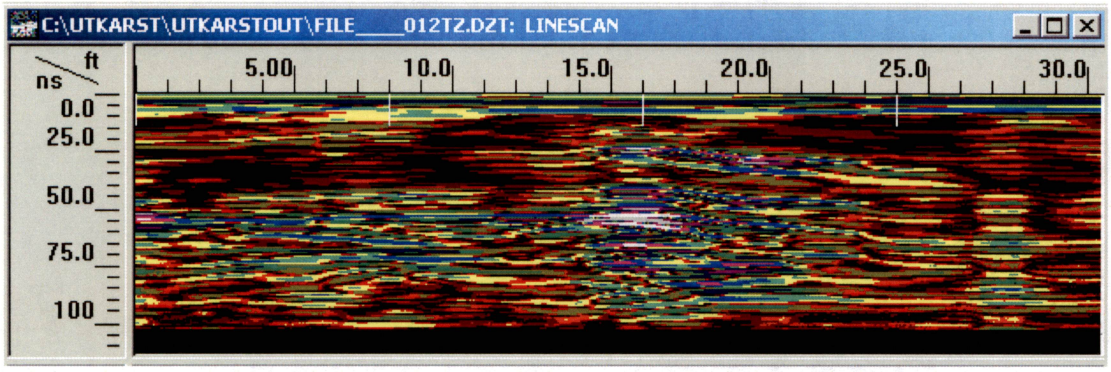
C:\UTKARST\UTKARSTOUT\FILE____012TZ.DZT: LINESCAN
ns
ft
0.0
25.0
50.0
75.0
100
5.00
10.0
15.0
20.0
25.0
30.0